

**Studiengang Systemtechnik**  
Vertiefungsrichtung Design and Materials

# Diplom 2010

*Camille Villettaz*

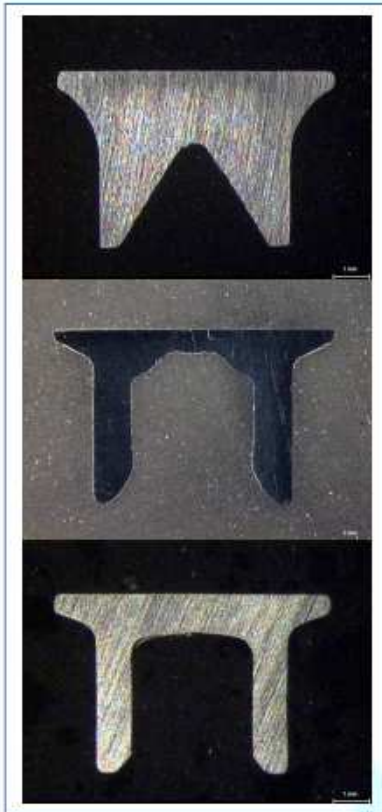
*Influence of the Geometry of  
Self-Piercing Rivets on the  
Joint Strength of High-Strength  
Thin Sheet Steel*

Dozent                    Dr. Jacques-Eric Bidaux  
Experte                    Dr. Alain Moreillon

# Influence of the Geometry of Self-Piercing Rivets on the Joint Strength of High-Strength Thin Sheet Steel

Diplomand

Camille Villettaz



Diplomarbeit  
| 2010 |

Studiengang  
*Maschinenbau*

Anwendungsbereich  
*Werkstofftechnik*

Verantwortliche/r Dozent/in  
*Prof. Dr. Anne Schulz-Beenken*  
[schulz-beenken@fh-swf.de](mailto:schulz-beenken@fh-swf.de)

Partner  
*Fachhochschule Südwestfalen*  
*Standort Soest*

HES-SO Wallis  
Route du Rawyl 47  
1950 Sitten

Tel. 027 606 85 11  
Web [www.hevs.ch](http://www.hevs.ch)

## Ziel des Projekts

Einfluss der Stanznietgeometrie auf die Verbindungsfestigkeit hochfester Stahlfeinbleche mittels eines Vergleichs zwischen verschiedenen Nieten zu untersuchen.

## Methoden / Experimente / Resultate

Es wird für diese Diplomarbeit 3 verschiedenen Nieten verglichen. Der ersten HF Niet wurde um Aluminium Blechen zu verbinden entwickelt. HD2 ist ein modernerer Niet der für das Fügen von Aluminium mit hochfesten Stahlfeinblechen realisiert wurde. Der G Niet ist noch ein Prototyp, dass hochfesten Stahlfeinblechen verbinden können soll.

Es wird 3 Fügeworkstoffen gebraucht für die Proben Vorbereitung. Davon, zwei sind hochfester Mehrphasenstähle: DP-K 34/60 und CP-W 800. Dazu kommt noch ein hochfester Edelstahl, den H400.

Um diese Nieten zu untersuchen, werden sie zuerst als ein Punkt Proben durchgeschnitten um die optimale Parametern zum stanzen zu finden. Dann werden die optimierenden Scherzugproben mit einer Universalprüfmaschine getestet. Schlussendlich, werden Zwei-Punkt-Scherzugproben für die Schwingfestigkeitsprüfung versucht.

Dieser Diplomarbeit hat gezeigt, dass die aktuelle Fertigung der G Niet noch nicht testbar ist.

Es wurde auch gefunden, dass der Hinterschnitt nicht einen grossen Einfluss auf die Verbindungsqualität hat. Es muss nur nicht unter eine kritische Grenze gehen.

Andererseits, die HF und HD2 Nieten können alle Kombinationen von die getesteten hochfester Stahlfeinbleche zusammenfügen. HD2 Nieten sind besser für quasi-statische Versuche und die HF Nieten sind besser für die dynamische Ermüdungsversuchen.

Die HF und HD2 Nieten sind weit hinter her die Festigkeiten des hochfesten Stahlfeinblechs. Das entwicklungspotential bleibt noch riesig.

# Résumé

## Objectif

Actuellement, des nouveaux prototypes de rivets sont conçus pour joindre des tôles d'aciers à haute résistance. Le but de ce travail est de tester et de comparer ces prototypes de rivets auto-poinçonneurs aux rivets pour acier à haute résistance déjà commercialisés. Il s'agit d'analyser l'influence de la géométrie de ces rivets sur la qualité des liaisons entre les tôles.

## Méthodologie

Les rivets auto-poinçonneurs sont de plus en plus utilisés dans l'industrie automobile. Pour ce travail, des tests ont été effectués avec des combinaisons de trois tôles différentes (DP-K 34/60, CP-W 800 et H400), issues de cette industrie.

Les assemblages ont été réalisés avec trois types de rivets, dont deux déjà commercialisés (HF et HD2). Le rivet HF a été conçu pour lier des plaques d'aluminium, tandis que le rivet HD2, développé plus récemment, est destiné pour joindre les nouveaux aciers hautement résistants avec de l'aluminium. Finalement, le rivet G, un prototype décliné en plusieurs variantes avec des modifications au niveau de la géométrie des pieds.

Pour analyser la qualité des liaisons de ces rivets, des coupes des différentes combinaisons d'assemblage ont été faites, ainsi que des essais de traction et des essais de fatigue.

## Conclusions

La qualité de la mise en forme et de la composition chimique du rivet G n'est pas encore suffisante pour être testé.

Les rivets de type HF et HD2 sont capables de lier des tôles en acier à haute résistance, mais la qualité de leur liaison ne parvient pas à mettre à profit les propriétés remarquables de ces nouveaux aciers.

Le rivet HF nécessite une trop grande force d'insertion, mais a une assez bonne résistance à la fatigue.

Le rivet HD2 quant à lui forme des assemblages qui résistent assez bien aux essais de traction.

Mots clés: rivet auto-poinçonneur, HF, HD2, géométrie du rivet, tôle en acier à haute résistance, essai de traction, essai de fatigue, courbe de Wöhler

# Abstract

## Purpose

New prototypes of self-piercing rivets (SPR) designed for bonding ultra high-strength steel (UHSS) have been developed. The aim of this project is to analyze the influence of the geometry of these SPR on their joint strength. Finally a comparison with other already commercialised rivets also usable for UHSS has to be done.

## Approach

The SPR, as well as the part of new UHSS, are increasingly used in the automobile industry. There is a need for new rivets able to bond these UHSS. In this study, three different modern UHSS were used. The poly-phase steels DP-K 34/60 and the CP-W 800. The third is an austenitic stainless steel, H400.

To join these sheets, three SPR were tested. Two of them, the HF and the HD2 rivets are already commercialised. The HF rivet was basically conceived for aluminium sheets. The HD2 is more recent and was designed for mixed construction with aluminium and high-strength steels. The third type of studied rivet is the new developed prototype for UHSS, named G. This prototype exists in several versions with small differences of the feet geometry.

To analyse the quality of the rivets bonding, sections of the different assembly combinations have been done. Finally, quasi-static shear tests as well as fatigue tests have been made.

## Conclusion

The actual quality of the chemical composition and the shaping process used for the G rivet is not good enough for running tests.

HF and HD2 rivets are able to bind ultra high-strength sheet steel, but they are not good enough to fully use the new ultra high-strength capacity.

The HF rivet requires a too big punching force, but has a good resistance for fatigue tests.

HD2 rivet is better for quasi-static shear tests.

**Keywords:** self-piercing rivet, HF, HD2, rivet geometry, ultra high-strength sheet steel, quasi-static shear test, fatigue test, Wöhler curve

# Contents

Résumé .....	i
Abstract .....	ii
Contents .....	iii
Nomenclature .....	v
1. Introduction.....	1
1.1 Background .....	1
1.2 Scope of the Research.....	2
2. Literature Review .....	3
3. Methodology.....	5
3.1 Objective .....	5
3.2 Methods of Investigation.....	5
4. Self-Piercing Rivets Technology.....	6
4.1 Classification of Self-Pierce Riveting in the Joining System.....	6
4.2 Self-Peirce Riveting Process .....	7
4.3 Main Parameters for Self-Pierce Riveting Process.....	9
4.3.1 Parts to be Joined Main Parameters.....	9
4.3.2 Rivet Main Parameters .....	10
4.3.3 Rivet Setting Main Parameters .....	10
4.4 Self-Piercing Rivets .....	11
4.5 Self-Piercing Rivet Die.....	14
5. High-Strength Sheet Steel.....	15
5.1 Multi-Phase Steels.....	15
5.1.1 DP-K 34/60 .....	15
5.1.2 CP-W 800 .....	16
5.2 Austenitic-Based Steels.....	16
5.2.1 H400 .....	16
5.3 Mechanical Properties of the High-Strength Steels .....	16
5.4 Chemical Composition of the High-Strength Steels.....	17
6. G Rivet Prototype .....	18

7.	Experimental Test Set-Up and Procedure .....	19
7.1	Tested Rivets .....	19
7.2	Tested Die for the Riveting .....	20
7.3	Riveting .....	21
7.3.1	Rivet Joint Sections .....	21
7.3.2	Self-Pierce Riveting Machine .....	25
7.4	Rivets Hardening .....	28
7.5	Quasi-Static Shear Tests .....	31
7.6	Fatigue Tests .....	33
8.	Results and Discussions .....	37
8.1	G Rivet Prototype .....	37
8.1.1	Cold Shaped Rivet .....	37
8.1.2	Machined Rivet .....	39
8.2	HF vs. HD2 Comparison .....	41
8.2.1	Dimensional Stability .....	41
8.2.2	Rivet Setting .....	46
8.2.3	Jointed Sheets Hardness .....	49
8.2.4	Quasi-Static Shear Tests Comparison .....	51
8.2.5	Fatigue Tests Comparison .....	55
9.	Conclusions and Recommendations .....	60
9.1	Conclusions .....	60
9.2	Recommendations .....	60
10.	References .....	61
11.	Acknowledgment .....	62
12.	Appendices .....	63
12.1	HD2 Rivet Joining Formation .....	63
12.2	HF Rivet Joining Formation .....	68
12.3	G Rivet Joining Formation .....	73
12.4	Quasi-Static Shear Test Comparison .....	74
12.5	Fatigue Shear Test Rivet Comparison .....	81
12.6	Fatigue Shear Test Frequency Comparison .....	83

# Nomenclature

CP:	A complex phase steel CP-W 800
CP-DP:	Combination of two sheets with CP on the punch side and DP on the die side
CP-CP:	Combination of two sheets of CP steel
DP:	A dual phase steel DP-K 34/60
DP-CP:	Combination of two sheets with DP on the punch side and CP on the die side
DP-DP:	Combination of two sheets of DP steel
DP-H400:	Combination of two sheets with DP on the punch side and H400 on the die side
$F_a$ :	Force amplitude for a fatigue test
$F_{max}$ :	Ultimate strength for a shear test
G:	Prototype of self-piercing rivet from Dr. Singh
H400:	A stainless steel H400
H400-DP:	Combination of two sheets with H400 on the punch side and DP on the die side
H400-H400:	Combination of two sheets of H400 steel
HD2:	Self-piercing rivet from the company <i>Böllhoff GmbH</i>
HF:	Self-piercing rivet from the company <i>Ribe GmbH</i>
k:	Deformation grade for a fatigue test
LVDT:	Linear Variable Differential Transformer
R:	Minimum versus maximum load ratio for a fatigue test
$R^2$ :	Coefficient of determination for a fatigue test
SPR:	Self-Piercing Rivet
UHSS:	Ultra High-Strength Steel
W30:	Realistic deformation energy for a shear test

# 1. Introduction

## 1.1 Background

The recent development of high-strength steels allows new conceptions and designs especially for the automotive field. These materials called ultra high strength steels (UHSS) have not only a higher resistance than the already existing steels, but also a better formability. These new steels, in sheet shape, are increasingly used in automobile range. The same development occurs for the stainless steel like for example the H400 steel which is able to withstand a huge energy deformation. This steel is therefore used for crash relevant pieces.

Due to the high-strength steels, it's possible to construct lighter structures that resist the corrosion without an external coating. The portion of high-strength steel is growing after every new generation as for example for the DC-E it increased of 27% over the last model.

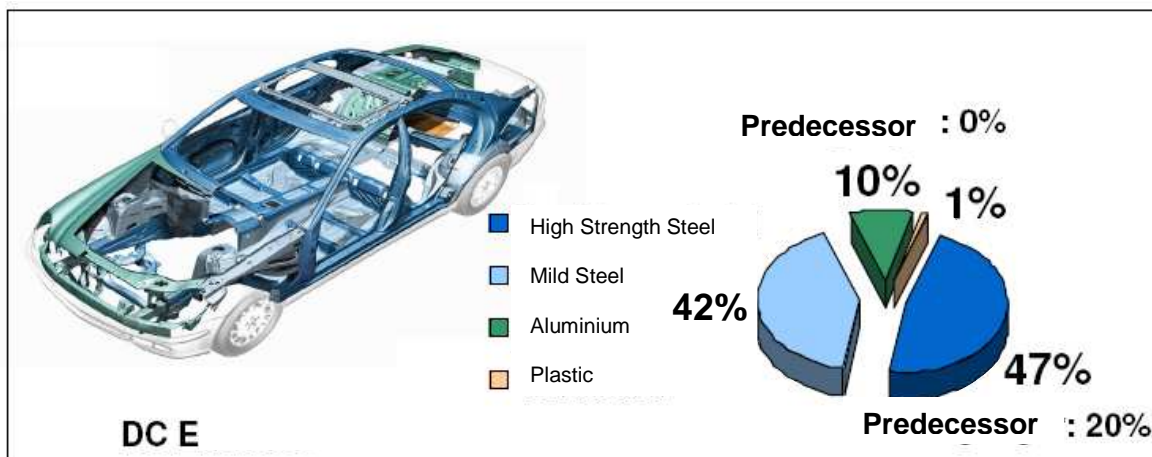


Fig. 1 Material composition of the DC-E / Source: DaimlerChrysler AG

These new poly-phase steels require a development of the joining methods that can be reproducible and also efficient with mixed materials. The UHSS produced in the last years have an ultimate tensile stress between 600 MPa and 1200 MPa. Most of the materials in the industrial production lines with an ultimate tensile stress of 600 MPa or less are joined with rivets. To be able to use the latest developments of the high-strength steels, it's necessary to improve the bonding technique.

Recently, new SPR for UHSS have been conceived. The success of a possibly commercialization depends on the performances of these SPR compared to the existing ones. The conception of a rivet is at the beginning made on a computer with an FEM program. It permits to simulate the bonding of SPR with different geometries. The second step of this development is to produce some prototypes and then to test them.

## 1.2 Scope of the Research

In this paper, study was carried on the influence of the geometry of self-piercing rivets (SPR) on the joint strength of high-strength thin sheet steel.

The quality of a connection depends on many parameters. One important is what kind of joined sheets are used and in which order. By order it is meant, which sheet is on the top, the punch side and which is down, the die side. For this study, 3 different sheets were used: DP-K 34/60, CP-W 800 and H400. They all belong to the ultra high-strength steels (UHSS).



**Fig. 2 Photo of a self-piercing rivet and a section of a self-piercing rivet joint / Source: Böllhoff GmbH**

The different combinations of the UHSS were assembled with 3 different rivets: HD2, HF and G. The samples were then cut to obtain a section of the SPR bonding and so to allow characterising the specific dimensions. Quasi-static shear tests as well as dynamic fatigue tests were done with other samples.

## 2. Literature Review

With an improving number of high strength steel parts, difficulties occur with joining technologies previously used with milder steel. Even if more high strength steel will make the mechanical joining more difficult, it will also increase the use of mechanical joining like self-piercing rivets (SPR), especially because of the good fatigue properties [01].

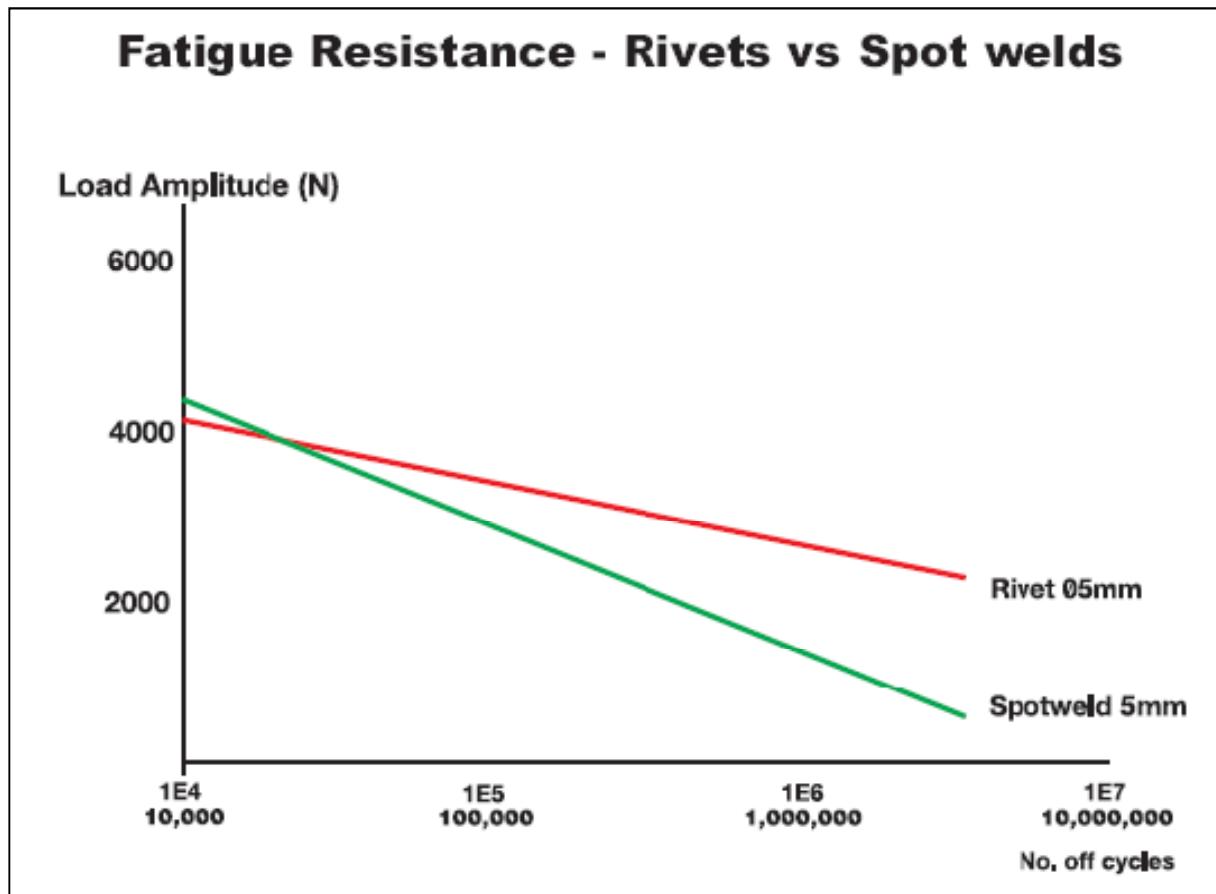


Fig. 3 Fatigue test for rivets versus spot welds / Source: Henrob Ltd

The heat brought by the spot welding changes the mechanical properties of the sheet in the heat-affected zones which is bad under oscillating loads. The fig. 3 and 4 show clearly that the Rivets become much better than the spot welds after 100'000 cycles and the trend increases with the number of cycles. There is no heating with the rivets and it allows mixed building structures when welding technologies cannot always bind.

The mechanical bonding applications are essentially the self-pierce riveting, because the clinching has a weaker joint strength (fig. 4).

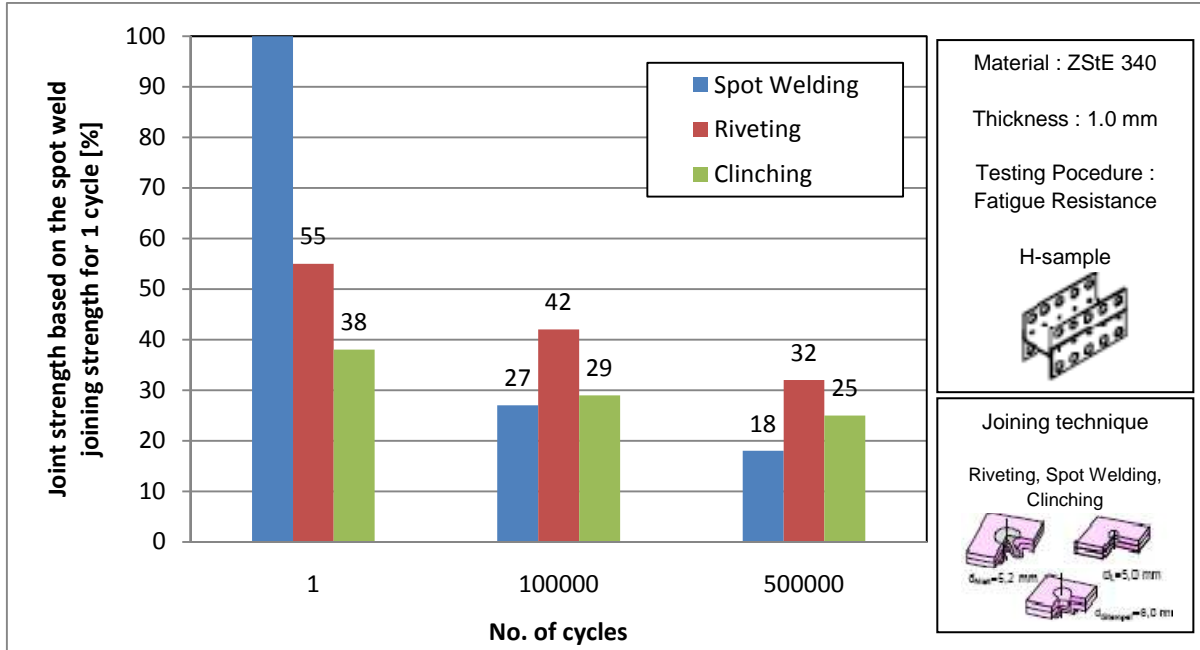


Fig. 4 Comparison between tensile stress and dynamic fatigue of spot welding, riveting and clinching / Source: LWF, Uni. Paderborn

The self-pierce riveting technique is first of all used in the automobile industry. Its importance increased considerably during the last 20 years (fig. 5). The self-piercing rivets (SPR) have proven their quality in aluminium joining for several years. They replace more every year the conventional welding, especially the spot welding.

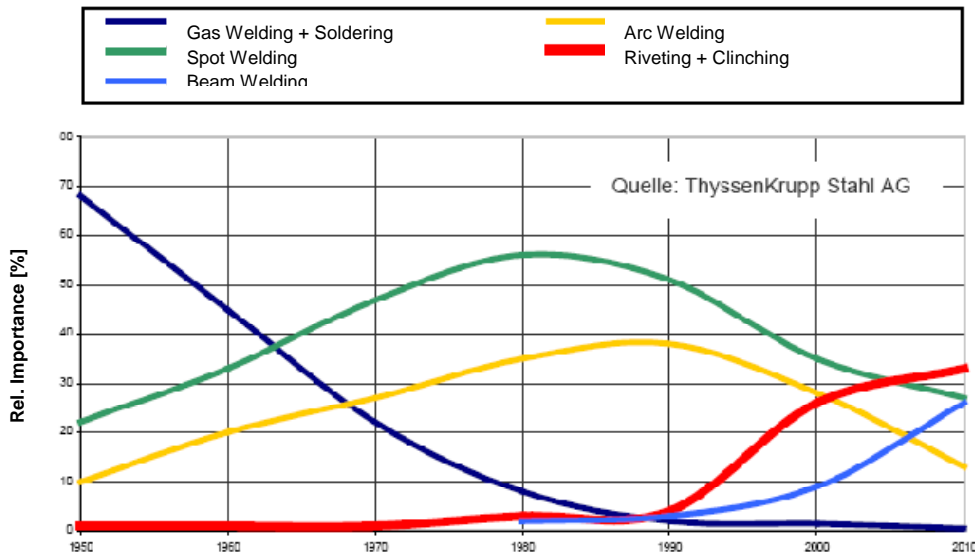


Fig. 5 Evolution of bonding technique / Source: ThyssenKrupp

The self-pierce riveting technique is a very good solution for high-strength steels but it needs to be enhanced for this new field of applications. In order to reach this objective, the researches and developments for SPR are done by the bonding manufacturers in collaboration with the research institutes.

## 3. Methodology

### 3.1 Objective

With the increasing resistance of the sheets steel, the bonding technique with the self-piercing rivets (SPR) is getting more complex. There is always more ultra high strength steels (UHSS) parts build in a car. The SPR are well suited for the joining of these kinds of pieces, but it's necessary to develop new rivets specifically designed for the UHSS.

The aim of this study is to understand the influence of the geometry of SPR on the quality of the bonding of high-strength sheets steel.

### 3.2 Methods of Investigation

In this study, 3 different modern UHSS were used. The DP-K 34/60 and the CP-W 800 belong to the poly-phase steels. H400 is the third UHSS; it is an austenitic stainless steel. All of the three materials are increasingly used in the sheet machining industry.

The joints were made with 3 different SPR. Two of them, the HF and the HD2 rivets are already commercialised. The HF rivet was basically conceived for aluminium sheets. The HD2 is more recent and was designed for mixed construction with aluminium and high-strength steels. The third type of studied rivet, named G, is a prototype developed for UHSS. This prototype exists in several versions with small differences of the feet geometry.

To analyse the quality of the rivets bonding, different sheet combinations have been assembled.

		Sheet on the Punch Side		
		DP-K 34/60	CP-W 800	H400
Sheet on the Die Side	DP-K34/60	HD2 / HF / G**	HD2 / HF	HD2 / HF*
	CP-W 800	HD2 / HF	HD2 / HF	–
	H400	HD2 / HF*	–	HD2 / HF*

Fig. 6 Samples combinations on which were made: a bonding section, a shear test and a fatigue test

\*: without fatigue test

\*\* : only bonding section

– : no sample

The samples have been cut in order to get a section of the joint and be able to measure the important dimensions and also to optimise the process parameters. Another series of samples has been tested with a quasi-static shear stress. Finally, a fatigue test has been made for a last series of samples.

# 4. Self-Piercing Rivets Technology

## 4.1 Classification of Self-Pierce Riveting in the Joining System

The self-pierce riveting existed already in the fifties for sheets bonding. But the developments achieved in welding and in gluing techniques made the riveting less important. The increasing automation and the diversification of the bonding materials in industries like the automobile industry made the self-pierce riveting technique come back. The conventional rivets technology requires a pre-punching operation which results in additional costs in the automation process. To reach a better productivity, it's necessary to reduce the number of operations in a process. The self-piercing rivet makes the joining without a pre-punching and is in this way an interesting solution for bonding processes.

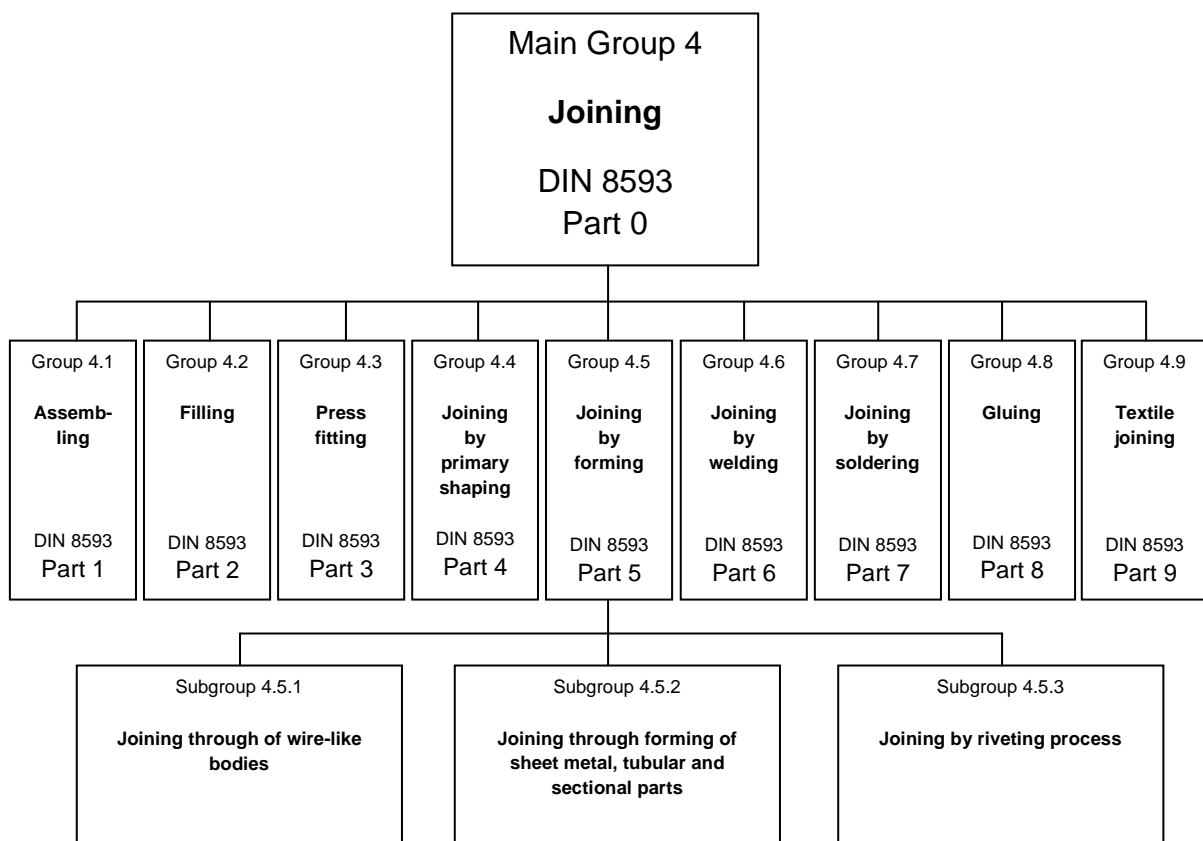


Fig. 7 Representation of bonding technique according to DIN 8593

According to DIN 8593, joining means a durable bonding of at least two components and this bonding can be firmly fixed or loose. The joining by forming involves a local plastic deformation of the components without a thermal influence on their structure and produces that way a form-locking bonding. The self-pierce riveting belongs to the subgroup 4.5.3 of joining by forming (fig. 7).

Rivet systems						
Connecting task / element	Connecting with rivet elements			Connecting with dismountable elements		
Preparation of parts to be joined	with prepunching		without prepunching	with prepunching		without prepunching
Accessibility / kinematics	One-sided connection	Two-sided connection	Two-sided connection	One-sided connection	Two-sided connection	Two-sided connection
Joining Technique	Blind rivet	Solid-, semi-tubular and tubular rivets, lock-ring bolts	Self-piercing rivet	Blind rivet nuts and bolts	Rivet nuts and bolts	Self-piercing nuts and bolts

Fig. 8 Characterisation of conventional riveting systems / Source: LWF, Uni. Paderborn

## 4.2 Self-Pierce Riveting Process

The self-pierce riveting process is done in one single operation that can be divided in 6 steps:

1. Positioning: the two sheets have to be positioned for the bonding
2. Fixing: the blank-holder is clamping the two sheets to prevent lateral movements
3. Penetrating: the self-piercing rivet is penetrating the punch side sheet
4. Stamping: the punch is stamping the rivet in the sheets, both sheets are plastically deformed and the shape is given by the die
5. Forming: the rivet encounters the die side sheet and start to spread thank the die
6. Setting: the rivet is upsetting and so closing the free spaces

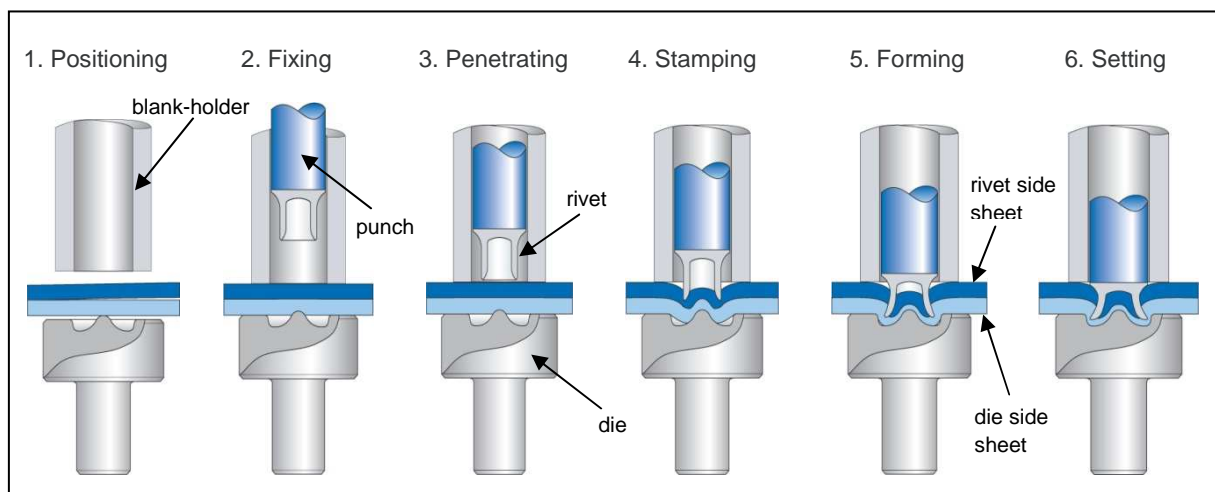


Fig. 9 Process step by step of a self-pierce riveting / Source: Böllhoff GmbH

In a single operation, self-piercing rivet (SPR) joins multiple layers of similar or dissimilar materials with varying thickness. During the assembly process, a SPR is driven into material stack at a controlled force, piercing the top layer or layers. The rivet radially expands into the bottom layer forming mechanical interlock and creates a button in the bottom sheet.

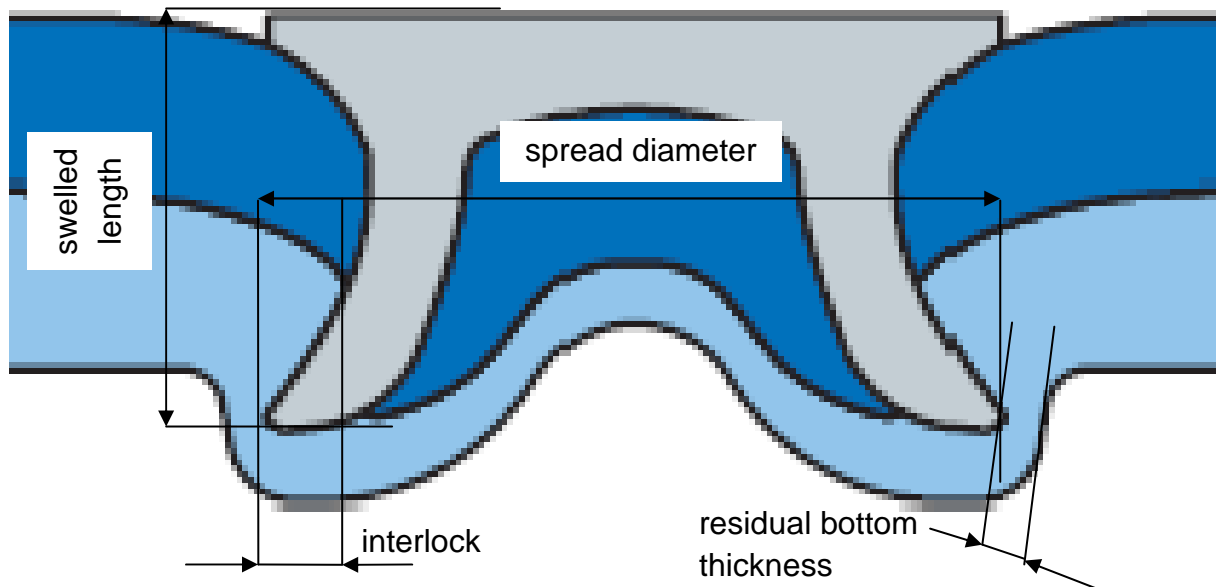


Fig. 10 Schematic Diagram of Physical Attributes of self-piercing riveted joint

The die influences deeply the piercing process as well as the spreading process which creates the undercut of the rivet. Since the lower sheet is not pierced the resulting joint is resistant to gas and liquid from the die side and therefore also resistant to corrosion. The entire process takes less than 3 seconds, depending on the machine stroke and rivets feeding mechanism. No need for pre-punching operations significantly increases attractiveness of the process for industry application because of speed and relatively easy automation of process. Ecological aspects like low noise emission, lack of gas and heat generation and low energy consumption are of notable importance, too. On the other hand, this process requires an access on both sides, but the rivet can be inserted in the two directions.

## 4.3 Main Parameters for Self-Pierce Riveting Process

The quality of the joint formation depends on a lot of different parameters. To optimise the settings it is necessary to perform many tests. The main parameters are listed in the following table [02].

Parts to be joined	Rivet	Rivet setting
Thickness	Geometry	Punch force
Positioning of the parts	Dimensional stability	Clamping force
Mechanical properties	Material	C-frame rigidity
Coating	Hardness	Die geometry
	Coating	

Fig. 11 Main parameters for self-pierce riveting process

### 4.3.1 Parts to be Joined Main Parameters

#### Thickness

The thickness determines the required punch force for the riveting. It will also give the rivet length. If the two sheets to be joined have different thickness, the thickest should be placed on the die side. This allows a better interlock, gives a wider residual bottom thickness and minimise the risk of cracks in the die side sheet [03].

#### Positioning of the parts

As mentioned above, the thickness should influence the positioning choice. Another point is to have the more ductile sheet on the die side, because the deformation of the sheet is much bigger on the die side than on the punch side.

#### Mechanical Properties

The mechanical properties of the materials indicate if the elements are well suited for the riveting process. A material with a low tensile strength and a high ductility is normally much easier to join with riveting than a material with a lower ductility and a higher tensile strength.

#### Coating

A coating on the sheets can help, even if the effect is small, to minimise frictions during the rivet setting.

## 4.3.2 Rivet Main Parameters

### Geometry

The geometry of the rivet has a big influence on the quality of the joining. Dimensions like the rivet length, the rivet diameter, the shank hole depth or the foot geometry are very important.

### Dimensional Stability

Rivets are shaped with a cold extrusion process. The dimensions can change, especially because of the billet mass fluctuations. The shaping of the shank hole can create shape concentrations near the head region which increases crack risks.

### Material

For rivets made of stainless steel, the tensile strength will increase during the setting process because of the bake-hardening effect.

### Hardness

The rivet must be hard enough to penetrate the punch side sheet and ductile enough to spread in the die side sheet. The hardness of the rivet has to be two times higher than the sheets.

### Coating

Rivets made of steel are usually coated to protect them from corrosion. The coating is generally softer than the rivet material. During the rivet setting, the coating helps a little bit the process by reducing the frictions.

## 4.3.3 Rivet Setting Main Parameters

### Punch Force

For the new high-strength steels, the punch force required is very high and reaches the limit of what the actual machines can do. The punch force needed for these steels is from 50 to 100 kN.

### Clamping Force

The clamping force avoids a deflection of the sheets and helps the penetration of the rivet in the punch side sheet. It also permits to control a little bit the flow of the die side sheet [04]. The more rigid the sheets are, the more high must be the clamping force.

## C-Frame Rigidity

The punch force needed for the rivet setting is supported by the C-frame of the setting machine. The C-frame must be rigid enough to be able to avoid lateral and angular displacements while setting the rivet [05].

## Die Geometry

The die helps the rivet to spread and therefore, helps for the creation of the interlock. It allows also the sheet material to flow and build this way a button [02].

## 4.4 Self-Piercing Rivets

The self-piercing rivets (SPR) exist in two different variants. One is named semi-tubular rivet and is hollow, the other is called solid rivet. The two types are different by geometry, by joint formation and by load capacity. For this work, the denomination of self-piercing rivet will always refer exclusively to the semi-tubular rivet.

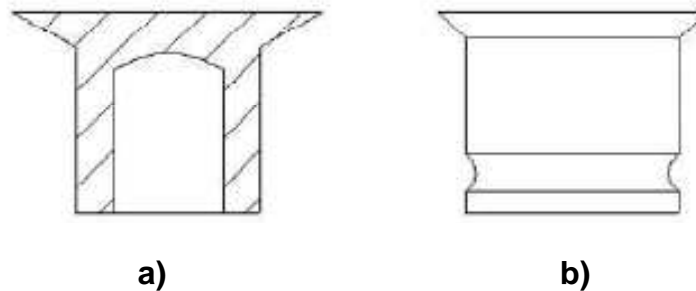


Fig. 12 Schematic representations of self-piercing rivets: a) semi-tubular rivet b) solid rivet

SPR are mainly described with the following dimensions:

$D_K$  = rivet head diameter

$D_S$  = rivet diameter

$D_I$  = rivet interior diameter

$\alpha$  = rivet cutting edge

$S_K$  = rivet head thickness

$L$  = rivet length

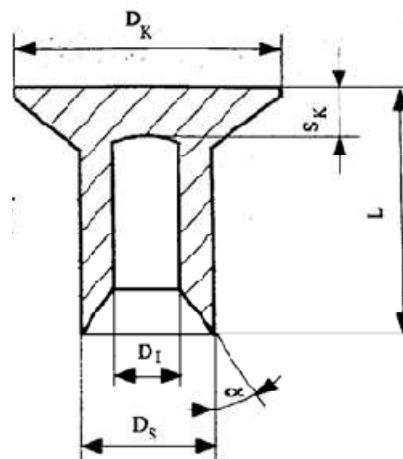
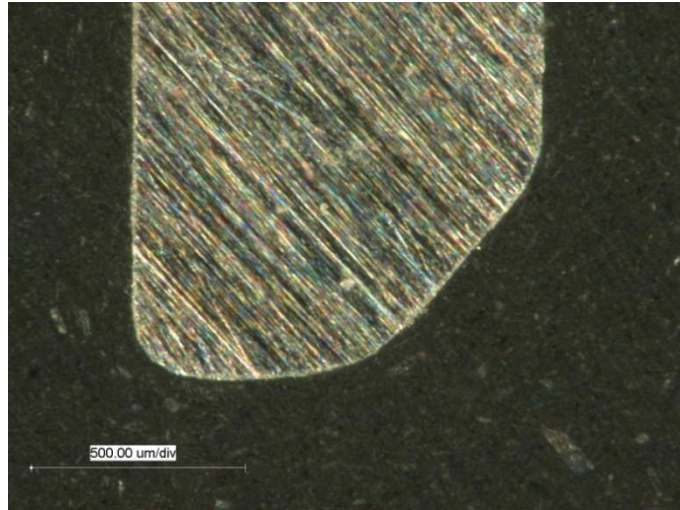


Fig. 13 Schematic section of a self-piercing rivet with the main dimensions

The geometry of the SPR can be much more complicated, especially for the foot geometry (the bottom part). For example, the foot geometry of a HD2 rivet is obtained with several radiuses and not just a rivet cutting edge as shown in fig. 13.



**Fig. 14** Left foot section of a HD2 rivet

The rivet must be stiff enough for piercing the upper sheet but also ductile to allow the radial expansion in the lower sheet. This means that the rivet hardness must be adapted to the sheets materials. SPR are generally made with impact extrusion. This is a cold extrusion process which presses the billet at a high velocity and extreme force into a die to give the shape. To get the final shape, the process is generally divided in 5 steps.



**Fig. 15** Billet for a G rivet

Once the shape is obtained, the rivet is hardened and tempered to optimise the penetration and spreading in the sheets. Finally, rivets are often coated to protect them from corrosion.

The rivets producers have defined hardness grades for the rivets. The hardness is written with the letter H and then a number from 0 to 6. Each number represents an interval of hardness measured in Vickers with a tolerance of  $\pm 25$  to 30 HV. A higher grade is necessary for rivets used for high-strength steels, so the grade 7\* was created [06].

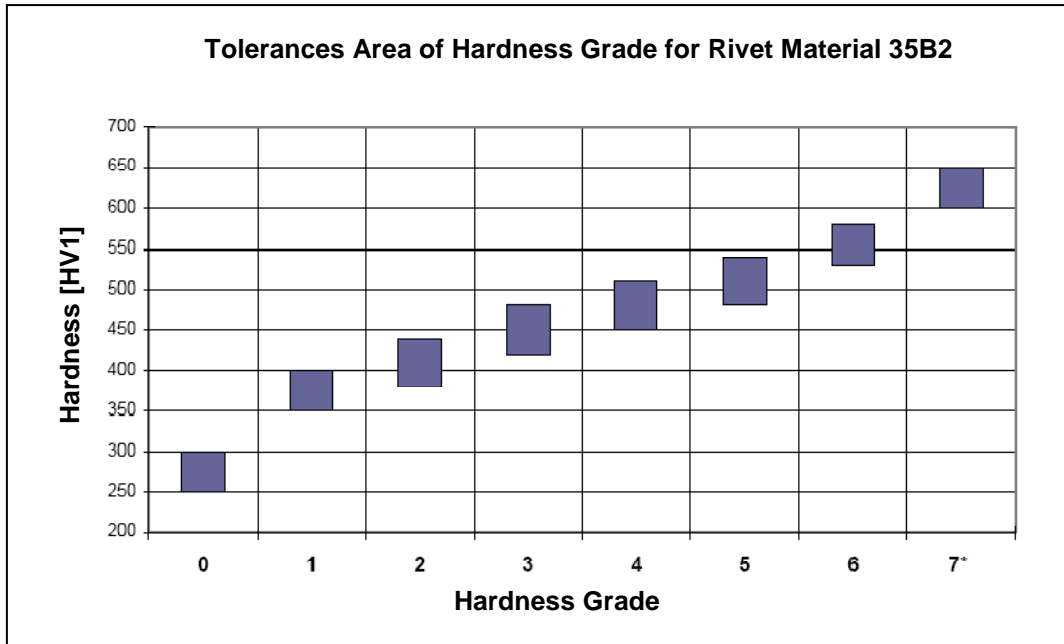


Fig. 16 Hardness grade for rivets, material 35B2 / Source: Böllhoff GmbH

## 4.5 Self-Piercing Rivet Die

One of the most important elements of the self-pierce riveting is the die. It's not only the counter holder. The die helps for the spreading of the rivet and so for the creation of the interlock. It allows also the sheet material to flow and build this way a button.

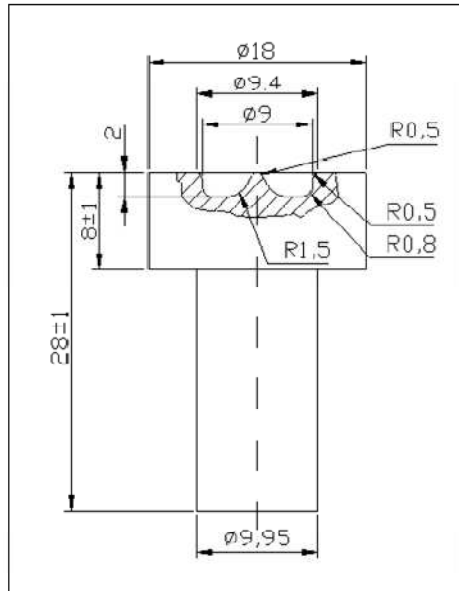


Fig. 17 Die with a tip for mild bonding sheet

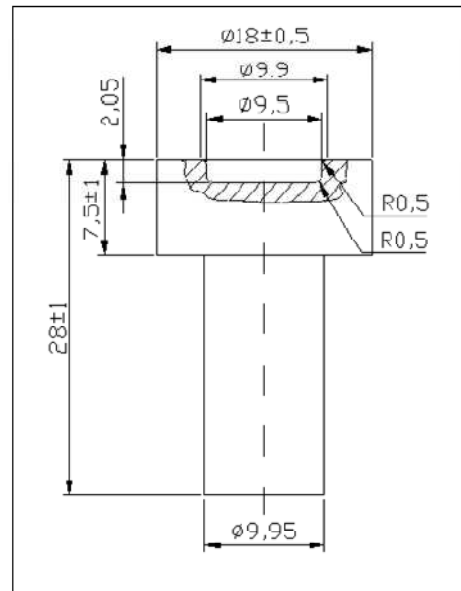


Fig. 18 Flat die for high strength bonding sheet

Dies with a tip are used for ductile bonding materials like aluminium or mild sheet steel to help for the spreading of the rivet. For high-strength steel, it is better suited to use flat dies because of the difficulty for the sheet to flow and so the risk of cracks [02]. The geometry of the die depends not only on the bonding materials but also on the geometry of the rivet. Some rivets because of their shape, need to be helped during the spreading phase and therefore, a die with a tip will be used.



Fig. 19 Different dies for SPR developed at the FH Soest

## 5. High-Strength Sheet Steel

New ultra high-strength steels (UHSS) for automobile industry have been developed. These UHSS have a better ratio of tensile strength under elongation than the conventional steels (fig. 20). The high strength allows constructing with thinner elements and sparing weight this way. The excellent elongation's rate suits well for pieces designed to absorb the energy due to a crash.

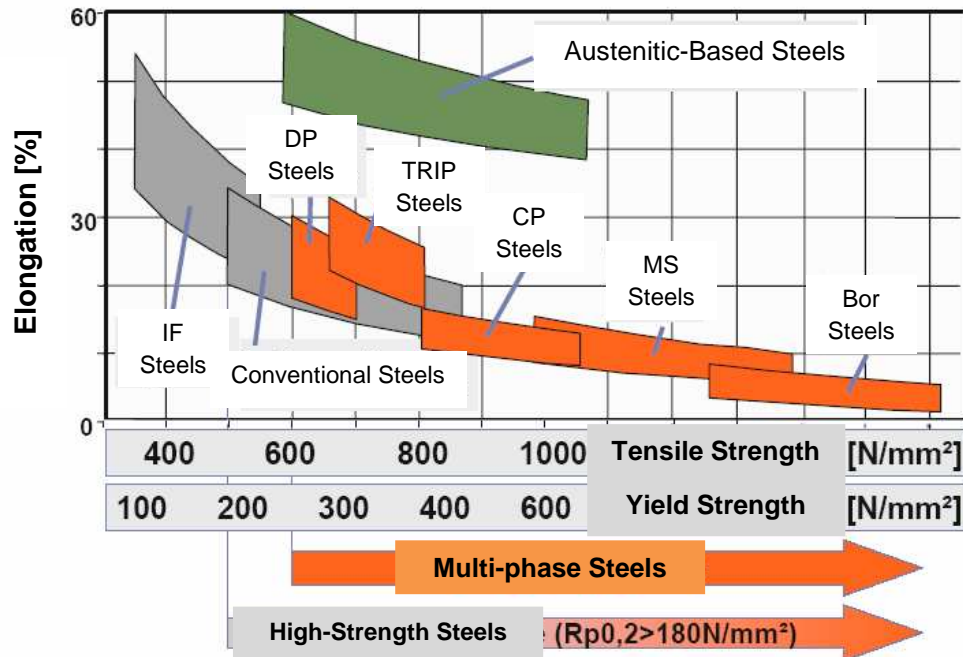


Fig. 20 Tensile strength vs. elongation of different steels

### 5.1 Multi-Phase Steels

Multi-phase steels have a softer ground matrix structure containing islands of stronger phases. There are many different kinds of multi-phase steels. For this study, two types have been tested.

#### 5.1.1 DP-K 34/60

It is a dual-phase steel that has a ferrite and martensitic microstructure. This steel has a high strength and a good deformation's rate. It is used for lightweight constructions and has a bake-hardening potential of approx. 30 N/mm<sup>2</sup>. This steel 34/60 has a maximum tensile strength of 600 to 700 MPa for yield strength of minimum 340 MPa.

### 5.1.2 CP-W 800

In this high strength steel, the structure contains more martensite than the DP-K 34/60. The very high tensile strength of this steel makes it interesting for crash relevant elements. The maximum yield strength is around 700 MPa and the tensile strength reaches 900 MPa.

## 5.2 Austenitic-Based Steels

Stainless steel is used for several years in the body making. Their high capacity of energy absorption makes them especially interesting for crash relevant pieces. The development in the last years increased the tensile strength of these austenitic-based steels.

### 5.2.1 H400

It is an austenitic chromium-nickel steel with a high tensile strength and a very high elongation's rate of approx. 45%. The maximum yield strength is between 400 and 450 MPa and the tensile strength goes up to 750 to 800 MPa. Because of the instable austenitic structure, the H400 gets easily hardened if it is cold worked, which makes it useful for absorbing crash energy.

## 5.3 Mechanical Properties of the High-Strength Steels

Material	Thickness [mm]	Coating	Rp <sub>0.2</sub> [N/mm <sup>2</sup> ]	Rm [N/mm <sup>2</sup> ]	Ag [%]	A <sub>80</sub> [%]
DP-K 34/60	1,50	Z 140	351	619	16,4	28,5
CP-W 800	1,50	Z 140	679	930	N.D. *	14,1
H400	1,50	-	434	782	43,1	53,5

Fig. 21 Mechanical properties of the high-strength steels

\*N.D. = No Data

## 5.4 Chemical Composition of the High-Strength Steels

Material	C	Si	Mn	P	S	Al	N	Cu	Cr	Ni	V	Mo	Ti	Nb	B
<b>DP-K 34/60</b>	0.14	0.50	2.00	0.04	0.01	1.50	N.D.*	0.50	N.D.*	N.D.*	N.D.*	0.50	0.15	0.15	0.005
<b>CP- W 800</b>	0.111	0.610	1.75	0.013	0.001	0.033	0.0035	0.029	0.300	0.035	0.012	0.005	0.094	0.005	0.0003
<b>H400</b>	0.039	0.36	6.71	0.03	0.004	N.D.*	0.152	N.D.*	18.06	3.69	N.D.*	0.19	N.D.*	N.D.*	N.D.*

Fig. 22 Chemical composition of the high-strength steels in mass percentage

\*N.D. = No Data

## 6. G Rivet Prototype

**Confidential**

# 7. Experimental Test Set-Up and Procedure

## 7.1 Tested Rivets

For this study, 3 different types of rivets have been tested.

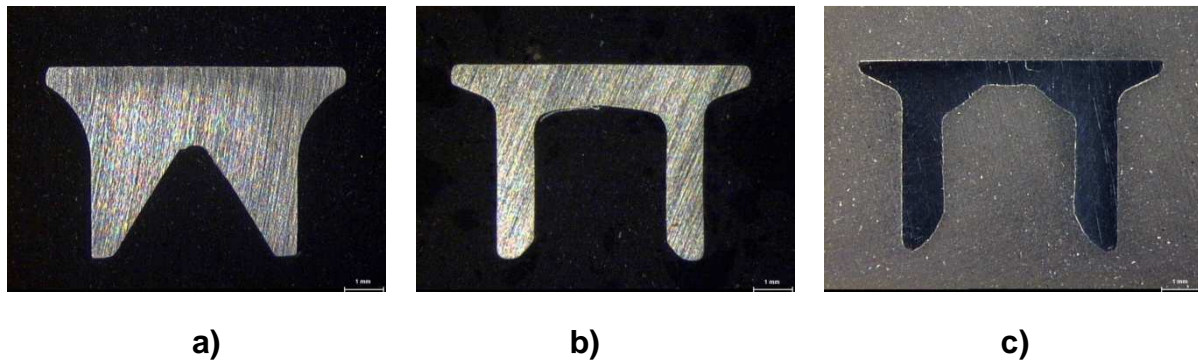


Fig. 25 Sections of self-piercing rivets: a) HF rivet b) HD2 rivet c) G rivet

The HF rivet is produced by *Ribbe GmbH* and was conceived for aluminium bonding. The HD2 rivet from *Böllhoff GmbH* is more recent and is designed for aluminium-steel joining. Finally the G rivet is a prototype developed by Dr. S. Singh for high-strength bonding.

All these rivets are 5 mm long and have a rivet diameter of approx. 5.3 mm.

The chemical composition of the rivet HD2 and HF used in this study is as shown in the figure below (fig. 26). For the G rivet, the chemical composition could not be determinate.

Material	C	Si	Mn	B	P	S	Cr	Mo	Ni	N
<b>35B2</b>	0.32 – 0.40	<0.40	0.50 – 0.80	0.001 – 0.005	<0.035	<0.035	N.D.*	N.D.*	N.D.*	N.D.*

Fig. 26 Rivet chemical composition in mass percentage

\*N.D. = No Data

HF and HD2 rivets have a mechanical coating called *Almac®*. It is a metal coating composed of zinc, tin and aluminium. This is a protection against corrosion.

## 7.2 Tested Die for the Riveting

Two different die have been used for this work. A flat die for all the different combinations of sheets for HD2 and G rivets. A second die with a tip was needed for HF rivets. There is just a small difference between the two dies, which makes the die parameter almost insignificant for the comparison of the rivets. The biggest difference is a small tip that is necessary for helping HF rivets to spread efficiently.

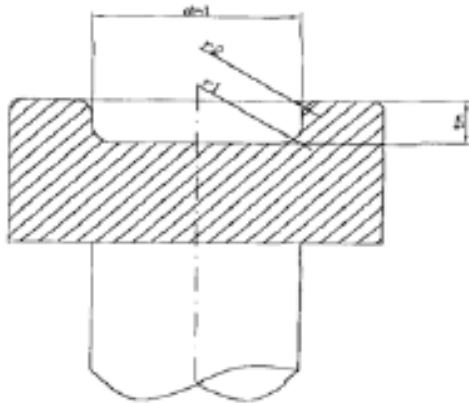


Fig. 27 Flat die G30 for the rivets HD2 and G

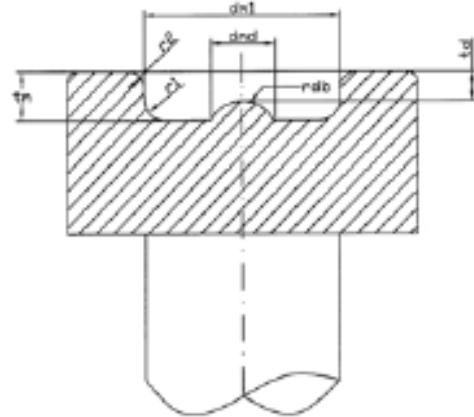


Fig. 28 Die with a tip for the rivet HF

Die	Type [mm]	dm1 [mm]	tm [mm]	r1 [mm]	r2 [mm]	td [mm]	rdb [mm]	dmd [mm]
<b>G30</b>	flat	8.8	2.0	1.2	0.8	-	-	-
<b>F61801</b>	tip	8.5	1.8	1.0	0.5	1.5	10.0	5.0

Fig. 29 Dimensions of the used dies G30 and F61801

## 7.3 Riveting

To study the influence of the geometry of self-piercing rivets (SPR) on high-strength sheet steel, it is necessary to prepare samples of riveted sheets and then to test them.

### 7.3.1 Rivet Joint Sections

The first measures are taken on unused rivets, in order to see the geometry differences between the rivets HD2, HF and G. Another aspect is to control the dimensional stability for these rivets.

To get the samples with a section in the exact middle, the following procedure was used:

- a) Measure the rivet diameter  $D_s$  of the chosen rivet (fig. 30.a)
- b) Cut this rivet near, but not in, the center (fig. 30.b) in the diameter length (with a cooling system)
- c) Measure the left thickness
- d) Embed the rivet with an Epoxy with mineral filler (*Durofast* in this work)  
Embedding steps: 20°C to 180°C in 4 min  
180°C to 190°C in 4 min and then at  
190°C during 13 min  
190°C to 20°C in 23 min
- e) Measure the height of the embedded rivet (fig. 30.c)
- f) Polishing the embedded rivet until the exact middle of the rivet  
Polishing steps: P120, P400, P2500 and finally P4000
- g) Corrode the rivet section with nitric acid  $\text{HNO}_3$  3% during approx. 10 sec
- h) Watch the sample on the stereomicroscope

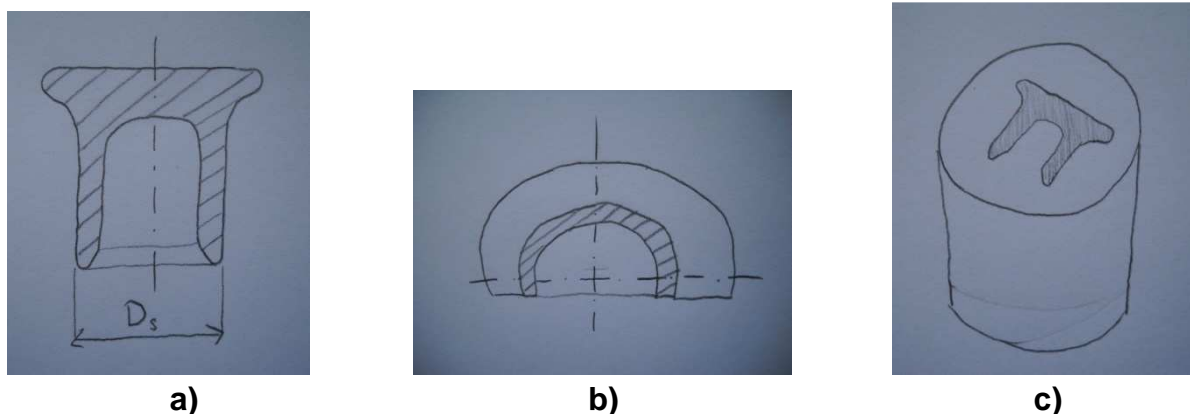


Fig. 30 Steps to get a section in the middle of the rivet

	<b>Embedding Machine</b>	
	<b>Model</b>	ATM
	<b>Version</b>	Opal 400

Fig. 31 Embedding machine for the rivet samples

The stereomicroscope is connected with a computer. The software from *Dietermann & Heuser Solution* permits to draw dimensions with the right scale (fig. 32).

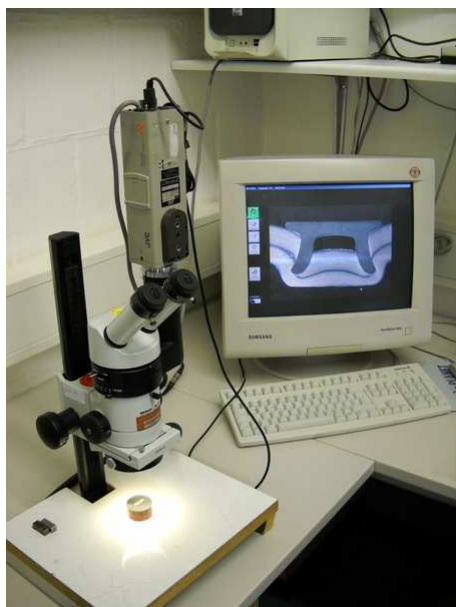
	<b>Stereomicroscope</b>	
	<b>Model</b>	Leica Microsystems
	<b>Version</b>	WILD M3Z
	<b>Enlarging</b>	6.5x – 40x
	<b>Camera</b>	JVC TK-1281
	<b>Software</b>	<i>Dietermann&amp;Heuser Solution</i>

Fig. 32 Stereomicroscope with the acquisition screen

A critical point to control is the rivet symmetry. For a good rivet joining it is necessary to have a good dimensional stability. This is also important for the repeatability of the process that has to be high, because the process must be automatable for the industry. The dimensions measured on a rivet depend on the type of the rivet, but it is always made to show if the symmetry is respected. For the HD2 and the HF rivet, the same measures have been done on 3 rivets.

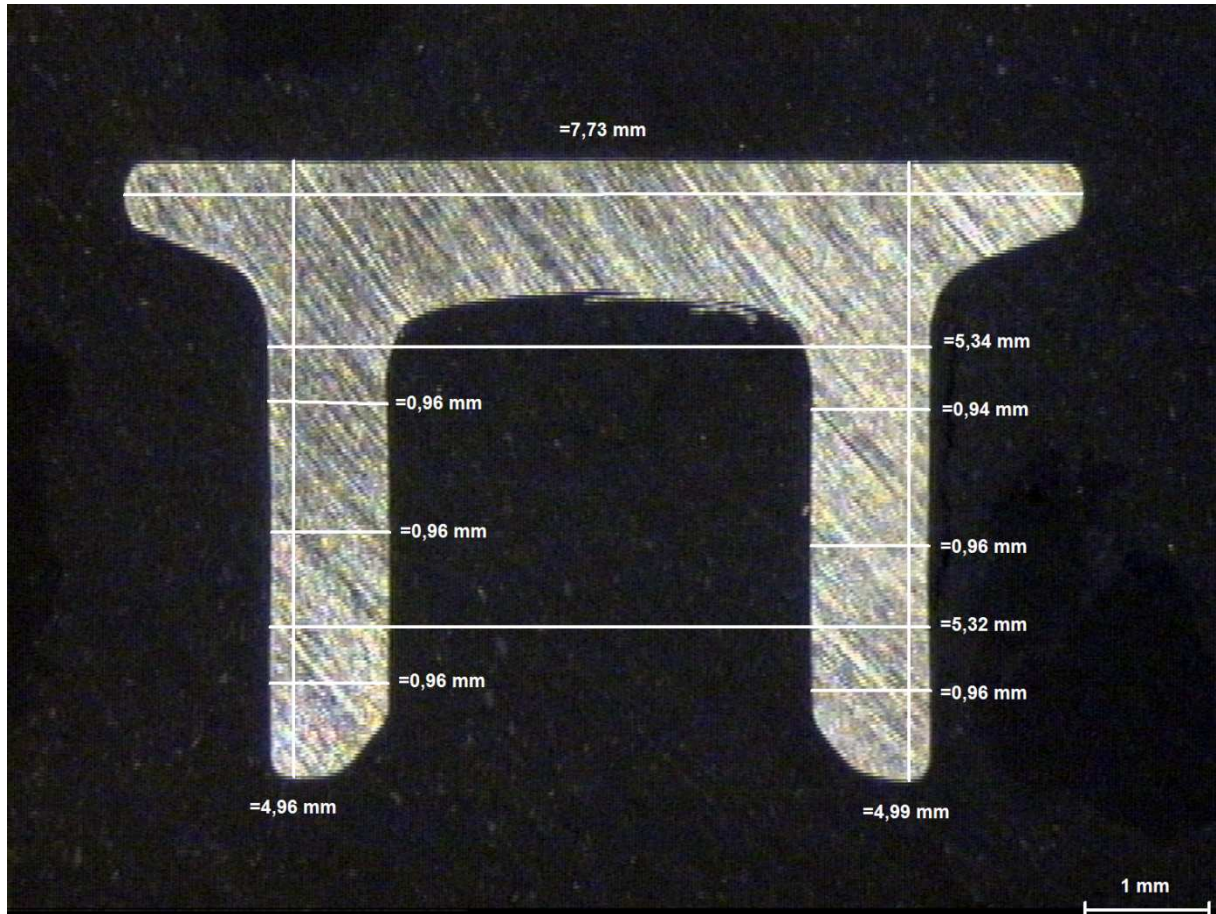


Fig. 33 Section in the middle of an embedded HD2 rivet with measure obtained with the stereomicroscope

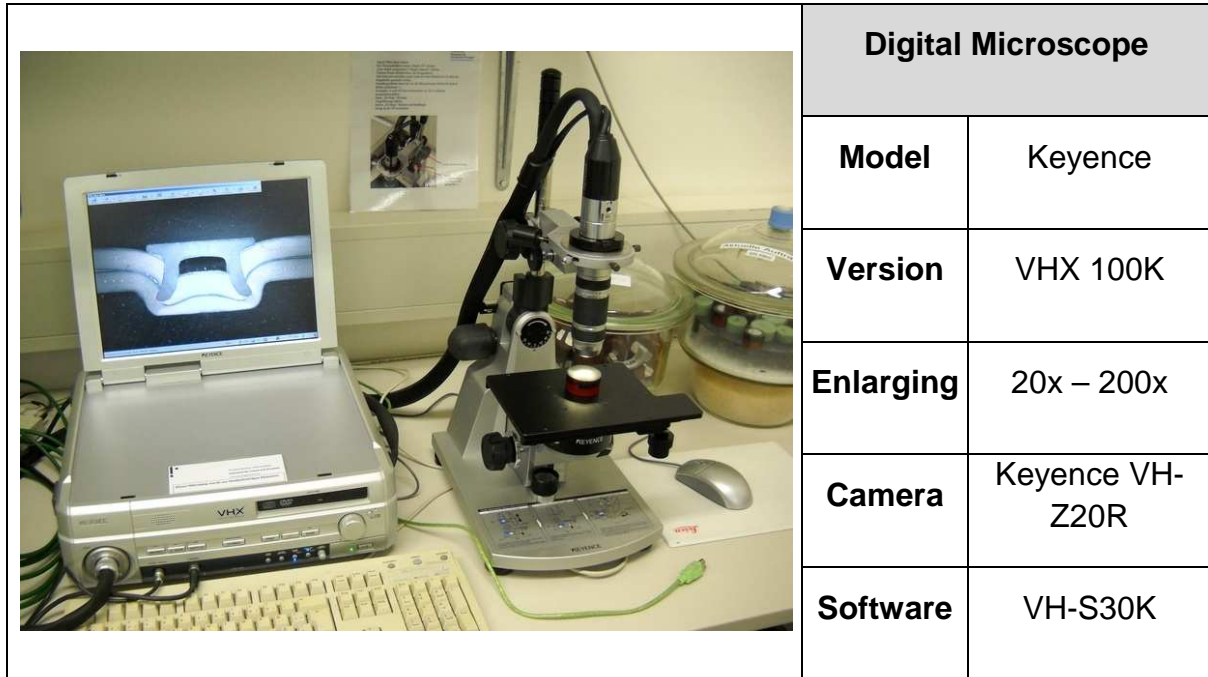


Fig. 34 Digital microscope with the data manager

Another tool allows measuring the complexity of the rivet foot geometry, the digital microscope (fig. 34). It is possible to enlarge 200 times and to draw circles that indicate the size of the radius. This can give the foot dimensions, by making the circles tangential to the curves of the foot geometry.

The digital microscope has been used for details enlargements and for comparison of foot geometry of the 3 samples of each HD2 and HF rivets.

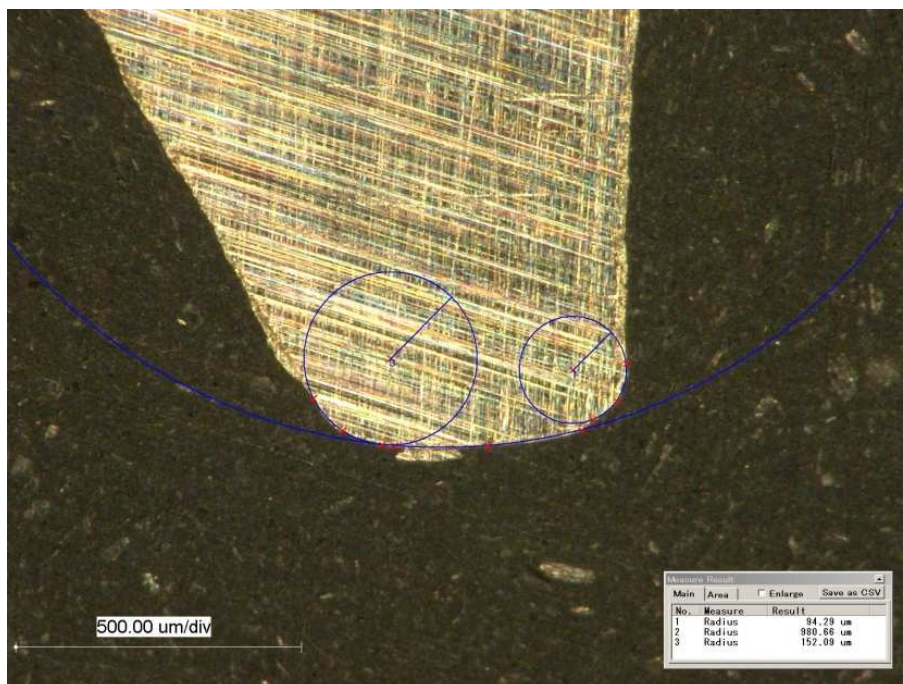


Fig. 35 Right foot of a HF rivet measured with a digital microscope

### 7.3.2 Self-Pierce Riveting Machine

For this work, high-strength steels are riveted which requires high forces to set the rivets. The self-pierce riveting machine used is a laboratory machine instead of an industrial one, because the laboratory machine can reach higher punch forces.

	Self-Pierce Riveting Machine	
	<b>Drive</b>	hydraulic
	<b>Working pressure</b>	max. 220 bar
	<b>Punch force</b>	max. 100 kN
	<b>Clamping force</b>	max. 100 kN
	<b>Punch speed</b>	max. 60 mm/s
	<b>Process program</b>	<i>BiForce 40</i>

Fig. 36 The laboratory machine for self-pierce riveting used in this work

This machine is composed of two separated hydraulic cylinders. One controls the clamping force and the other the punching force. The maximum force for both is 100 kN. The command of the machine is done with an SPS, which allows choosing the punching and the clamping force. There is also a Linear Variable Differential Transformer (LVDT) that measures the displacement of the rivet and a pressure sensor that measures the pressure used to set the rivet.

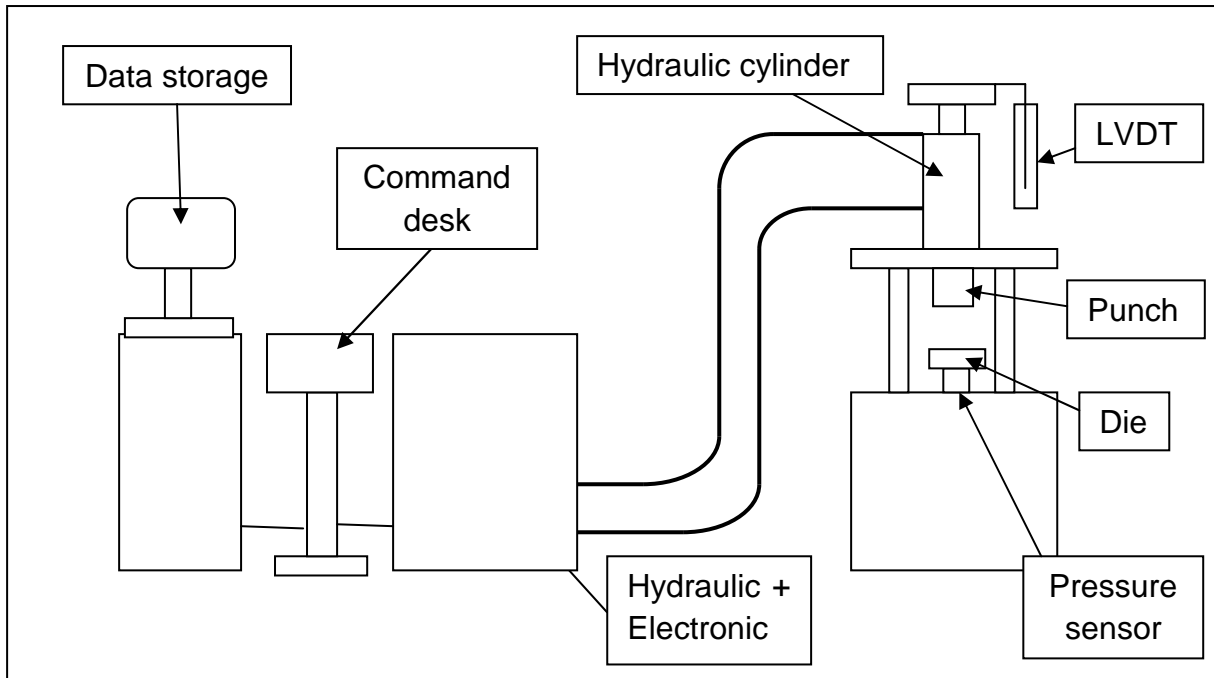


Fig. 37 Schematic plan of the laboratory self-pierce riveting machine

The information is collected with a computer, which finally delivers a Force vs. Displacement graphic (fig. 38). With this kind of figures, it is possible to see the influence of the geometry of the rivet on the different steps of the riveting (cutting, spreading and swelling).

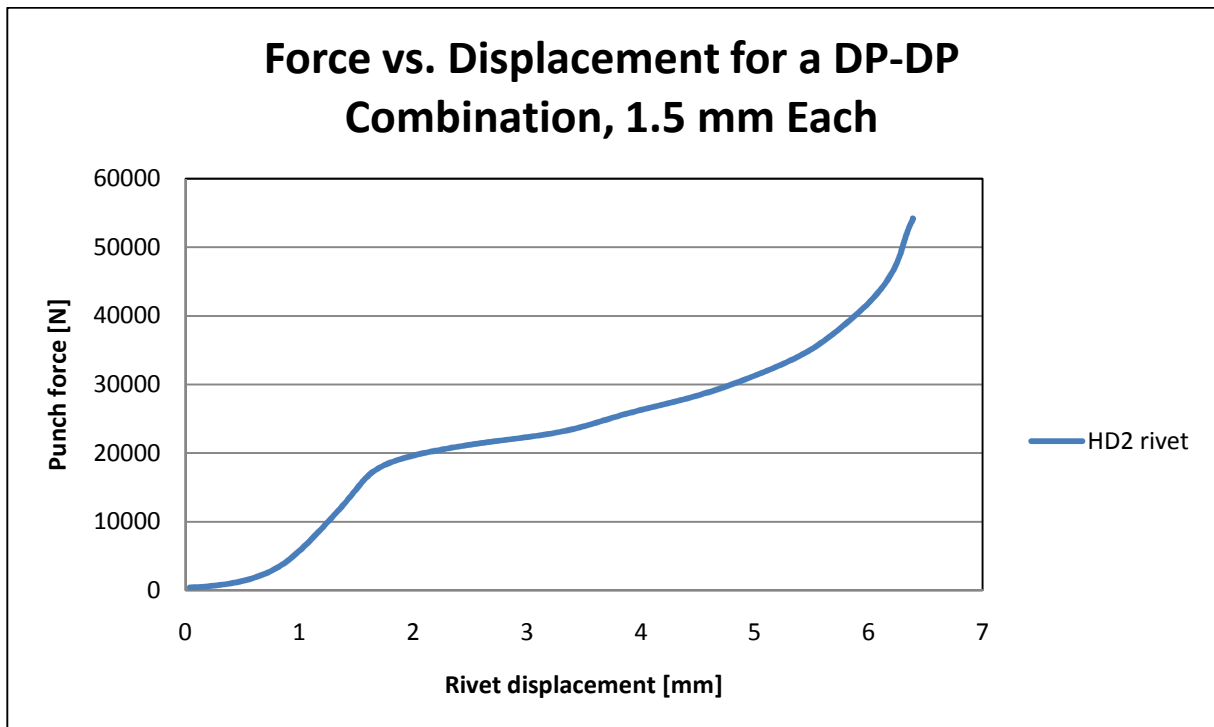


Fig. 38 Force vs. Displacement graphic for a HD2 rivet

The setting of the punching force and clamping force depends on the material combination, the die type, the rivet type and its hardness. Several tests are needed to find the optimum, which is the minimum force necessary to have a good joint with the smallest free space between the head of the rivet and the punch side sheet.



**Fig. 39** Section of a HD2 rivet binding with DP-H400 combination

The samples (fig. 39) are obtained as explained below:

- a) The two sheets steel are cut 50 mm long and 38 mm wide
- b) They are layered and a rivet is punched in the middle and 10 mm from the border
- c) The two joined sheets are turned 180° with still the same upper sheet and a second rivet is inserted like the first one
- d) One of the two rivet is cut in a way that a bit more than the half stays in the sheets, while the other rivet maintain the two sheets joined
- e) The cut rivet is polished until the centre of it with the following steps: 120P, 400P, 2500P and 4000P
- i) The rivet is corroded with nitric acid HNO<sub>3</sub> 3% during approx. 10 sec
- f) The section of the rivet can finally be watched with the stereomicroscope and the digital microscope

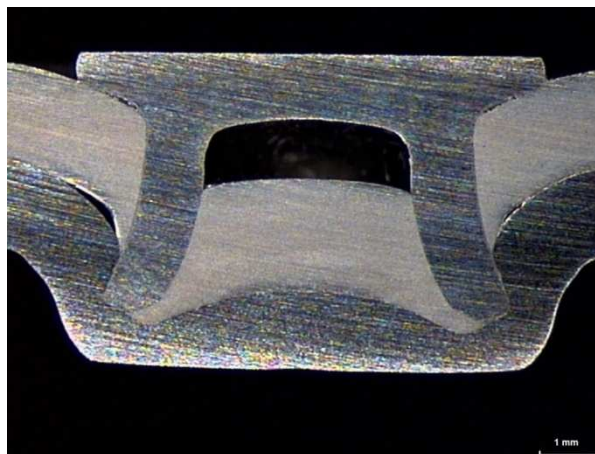


**Fig. 40** Example of a section of HD2 rivet with DP-H400 combination

All the possible sheet combinations between DP, CP and H400 have been tested except the combinations with CP and H400. This pair of sheets is too difficult to be joined with the tested rivets.

For one combination, the DP-DP, 3 samples for the HD2 and the HF rivet have been done. The outline of the rivet has been highlighted with the software CorelDrawX5 and then overlaid with the two other outlines. This allows to see how stable is the process of riveting.

## 7.4 Rivets Hardening

In some cases the rivet must be hardened to be able to join the high-strength sheets steel. The self-piercing rivets are available for a maximum hardness grade of H6, which means a hardness of 550HV  $\pm$ 25 HV. But for some sheet combinations, a hardness grade of H7 is required. This hardness grade represents 625HV  $\pm$ 25HV and to obtain this value, it is necessary to make a heat treatment on a softer rivet. The heat treatment parameters depend on the material composition of the rivet. For HF and HD2 rivets the treatment is, first a quenching and then a tempering:

- a) The oven for the quenching is preheated at 850°C (fig. 41)
- b) The number of needed rivets are put in a metallic basket that hangs on a magnetic lid, which closes the oven tube
- c) The oven pump evacuates partially the oxygen in the tube to minimize the corrosion
- d) The rivets are heated during 35 min
- e) A push on a button demagnetize the lid, which let the basket with the rivets fall and open in the same time the bottom trap of the oven tube
- f) The basket with the rivets falls in a container full of oil at room temperature

	Quenching Oven	
	<b>Model</b>	Thermal Technology
	<b>Version</b>	Termolab 1150
	<b>T° max.</b>	1150°C
	<b>Pump</b>	Alcatel, PASCAL 2005SD
	<b>Ultimate pressure</b>	$2 \times 10^{-3}$ mbar

Fig. 41 A tubular oven for quenching

After the quenching, the rivets have a tempering process to homogenize the hardness of the rivet structure:

- a) The tempering oven is preheated at 200°C
- b) The rivets at room temperature are put in the preheated oven
- c) The tempering lasts 40 min
- d) The rivets are taken out of the oven and let cooled down at room temperature

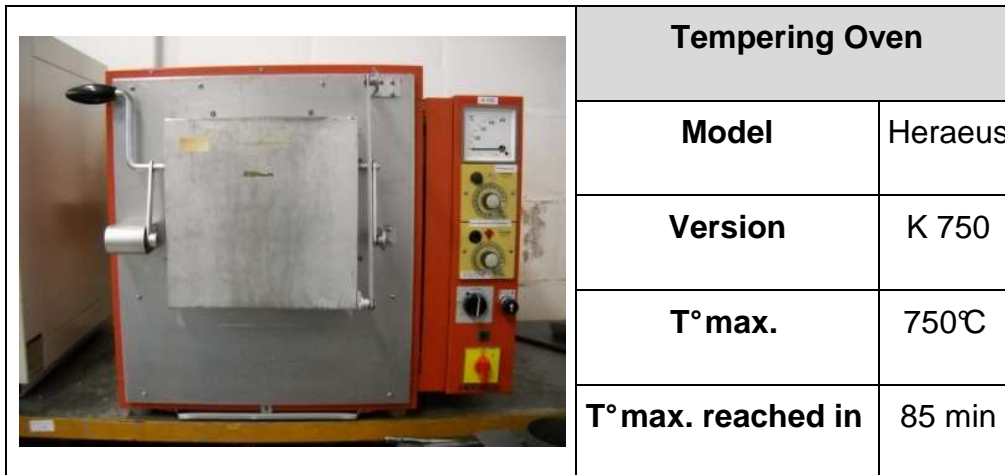


Fig. 42 A tempering oven

When the heat treatment is done, the rivets hardness is controlled with a micro hardness tester. The normal hardness test was made as explained below:

- a) 5 rivets have their head polished
- b) 3 measures are taken on each of the 5 rivets
- c) The arithmetic mean of the 3 measures for each rivet is calculated
- d) The final value is the arithmetic mean of the 5 means calculated previously

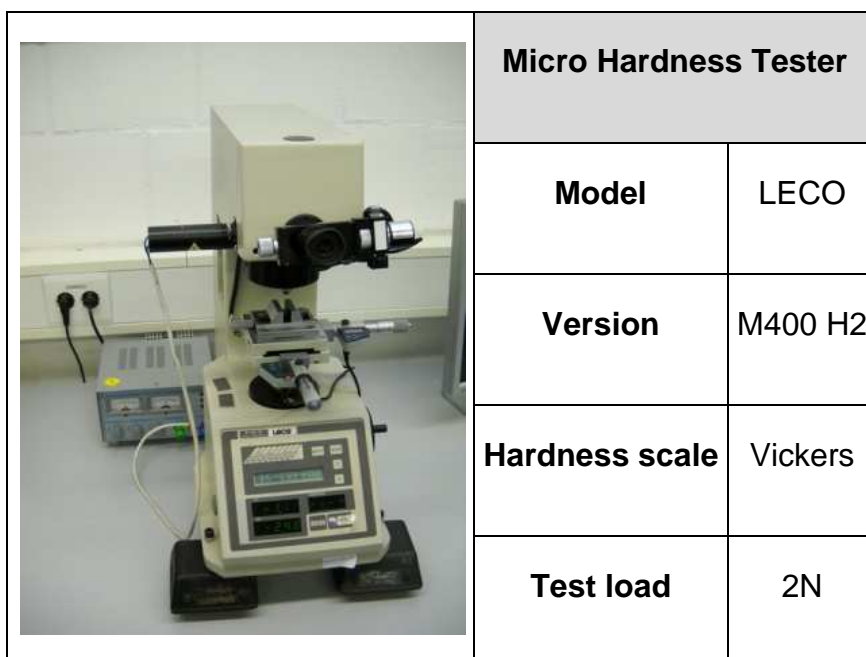
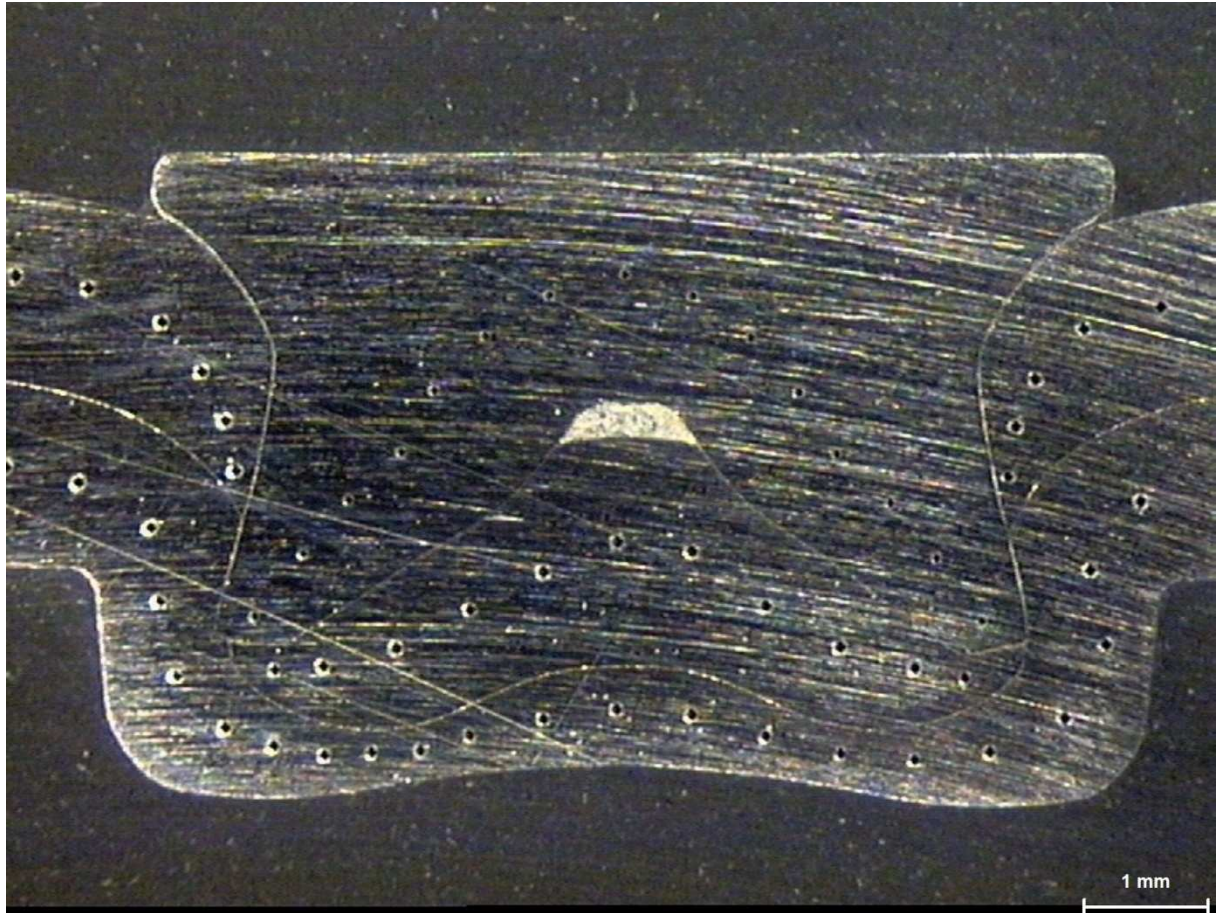


Fig. 43 Micro hardness tester

For every type of rivet, a deeper hardness test has been done. Instead of just measuring the hardness value on the head of the rivet, the measures have been taken on a section surface.

In the case of the HD2 and the HF rivet, the joined sheets have also been measured. This allows comparing which rivet geometry hardened the most the sheets, after the riveting process.



**Fig. 44** Hardness measures of a HF rivet joint of a DP-DP combination

The spacing between each measure point is approx. 0.5 mm.

## 7.5 Quasi-Static Shear Tests

A quasi-static shear test was done 3 times for each sheet combinations and this with the HF and the HD2 rivets. The tests were made with a tensile machine from Wolpert, version TUZ 300.

	Tensile Machine	
	<b>Model</b>	Wolpert
	<b>Version</b>	TUZ 300
	<b>Max. test force</b>	300 kN
	<b>Test speed</b>	10 mm/min
	<b>Cross stroke</b>	250 mm
	<b>Max. cross speed</b>	200 mm/min
	<b>Data logging</b>	Digital

Fig. 45 A Wolpert Tensile machine

The samples were clamped with a hydraulic system under a pressure of 200 bar.



Fig. 46 Hydraulic clamping system of a tensile machine

The samples were assembled and tested according to the norm ISO 14273. The sheets are overlapped for 16 mm and there is only one riveting joint.

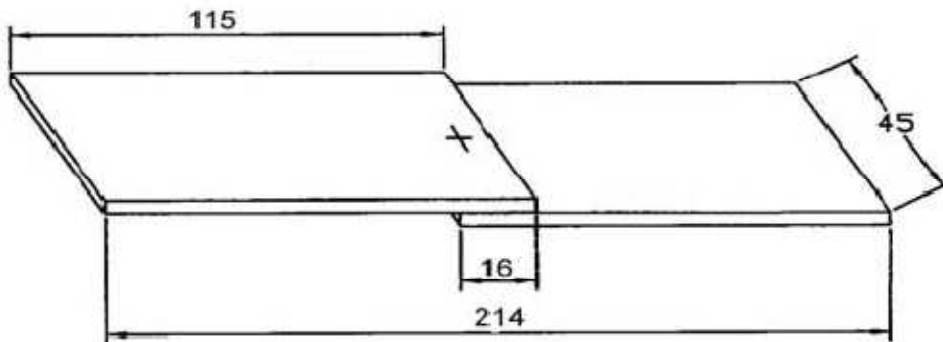


Fig. 47 Quasi-static shear test sample according to norm ISO 14273

During the test, the tensile machine measured the tensile force and the elongation. The results were treated with software named *Cadis* and a computer represented the data in a Force vs. Displacement graphic and showed the maximum force and the energy  $W_{30}$ .

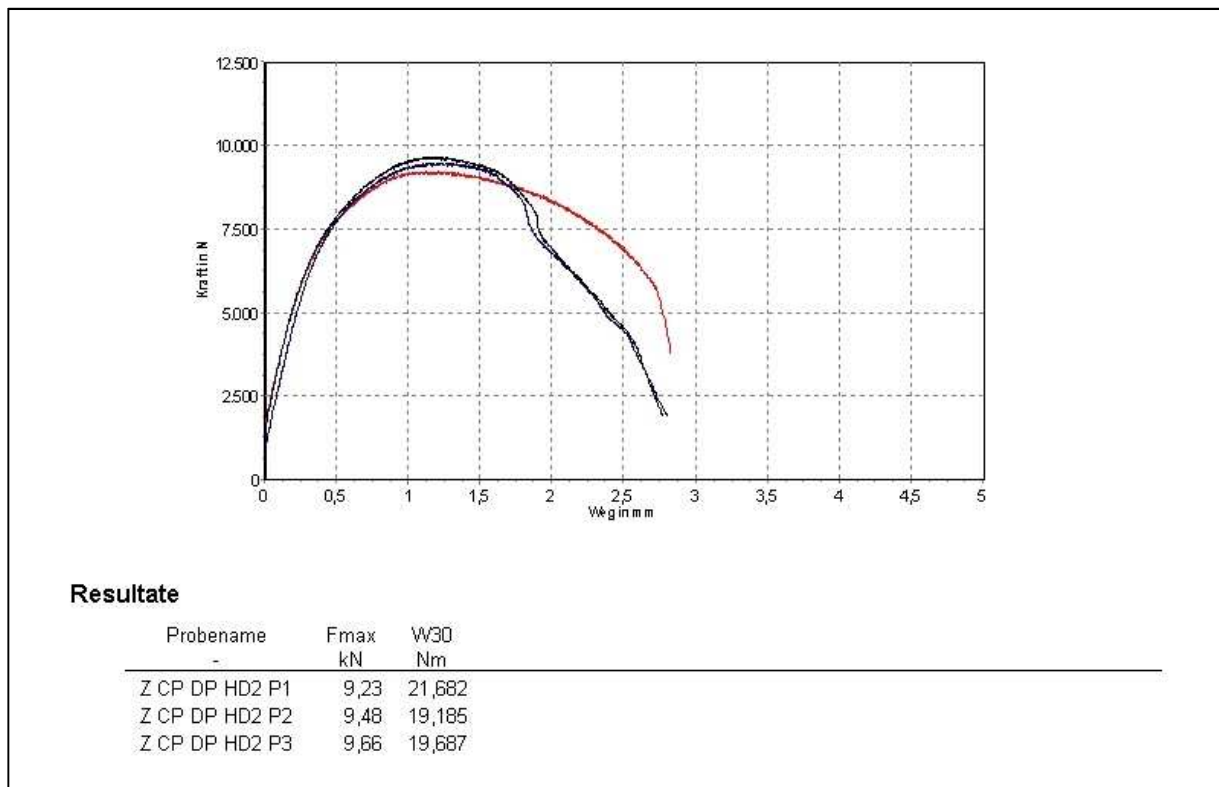


Fig. 48 Force vs. Displacement graphic of a quasi-static shear test with a CP-DP combination for a HD2

The  $W_{30}$  energy represents in fact the area from the tensile curve to the point  $0.3 \cdot F_{\max}$ . The entire area under the tensile curve is not considered, because of the too long sheet cracking phase that is not really bearing the load anymore.

## 7.6 Fatigue Tests

The samples for the fatigue test are almost the same than the ones for the quasi-static tests. The dimensions changes just a little bit and there is one more rivet.

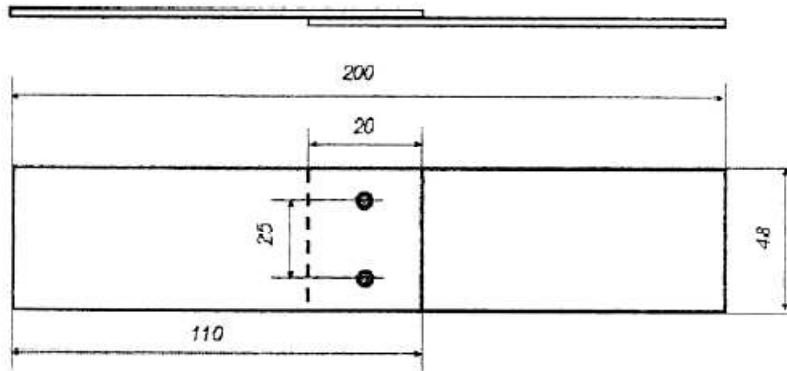


Fig. 49 Fatigue test sample dimensions

The samples are mounted and tested without breaks in the cycles. The minimum vs. maximum load ratio is the same for all the tests and is  $R = 0.1$ . This means that the samples are always under tension until the test ends, which interconnects and readjusts the fatigue frequency with the sample's rigidity.

	Resonant Testing Machine	
	<b>Model</b>	Russenberger Prüfmaschinen
	<b>Version</b>	AMSLER HFP 422
	<b>Max. static test force</b>	100 kN
	<b>Max. dynamic test force</b>	100 kN $\pm$ 50 kN
	<b>Test frequency</b>	-
	<b>Frequency measure precision</b>	0.01 Hz
	<b>Force measure precision</b>	0.5%
	<b>Software</b>	RUMUL TOPP

Fig. 50 A resonant testing machine from *Russenberger Prüfmaschinen*

The frequency is interconnected the rigidity, which is connected to the sample's degradation. Therefore, the frequency can be taken as a run-out condition for the fatigue tests.

A resonant testing machine from *Russenberger Prüfmaschinen* with the software *RUMUL TOPP* had been used. The only setting parameter is the force amplitude ( $F_a$ ), the frequency of the oscillations depends on the mounted sample. The resonant testing machine will try to keep the  $F_a$  as stable as possible.

The automatic ending conditions of the test can be selected. For this work all the samples have the two same ending conditions. First, as soon as the delta frequency is bigger than -20 Hz. After some pretesting, a negative difference of 20 Hz happens just before the fracture of the sample. If the test is not interrupted before the fracture, the two parts of the sample are violently clinking for a few cycles. The second ending condition is when the sample has endured  $2 \cdot 10^6$  cycles without breaking.



**Fig. 51 Hydraulic clamping system of a resonant testing machine**

The samples were clamped under a pressure of 200 bar. No guide system guaranteed a vertical positioning of the sample. The positioning was controlled with a measuring rod.

For the first test of the HF and the HD2 rivets, to have an idea for the order of magnitude of the  $F_a$ , a sample prepared like for the fatigue test (fig. 49) has been tested with the quasi-static tensile machine. To stay between  $10^3$  and  $10^7$  cycles, the  $F_a$  must be approx. the half of the measured yield strength.

For the following fatigue tests, a level of 0.5 kN had been added or subtracted. If the level of 0.5 kN were to big, a level of 0.2 or 0.3 kN was taken.

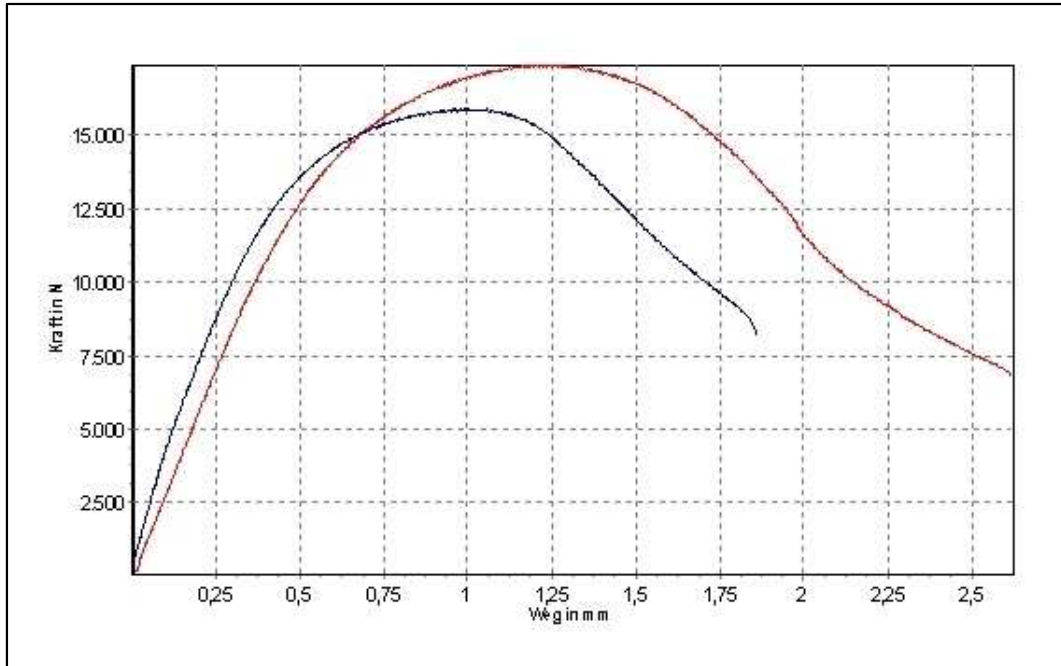


Fig. 52 Force vs. Displacement of a quasi-static test for a HD2 rivet with DP-DP combination

The resonant testing machine measures the frequency of the cycles, the number of cycles and the force amplitude. It is possible to build a Wöhler curve with the collected information (fig. 54).

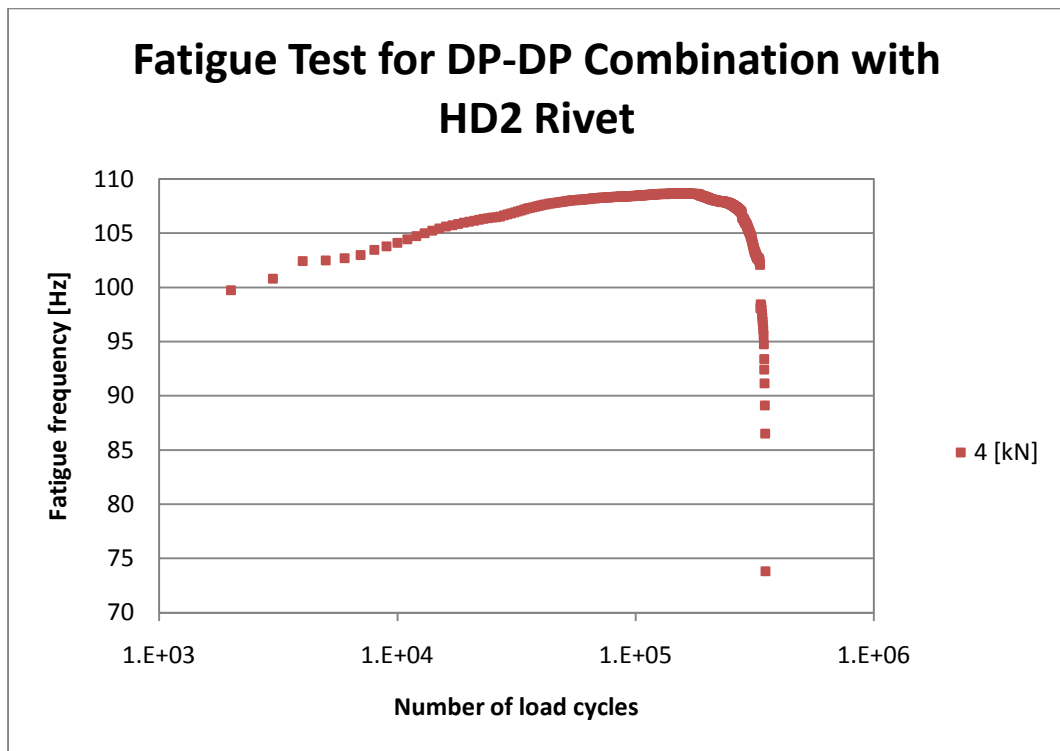


Fig. 53 Fatigue test for DP-DP combination with a HD2 rivet

In order to obtain a Wöhler curve, at least 6 samples of the same type but for different force amplitude are measured and this for different sheet combinations with HF rivets and HD2 rivets. The force amplitude are chosen so that the number of load cycles are between  $2 \cdot 10^3$  and  $2 \cdot 10^7$  cycles.

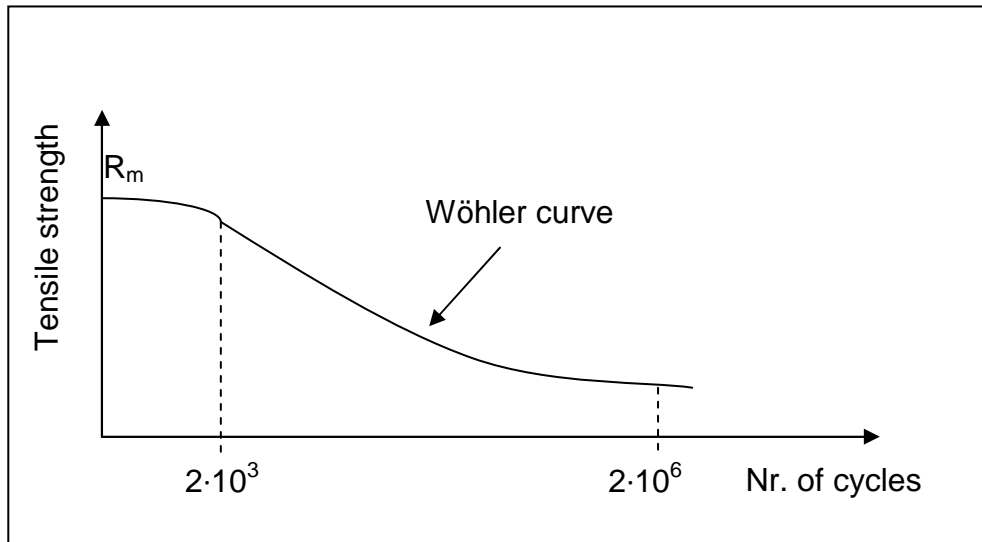


Fig. 54 Schematic representation of a Wöhler curve

## 8. Results and Discussions

*Because of the multitude of figures described in this chapter, they are incorporated in the appendices.*

### 8.1 G Rivet Prototype

Normally, the G rivet should be compared with the HF and the HD2 rivet. The quality of the received prototypes was not good enough to prepare samples and therefore, it was not possible to compare the G rivet with the other. The defaults of this rivet are detailed in this chapter.

#### 8.1.1 Cold Shaped Rivet

The first version of the G rivet prototype was shaped with an impact extrusion process. But the quality of this rivet was very bad.

First of all, the symmetry of the geometry is not respected. It is obvious, for example in fig. 55, that the geometry of the left foot is quite different from the right foot.



Fig. 55 Cold shaped G rivet

The head thickness is also really excessive. Besides, during the cold shaping process, interferences were created where the feet join the head. The enlargement of the left interference, in fig. 56, shows clearly how the material flow was during the shaping process. The process temperature was probably not high enough and there are maybe not sufficient steps in this cold shaping.

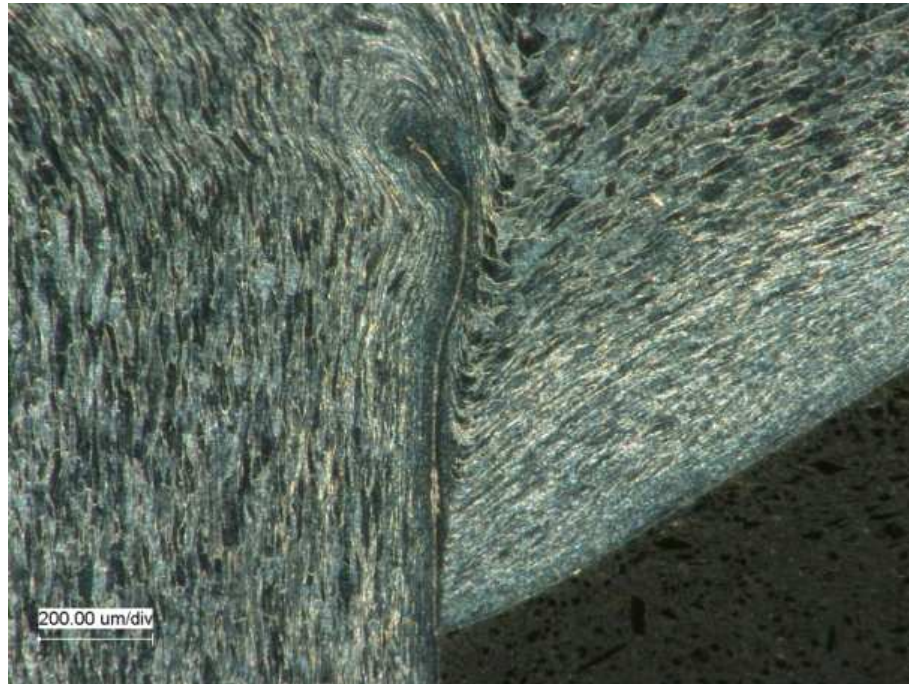


**Fig. 56** Left side interference enlargement on a cold shaped G rivet

As the quality of this rivet set is so poor, no further tests have been done on this set.

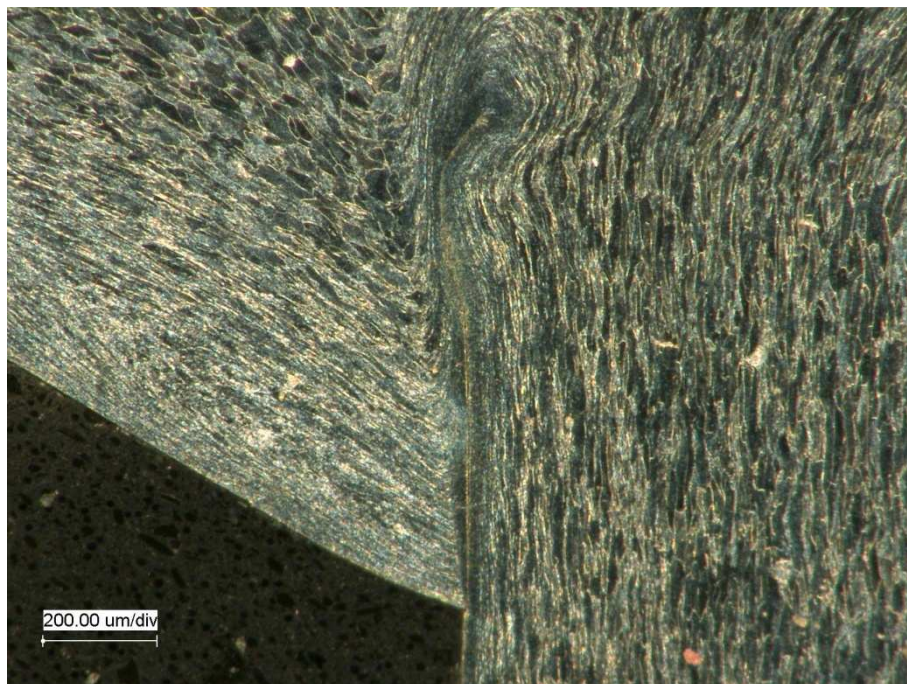


**Fig. 57** Right side interference enlargement on a cold shaped G rivet

### 8.1.2 Machined Rivet

The second set of G rivets is meant to be the same variation as the first set. The only difference between the two sets is that the rivets of this second one are machined and not cold shaped any more.

The geometry and the symmetry of this machined rivet are better, but the head thickness seems to be very thin this time.

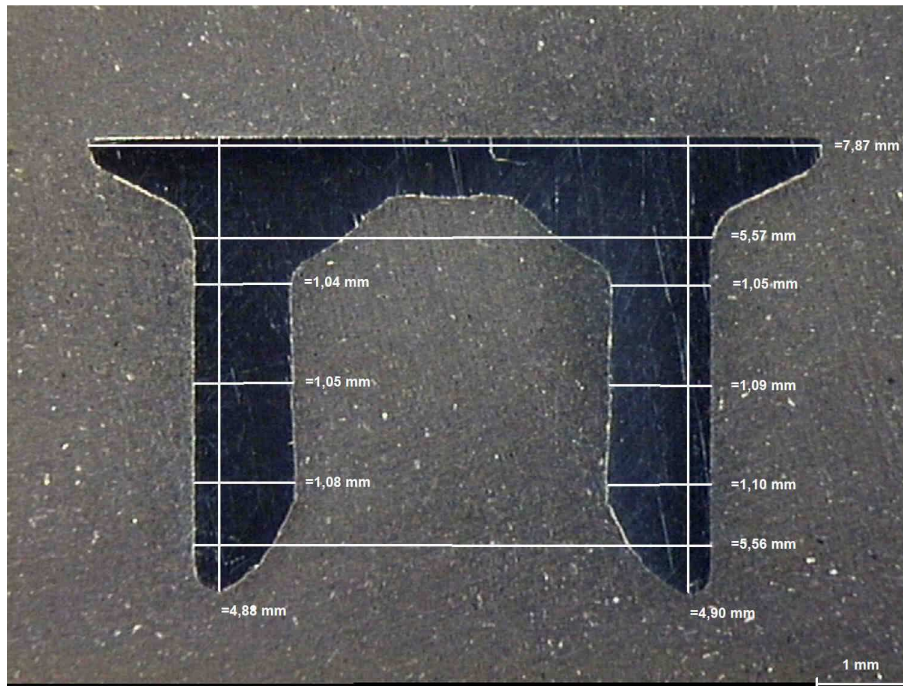


Fig. 58 Dimension stability of a machined G rivet

The first attempt to set one of these rivet in a DP-DP sheet combination was not successful. The rivet was much too soft even for the easiest combination to drill.

Next step was to try to harden the rivet. As it was not possible to know the chemical composition of these rivets, the right heat treatment was difficult to find.

The first heat treatment attempt was heating at 840°C during 40 min and quenched in Oil. The final mean hardness was 393 HV, which is not enough for high-strength steels.

The second try was the same procedure except that the heating temperature was at 880°C. The result was a bit better with 483 HV, but still not hard enough.

A third attempt was a heating at 880°C during 40 min and at the end water quench. The hardness shortly reached 400 HV, which is even worse than the second attempt.

Apparently, whatever the chemical composition is, it has a lack of carbon. This element is necessary for a heat treatment.

The fourth heat treatment was the same as the second, but with the rivets covered with coal during the heating. The result was about 30 HV better than the second attempt, the coal was a little bit absorbed and the hardness could finally be measured. But a hardness measure on a rivet section showed a large fluctuation, going from 400 HV to 620 HV. The softest parts were the external layers.

A tempering process was tried for the second heat treatment attempt. First, one with 200°C during 30 min and another try with 250°C during 40 min. The first reduced the hardness of 20 to 30 HV, second tempering lowered the hardness of 40 to 60 HV. But both tempering processes failed to homogenize a little the rivet hardness.

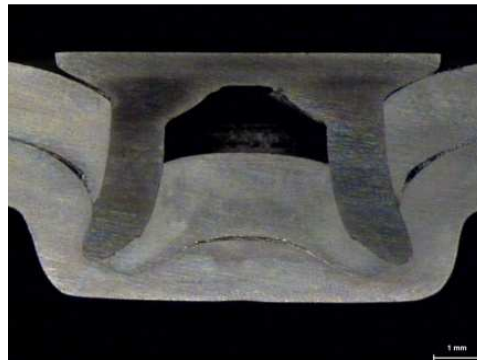


Fig. 59 A G rivet section of a DP-DP combination

Despite of the low hardness, a rivet setting was tested with the first tempered rivets (appendix 12.3). For the DP-DP, the free space between the two sheets and the upper sheet with the head are a sign of a bad joining. Besides, the space under the head is really too big, that weakens the joining. The feet are also too swelled in this DP-DP combination.

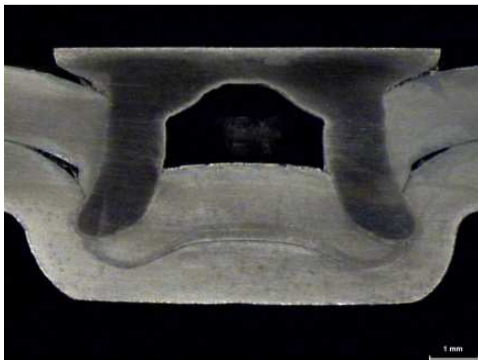


Fig. 60 A G rivet section of a CP-CP combination

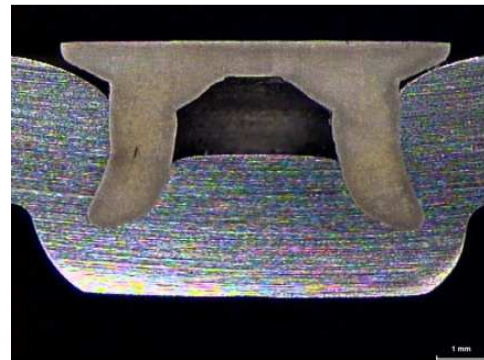


Fig. 61 A G rivet section of an H400-H400 combination

For the CP-CP sheets, the rivet is really too soft to make a bonding and it is even worse for the H400-H400 combination.

This actual version of G rivet is clearly behind the HF rivet and the HD2 rivet. But with the received quality it is impossible to deduct anything about the theoretical geometry of the G rivet.

## 8.2 HF vs. HD2 Comparison

### 8.2.1 Dimensional Stability

The self-pierce riveting is an industrial technology and therefore, it must be reproducible with an automated system. If the rivets have not a good symmetry, they will not have a good symmetrical cutting and spreading.

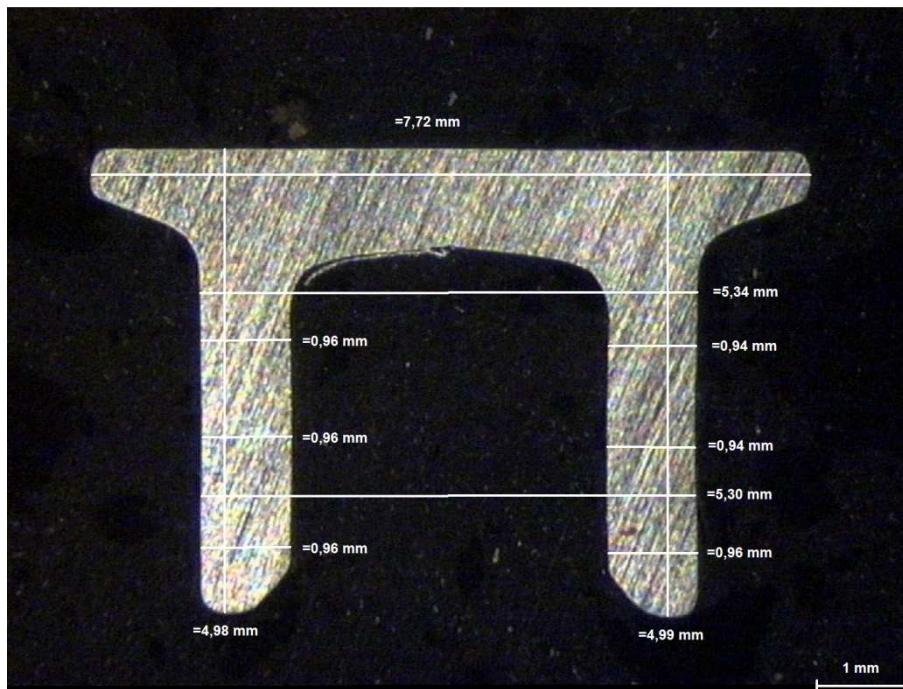


Fig. 62 Section in the middle of an embedded HD2 rivet with measure obtained with the stereomicroscope

The HD2 rivets have excellent dimension stability. Among 3 rivets, the biggest measured difference is of 0.04 mm for the symmetry in a same rivet and a difference of 0.05 mm between two rivets for a same dimension.

HD2 rivet nr.1 [mm]		HD2 rivet nr.2 [mm]		HD2 rivet nr.3 [mm]	
7.73		7.74		7.72	
5.34	5.32	5.35	5.34	5.34	5.30
4.98	4.99	4.99	5.02	4.98	4.99
0.96	0.94	0.94	0.96	0.96	0.94
0.96	0.96	0.93	0.96	0.96	0.94
0.96	0.96	0.94	0.96	0.96	0.96

Fig. 63 Main dimensions of embedded HD2 rivets, on each line, the same dimensions is considered

The HF rivet is a bit more difficult to measure than the HD2 because of the conical shank hole. The red line shows the symmetry axe of the rivet.

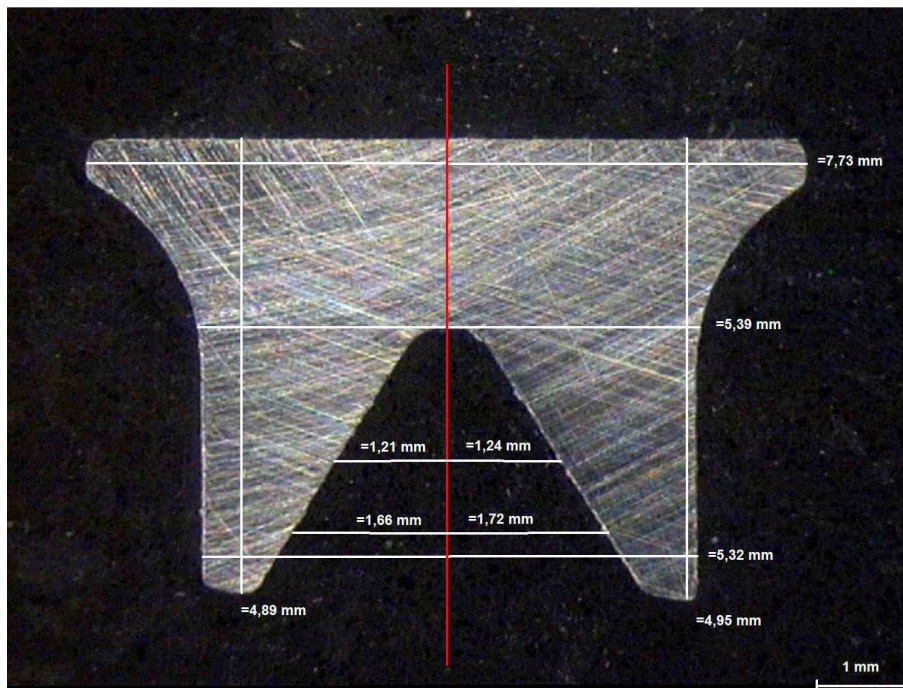


Fig. 64 Section in the middle of an embedded HF rivet with measure obtained with the stereomicroscope

The dimension stability of the HF rivet is very good. Among 3 rivets, the biggest measured difference is of 0.11 mm for the symmetry in a same rivet and a difference of 0.15 mm between two rivets for a same dimension.

HF rivet nr.1 [mm]		HF rivet nr.2 [mm]		HF rivet nr.3 [mm]	
7.73		7.88		7.73	
5.40	5.29	5.40	5.29	5.39	5.32
4.91	4.85	4.95	5.02	4.89	4.95
1.22	1.20	1.24	1.19	1.21	1.24
1.65	1.61	1.65	1.60	1.66	1.72

Fig. 65 Main dimensions of embedded HF rivets, on each line, the same dimensions is considered

The dimension differences are bigger for the HF rivet than for the HD2 rivet, but they are very small anyway.

The dimension measured on the foot geometry with the digital microscope gives precise values for the different radiuses. The problem with this technique is that the radius size can change a lot if the circle is more or less tangent to the rivet geometry (fig. 66 and 67). If you consider the radius of the inner part, it is 191  $\mu\text{m}$  for the left foot and 92  $\mu\text{m}$  for the right foot. Now if you compare the big radius, it is 925  $\mu\text{m}$  for the left and 2228  $\mu\text{m}$  for the right, but the real difference does not seems so big. Therefore, this method is not considered as totally reliable.

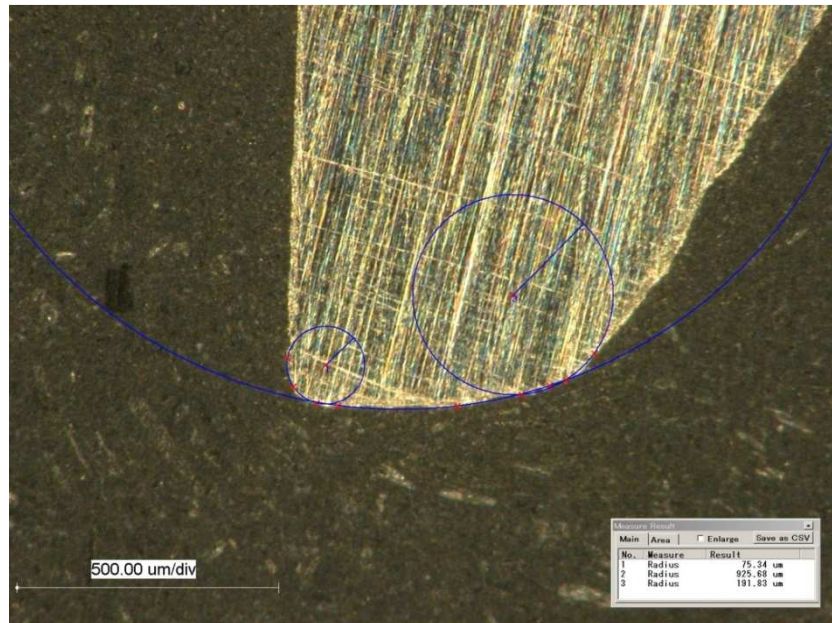


Fig. 66 Left foot geometry of HF rivet

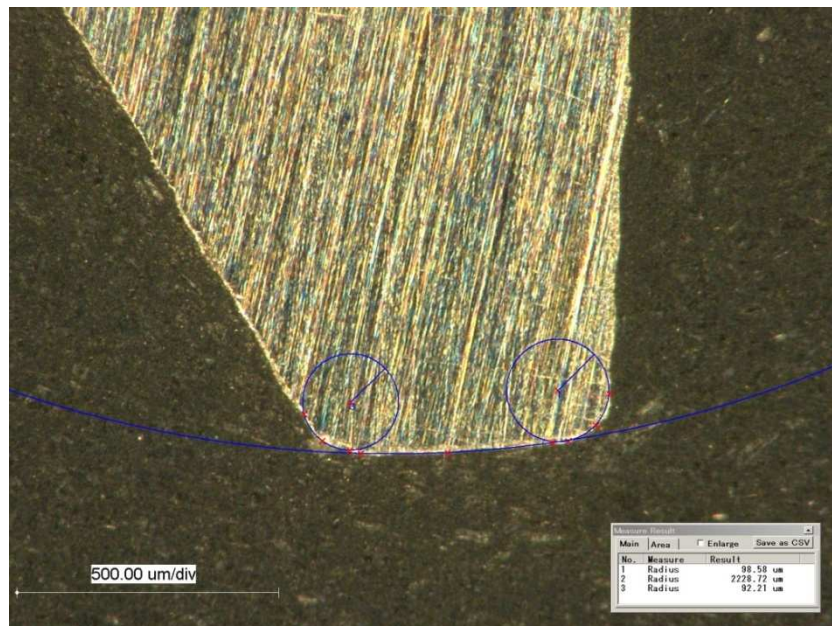


Fig. 67 Right foot geometry of HF rivet

Despite of that, the radiuses of the cold formed G rivet, of the HF rivet and of the HD2 rivet have, in most of the cases, a dimension difference smaller than 0.2 mm.

The stability of the setting process can be controlled on the figures below. The fig. 68 and fig. 70 were obtained by high lightening the rivet outline. The rivets come from three times a DP-DP combination.

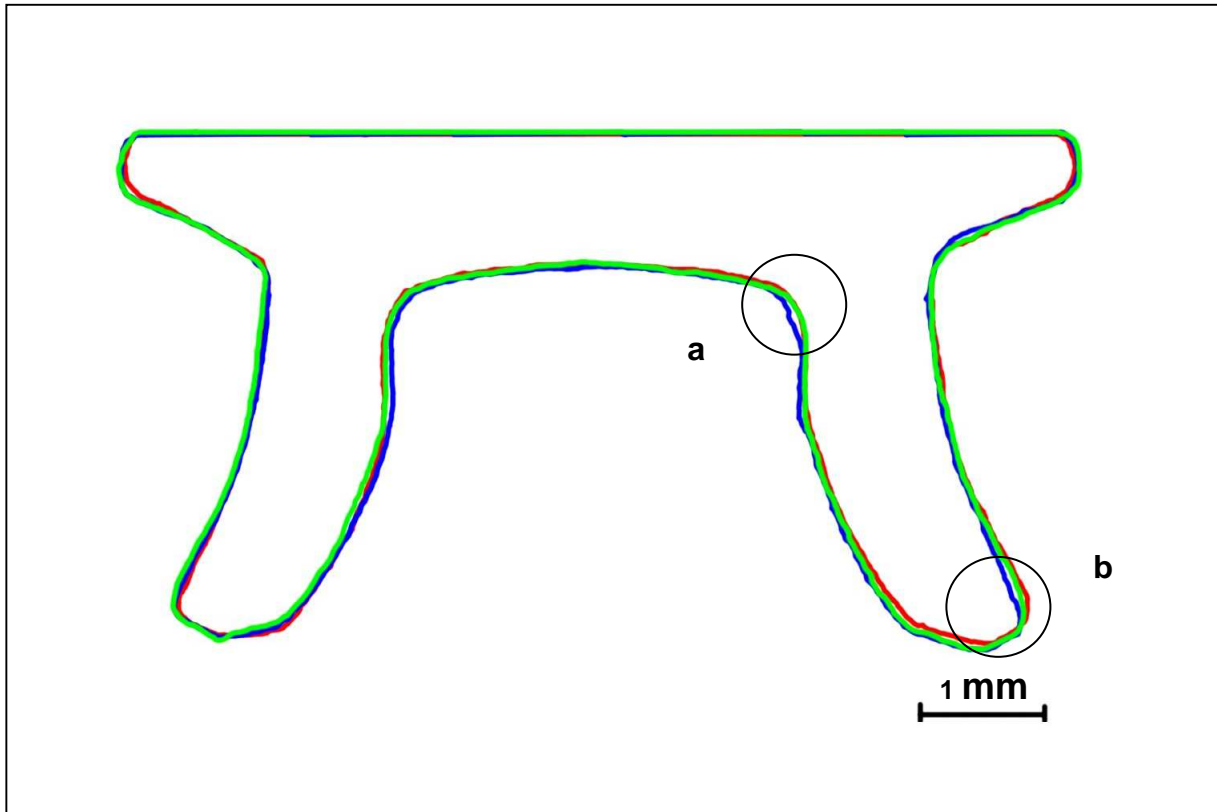


Fig. 68 Stacking of 3 HD2 joint sections with a DP-DP combination

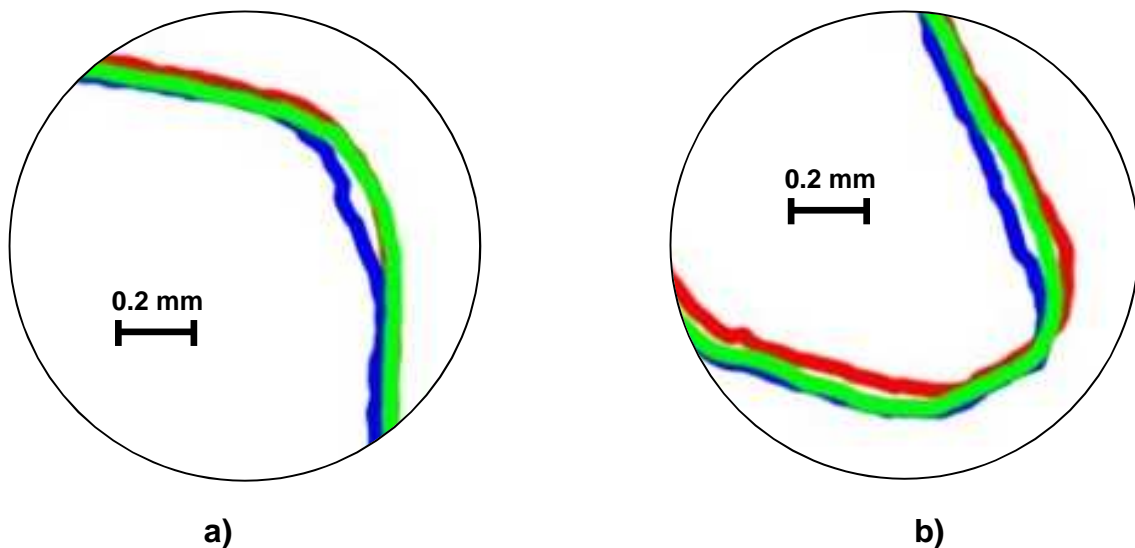


Fig. 69 Enlargement a) and b) of the stacking of 3 HD2 joint section with a DP-DP combination

The dimensional stability is excellent for the HD2 rivet. The biggest variation is smaller than 0.1 mm.

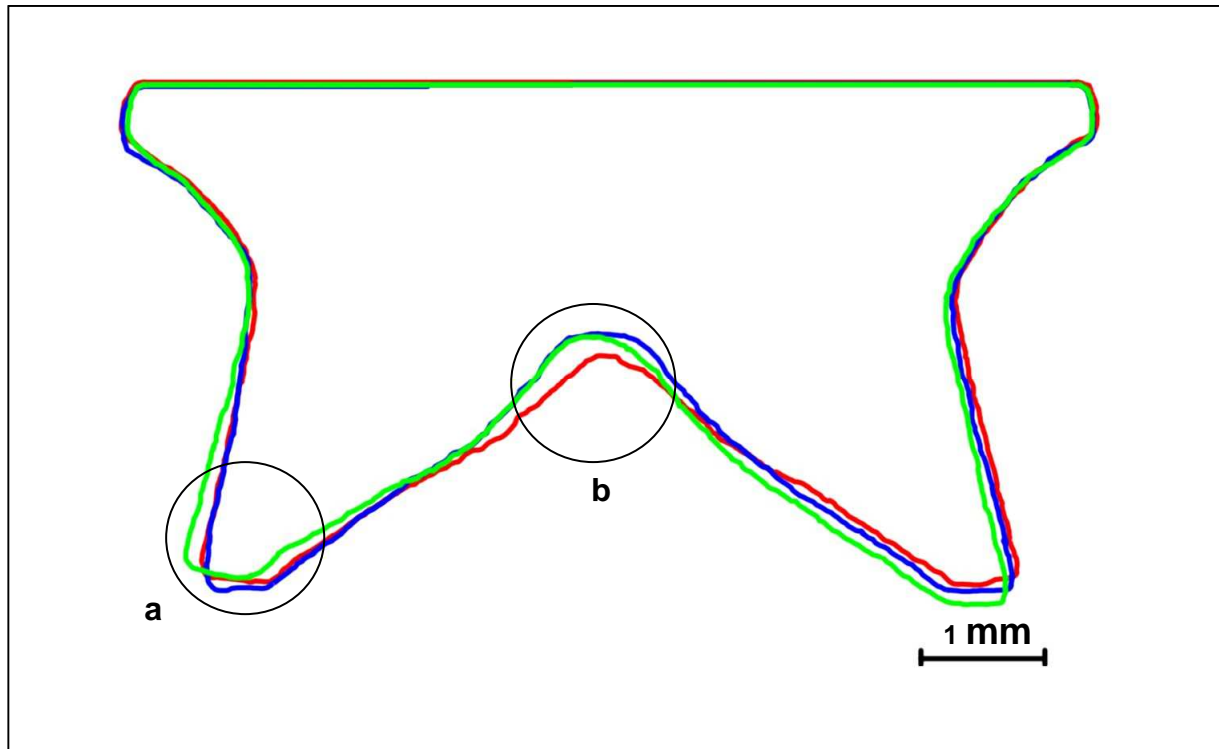


Fig. 70 Stacking of 3 HF joint sections with a DP-DP combination

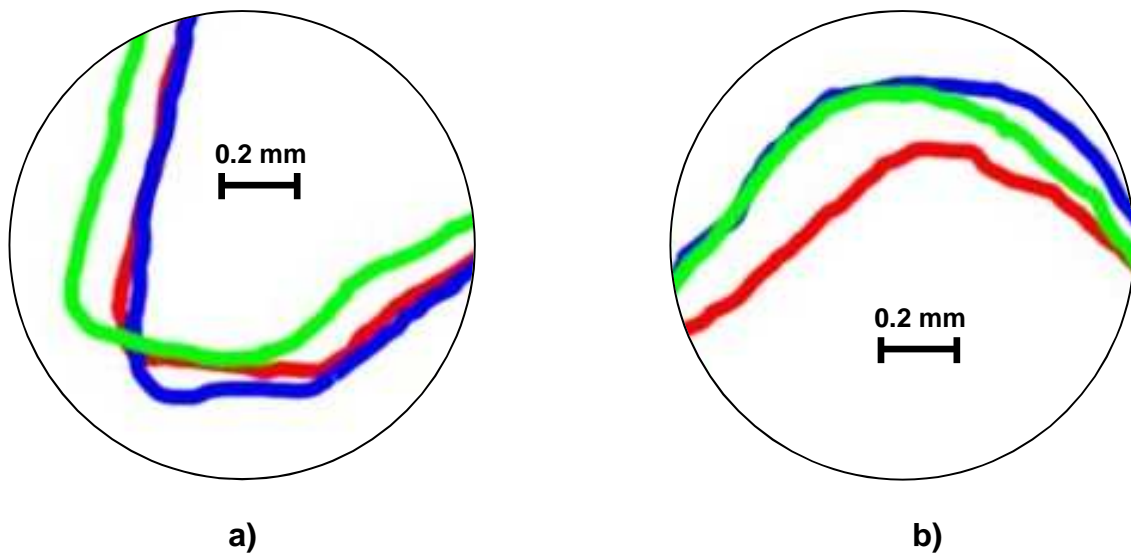


Fig. 71 Enlargement a) and b) of the stacking of 3 HF joint section with a DP-DP combination

The dimensional stability of the HF rivet is not as good as for the HD2 rivet. Here the variation reaches approx. 0.3 mm, which is 3 times bigger than for HD2.

These measured differences are much smaller than some found with the last method.

## 8.2.2 Rivet Setting

The differences between HF and HD2 rivets are similar for the possible sheet combinations (appendices 12.1 and 12.2). The Force vs. Displacement graphic below can be divided into three different parts: the cutting, then the interlocking and finally the swelling.

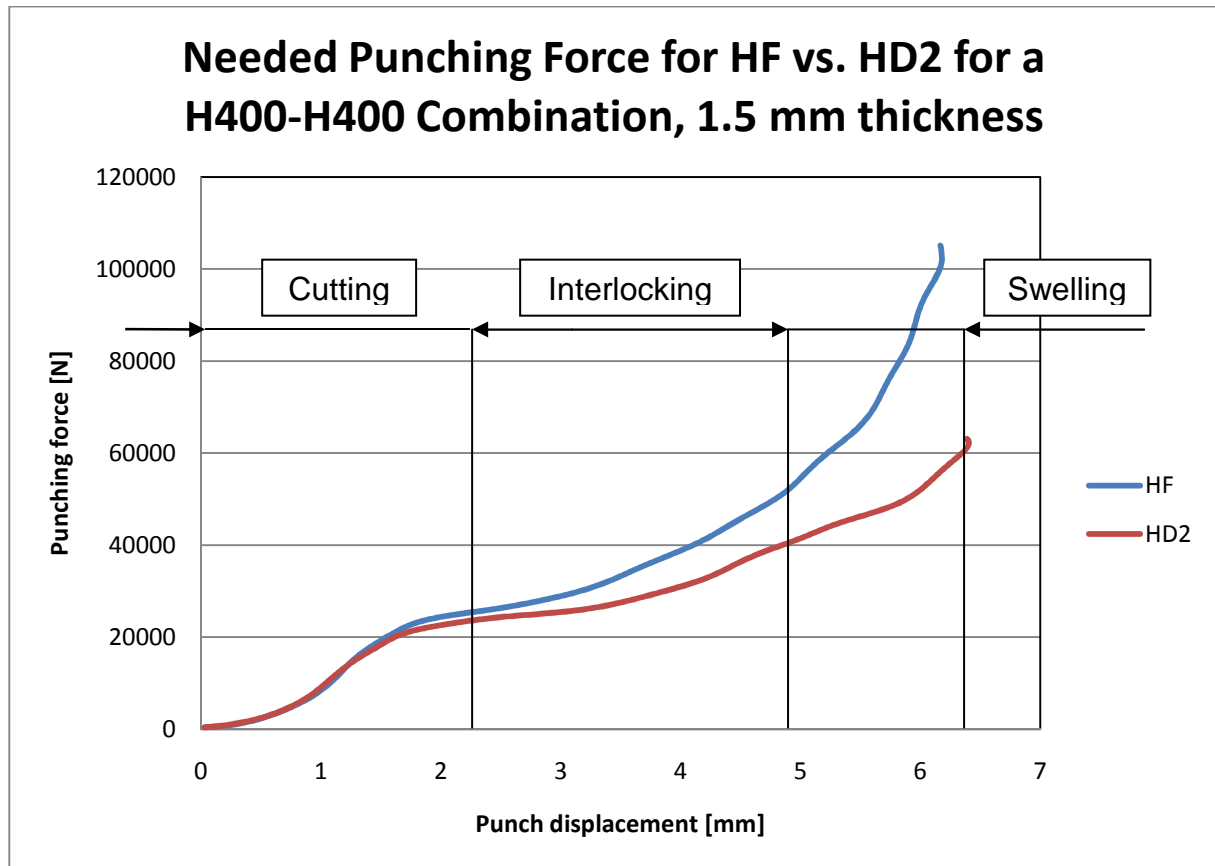


Fig. 72 Force vs. Displacement graphic for HF and HD2 rivet setting

### 8.2.2.1 Cutting

During this phase, the rivet is drilling the upper sheet. The two curves merge, but at the beginning the HF curve is a tiny bit lower than the HD2 curve. This is probably due to the sharper outside angle, which helps to cut.

### 8.2.2.2 Interlocking

For both rivets the force increases a lot, this is because an always bigger part of the rivet is deformed while the rivet is penetrating the sheets. The HF rivet requires at the beginning a little bit more force to spread. The difference increases with the displacement and is 25% bigger for the HF rivet at the end of the spreading. The reason is that the shanks of the HF rivet are getting thicker and more rigid on the upper part.

### 8.2.2.3 Swelling

This step requires a lot of force to swell the rivet in the sheets. As the shanks of the HF rivet are much thicker, they need much more energy for swelling than the HD2.

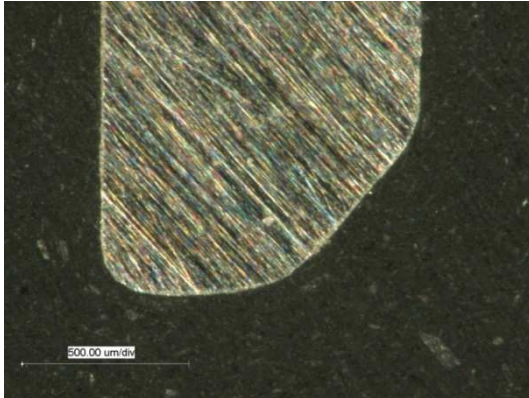


Fig. 73 Left foot of a HD2 rivet

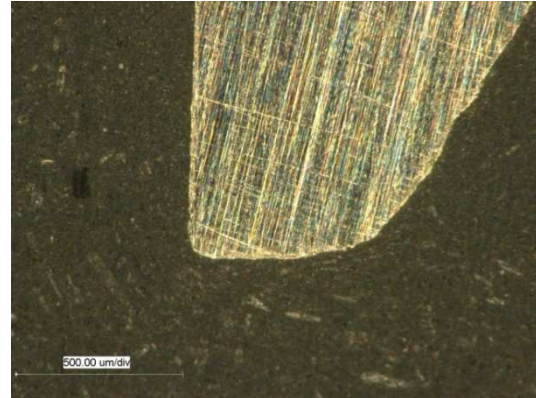


Fig. 74 Left foot of a HF rivet

HF rivets as well as HD2 rivets were able to join all the different combinations of ultra high-strength sheet steels.

The HF rivets need almost twice the force required for the HD2 rivets (fig. 75). This can be a problem, because the used forces correspond to the limits of the actual industrial riveting machines.

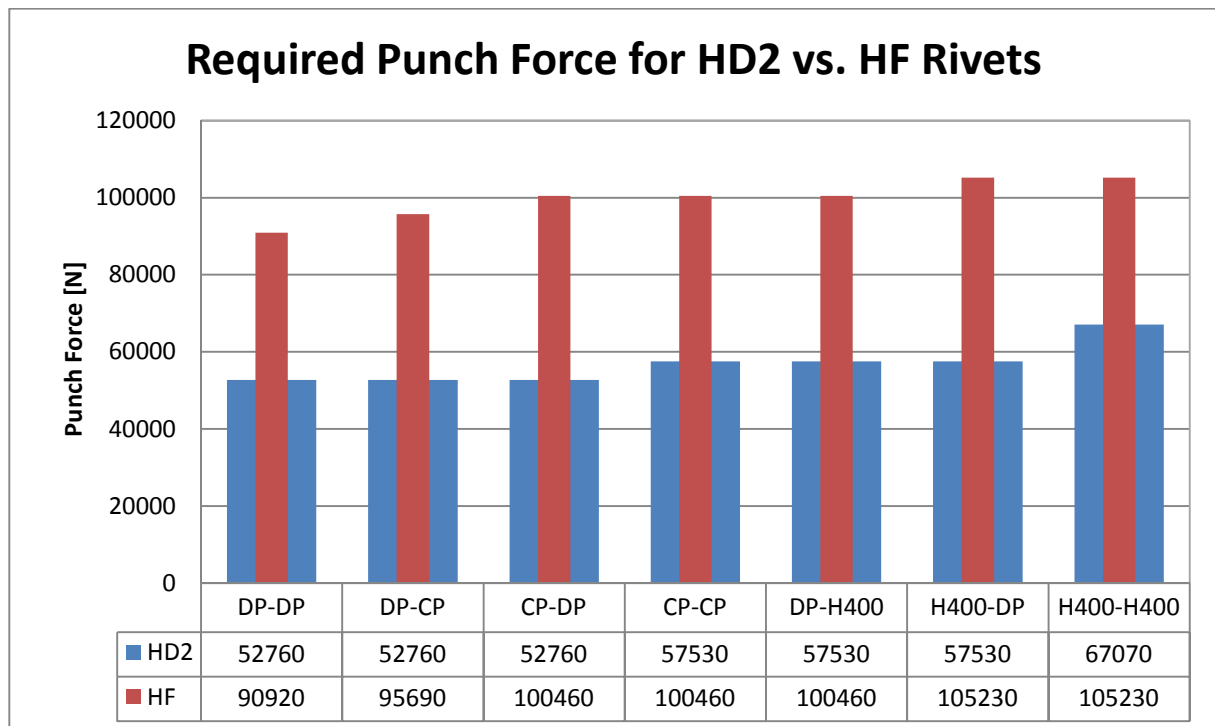


Fig. 75 Required punch force for the rivet setting of HD2 vs. HF

The difficulties to perform a self-piercing rivet (SPR) joint in high strength steel sheets are related to the reduced ductility of high strength steels. In particular, the lower sheet requires a sufficient ductility. The higher strength of the sheet material requires a higher strength of the rivet material to avoid collapse. At the same time, the rivet must exhibit, which will result in larger and heavier C-frames to maintain the parallel surface between rivet and die. The automated robots that will carry the C-frame may have problems if the mass or the size of the C-frame increases too much.

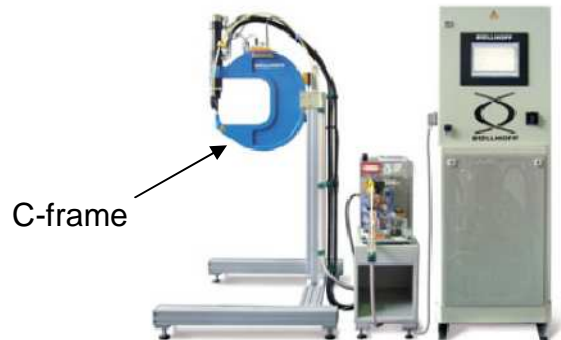


Fig. 76 Example of a self-pierce riveting machine / Source: Böllhoff GmbH

The main problem of high bonding forces isn't to be able to generate them, but much more the reaction forces applied on the C-frame. Two defaults can provide from a lack of rigidity of the C-frame. The stamped rivet can be inserted with a lateral displacement if considering the rivet and the die. According to Hahn and Philipskötter [05], if the displacement is bigger than 0.3 mm, the quality of the bonding is dramatically reduced. The second default is if the rivet is inserted with an angle compared with the vertical. In this case, an angle bigger than 2° will let a gap between the head of the rivet and the upper sheet. A large space like that is very favourable for corrosion.

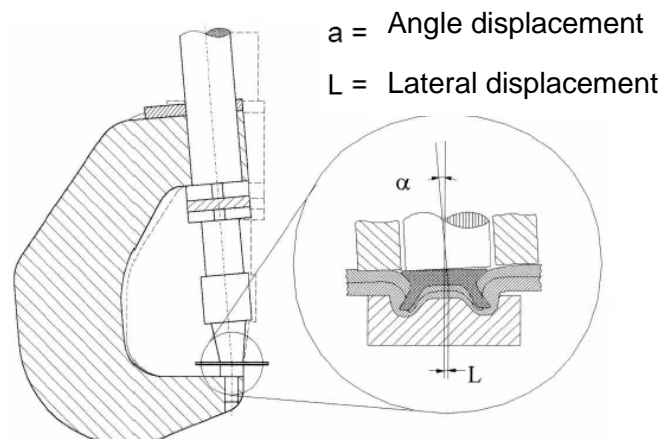


Fig. 77 Defaults due to a lack of rigidity of a C-frame [05]

### 8.2.3 Jointed Sheets Hardness

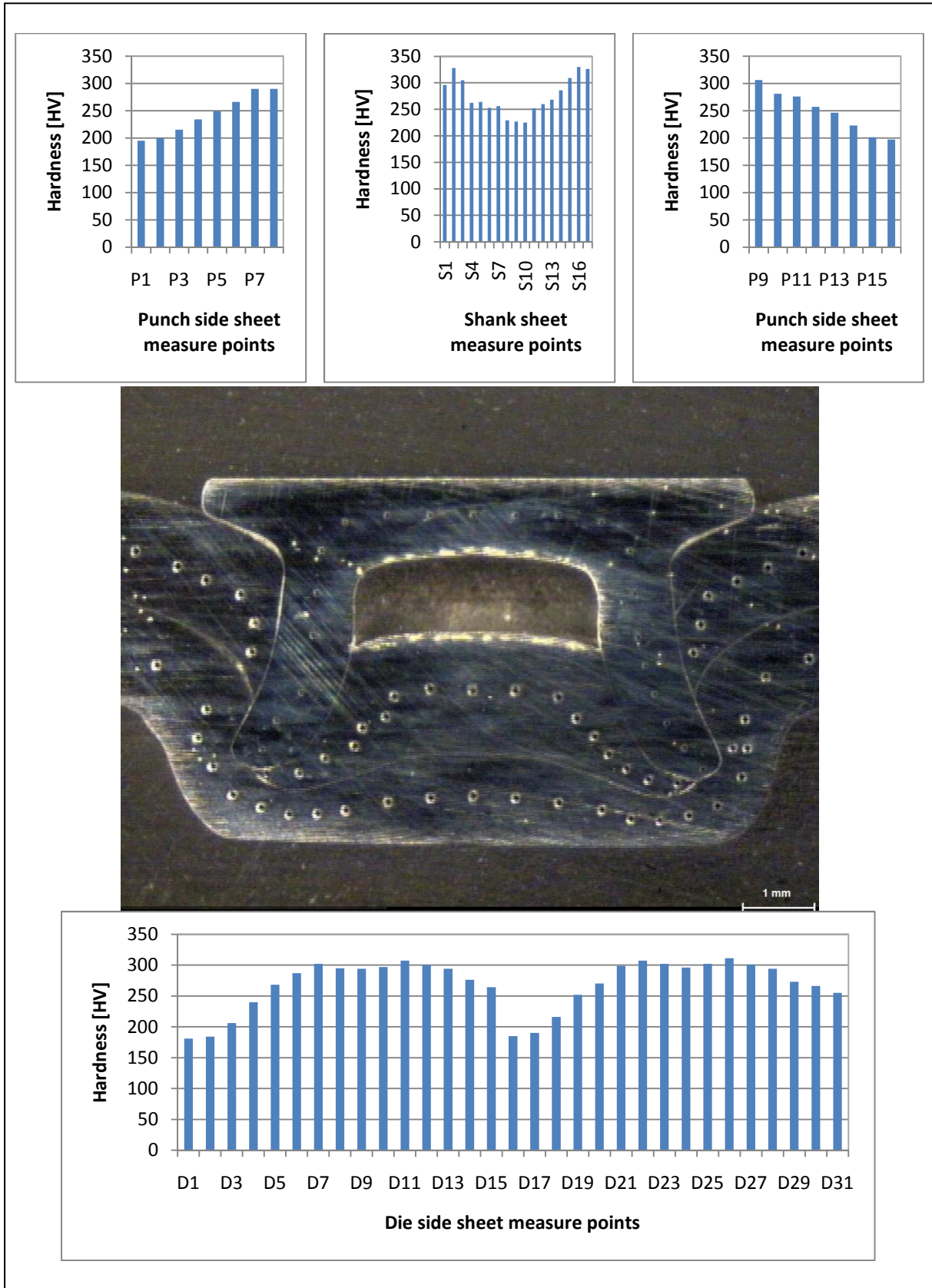


Fig. 78 Hardness measure of a HD2 joint section with a DP-DP combination

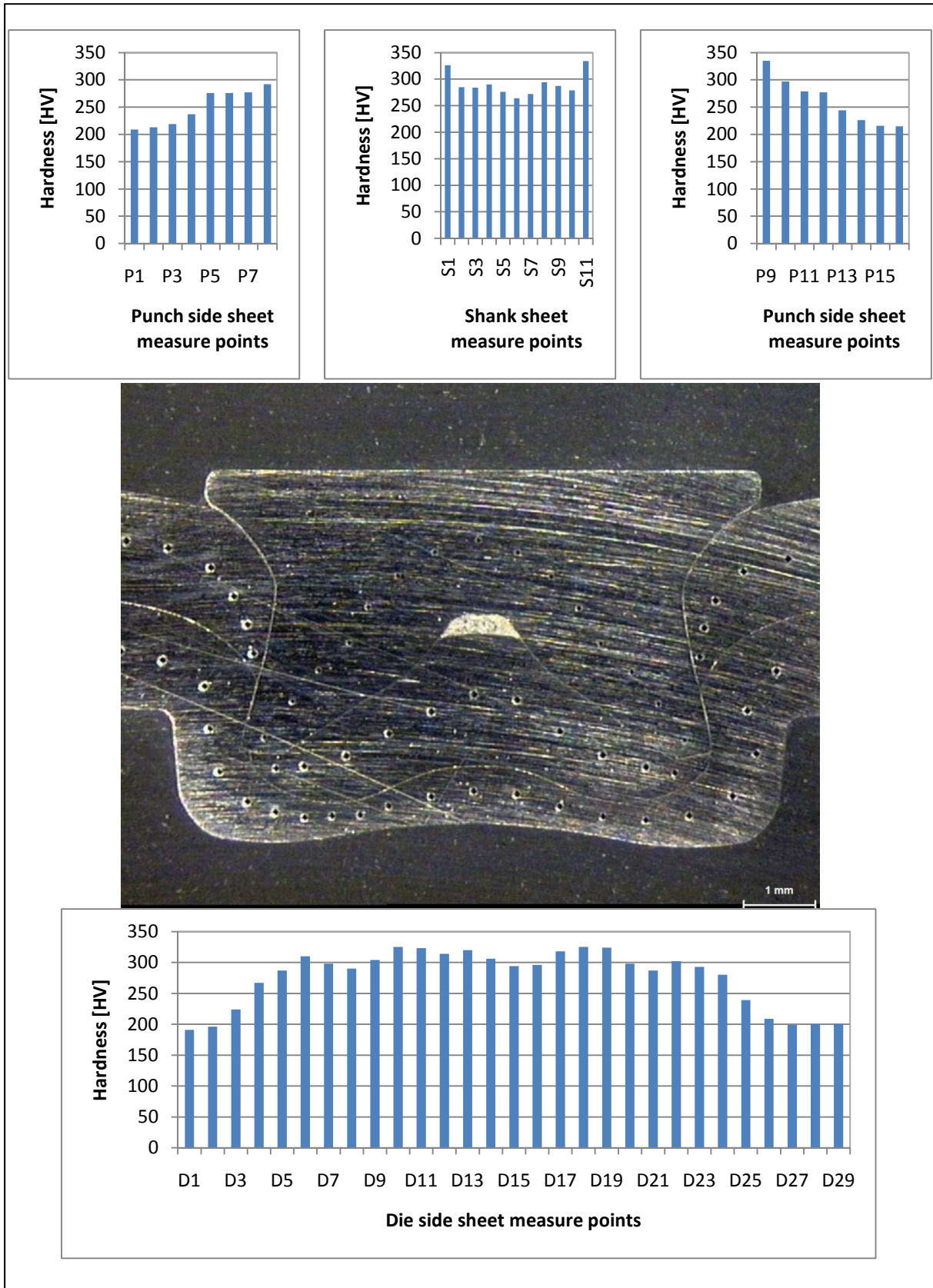


Fig. 79 Hardness measure of a HF joint section with a DP-DP combination

The process of riveting involves local important sheet deformations. This has for effect to harden locally the sheets (fig. 78 and 79). The DP steel, near the rivet feet, passes from approx. 200 HV to almost 350 HV.

Both of the HF and the HD2 rivets induce this cold impact hardening. The hardness gain is more or less the same for the HF joint sheets as for the HD2 joint sheets.

### 8.2.4 Quasi-Static Shear Tests Comparison

Except for one case (fig. 82), the interlock length has no significant influence on the ultimate strength or on the deformation energy for the quasi-static shear tests (appendix 12.4). For the H400-H400 combination, the rivet HD2 is not able to build a good joining. In this case, the much shorter interlock than for the other combinations is certainly responsible. In other words, if the interlock length is longer than a critical minimum, it has no real impact for quasi-static shear tests. Nevertheless, it will probably have a more important effect for peel tests and much more for cross tension loading tests. In those tests, tensile forces are concentrated on the interlock.

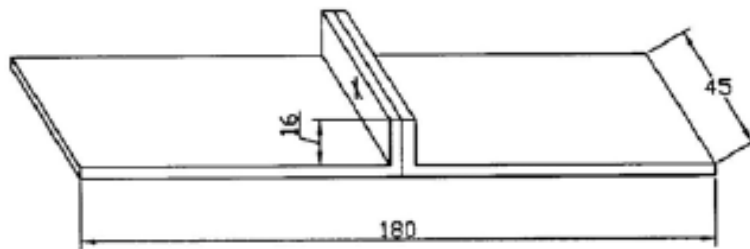


Fig. 80 A Peel test sample with one rivet bonding

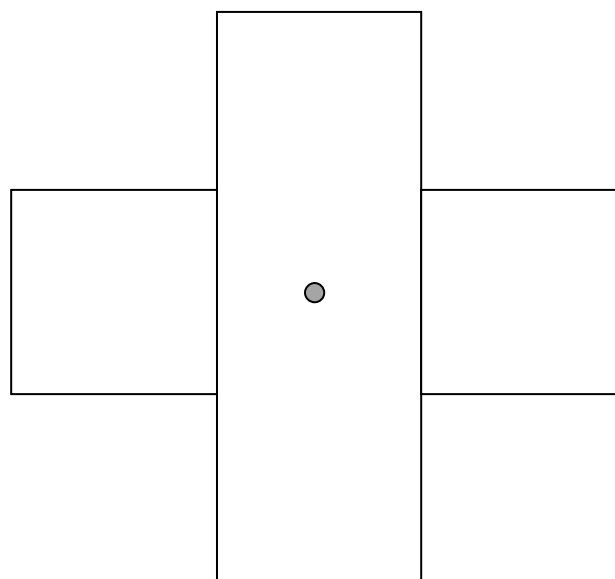


Fig. 81 Cross tension loading

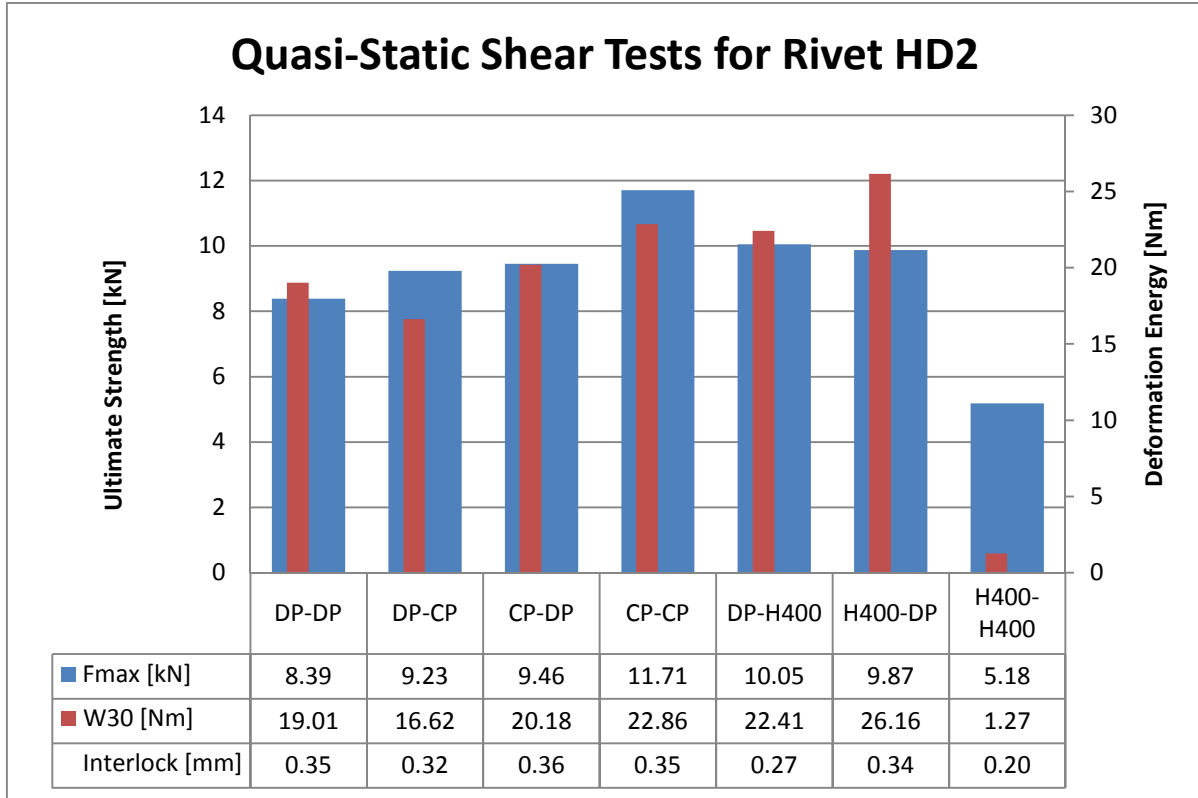


Fig. 82 quasi-static shear tests for HD2 rivets

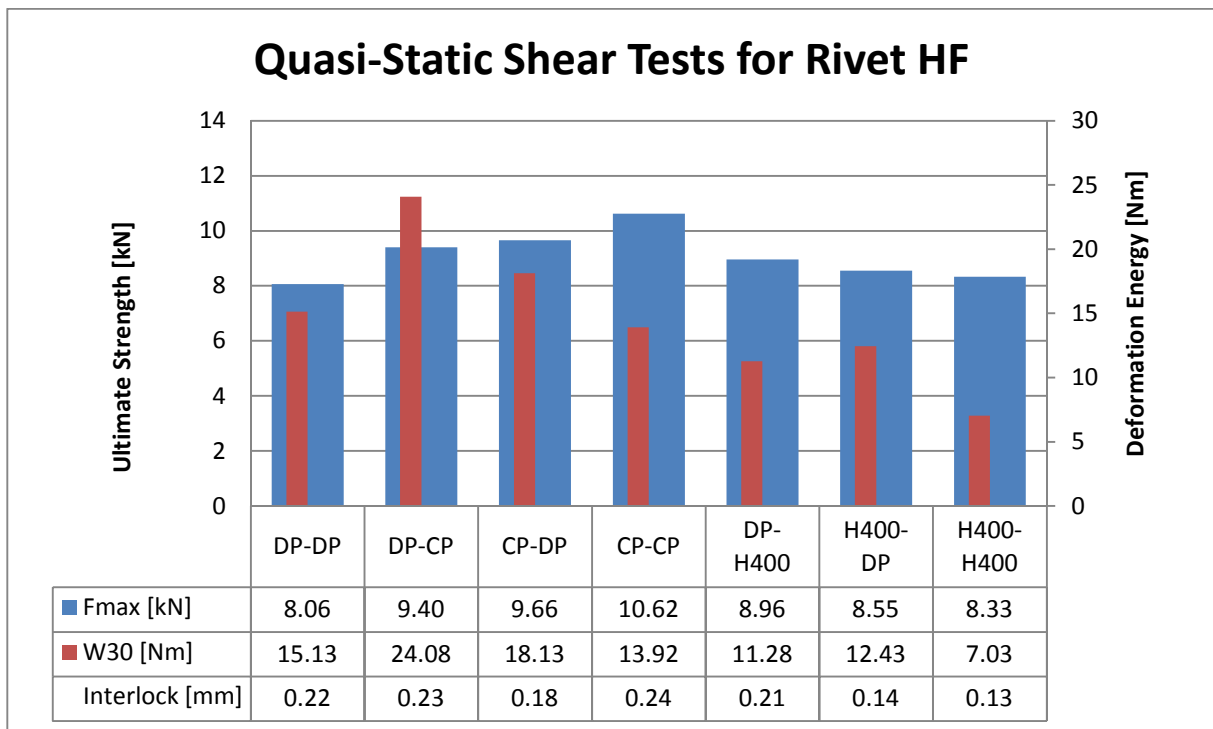


Fig. 83 Quasi-static shear tests for HF rivets

### 8.2.4.1 HD2 Rivet Quasi-Static Tests

The entire HD2 sample except with the H400-H400 sheets had the rivet head torn in the centre (fig. 84). This rivet deformation needs high shear strength and demands also a lot of deformation energy. This kind of rupture happens because of the big shank hole just under the head. This makes a free space under the rivet head interesting, but the head thickness must not be too wide to be able to crack.

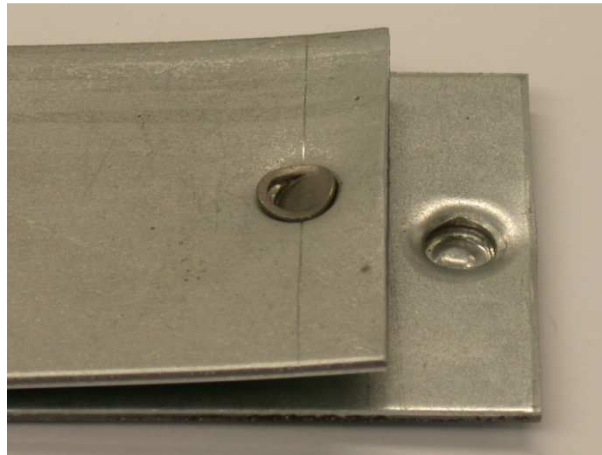


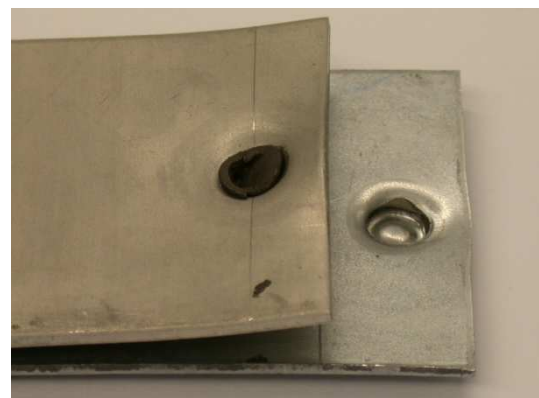
Fig. 84 A typical HD2 rivet failure mode with a CP-DP combination

The only combination where the HD2 rivet does not crack in the centre of the head is with the H400-H400 sheets. The reason is that the interlock is too short and the rivet is unbuttoned before the constraints become too big for the rivet's head.

The HD2 with H400-DP combination has an especially high ultimate strength. This is because the rivet is not only opened on the head, but the feet are completely deformed.



a)



b)

Fig. 85 HD2 rivet with H400-DP combination, a) view on the rivet feet b) view on the rivet head

### 8.2.4.2 HF Rivet Quasi-Static Tests

The HF rivet head is much thicker and the shank hole is very small, therefore a crack in the middle of the head will probably never happen. On the other hand, the interlock is shorter than the one created by the HD2 rivet. As written above, this does not make the HF rivet much worse than the HD2. But, the HF rivet generally fails with a small foot piece torn away (fig. 86).

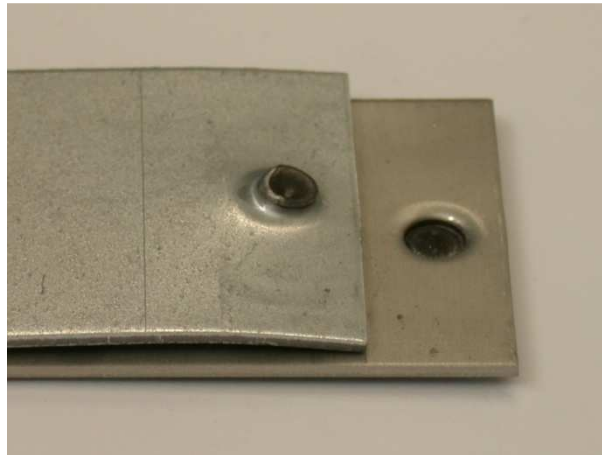


Fig. 86 A typical HF rivet failure mode with a DP-H400 combination

The DP-CP combination required a very high energy deformation to break the HF joint. The DP sheet is too soft for the HF rivet and therefore, the rivet deformed heavily the DP sheet before being unbuttoned.

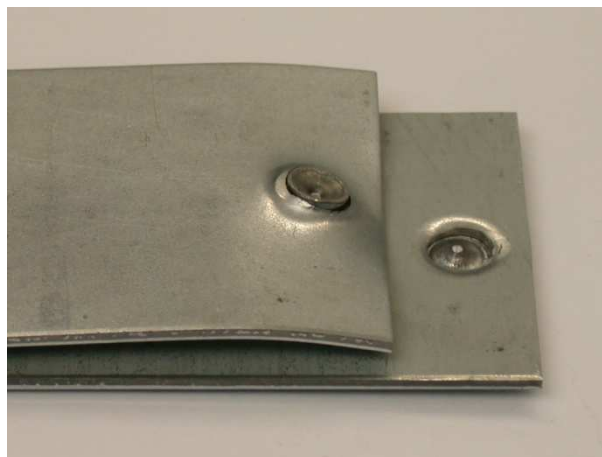


Fig. 87 A HF rivet with a DP-CP combination

The H400-H400 combination for this rivet is much more resistant than the same combination with the HD2 rivet. The main reason is probably the higher compression exercised on the shanks of the HF rivet. The pressure on the shanks comes not only from the outside like for the HD2 rivet, but also from the inside due to a filled shank hole.

### 8.2.5 Fatigue Tests Comparison

The automatic run-out condition for the program that executed the fatigue tests was chosen after a few preliminary tests. The testing showed that the fatigue frequency declined for all the samples very quickly after  $\Delta f = 8$  Hz. To stop the test shortly before the breaking of the sample, a delta frequency of 20 Hz was taken.

The frequency reference is the start frequency measured by the program. The frequency during the first  $10^3$  load cycles is unstable. Meanwhile the fatigue test, the frequency is first increasing, because at the beginning the rivet joint is shrinking [07]. When the maximum is reached, the frequency decreases slowly approx. for 5 Hz and then the reduction is sudden (fig. 88).

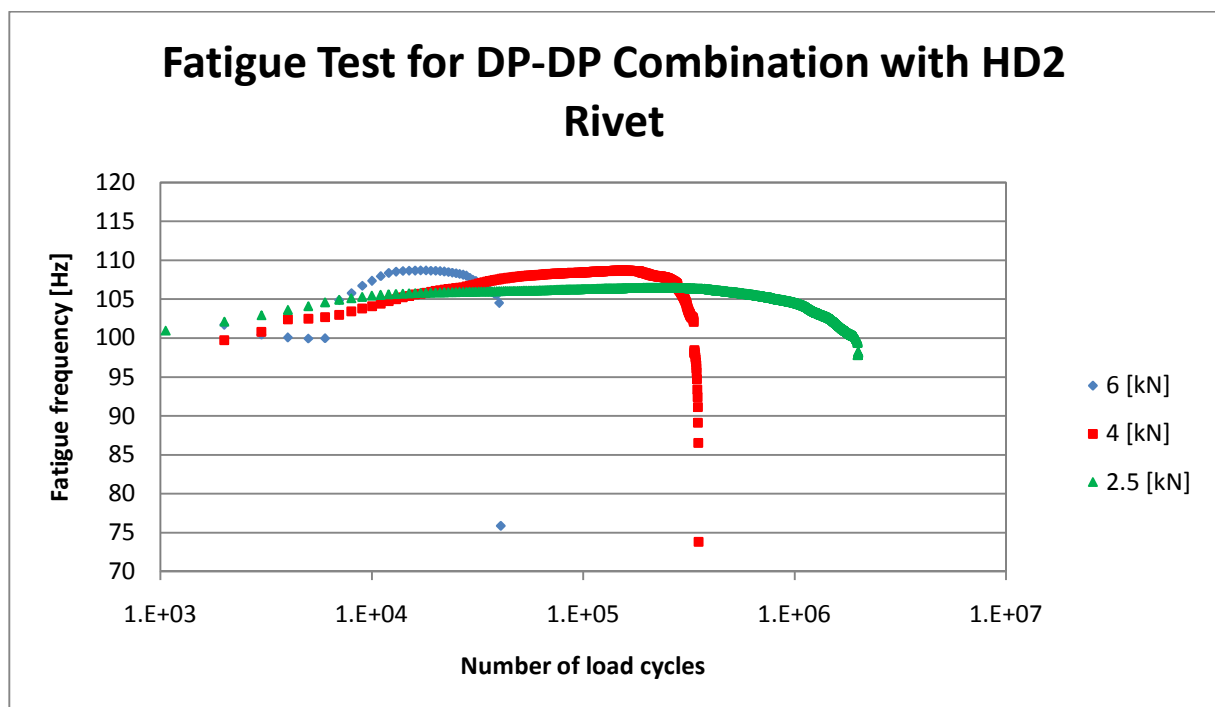


Fig. 88 Fatigue test for DP-DP combination with HD2 rivet

The research from Glowig et al. [07] have showed that cracks, that are approx. 1mm deep, could appear already after a frequency variation of 0.5 Hz.

For this work, in order to have fatigue values for samples without deep cracks, the number of load cycles was defined for a frequency variation of 0.1 Hz and the frequency reference is the maximum reached during the test (fig. 89).

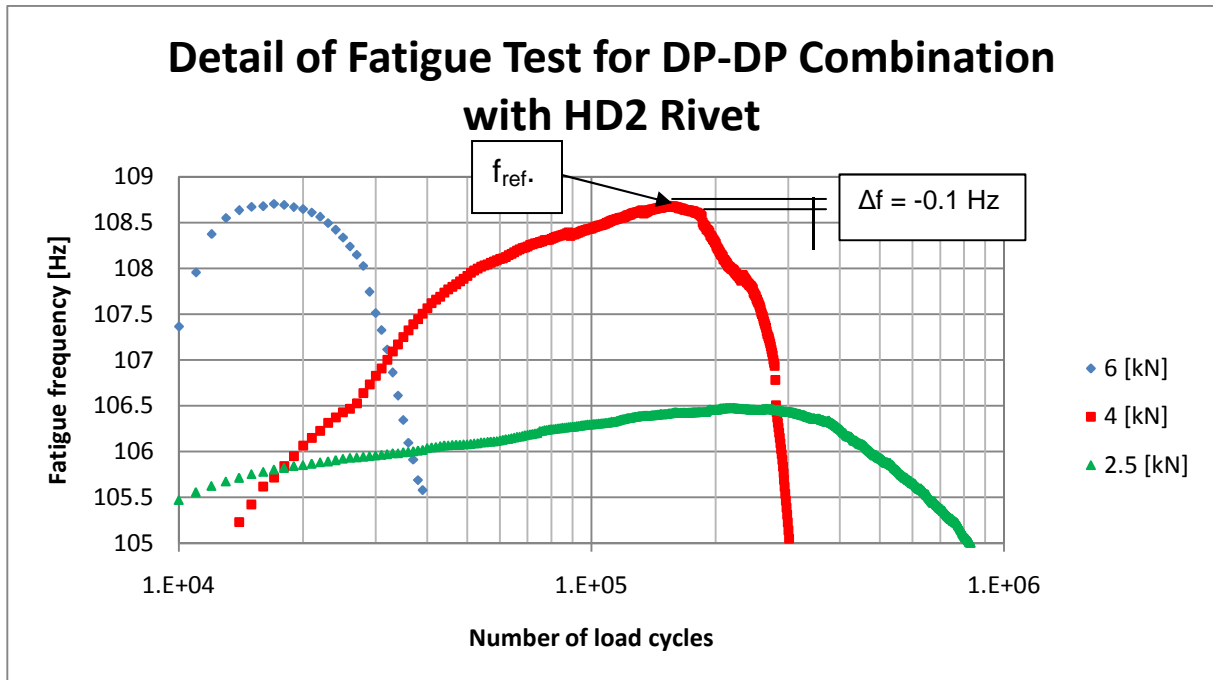


Fig. 89 Enlargement of a detail of the fatigue test for DP-DP combination with HD2 rivet

Wöhler curves for a delta frequency of 20 Hz as run-out condition are indicating better results than the curves with a delta of 0.1 Hz. For high force amplitudes, the difference is small, but the difference increases with the force amplitude decrease (appendix 12.6).

Deformation grades of curves with a delta of 0.1 Hz are smaller than curves with a delta of 20 Hz. Some samples are still firmly bound after having reached a delta of 20 Hz. Maybe the results with a delta of 0.1 Hz are lowering the real capacity of the tested rivets, but the risk of having cracks is unacceptable for mechanical structures.

The reason why the CP-CP combination is also shown (fig. 90) for the delta 20 Hz condition is that for the 0.1 Hz curve is drawn with only five points between 18000 and 70000 load cycles. With more measure points distributed on a wider range, the curve would certainly indicate the same ratio between the HD2 and the HF curve for 0.1 Hz than for 20 Hz. Anyway, there are no apparent reasons for the 0.1Hz curve for being so weak compared to the other sheet combinations.

The samples for the HF rivet with H400 combinations have not been tested because of a lack of time.

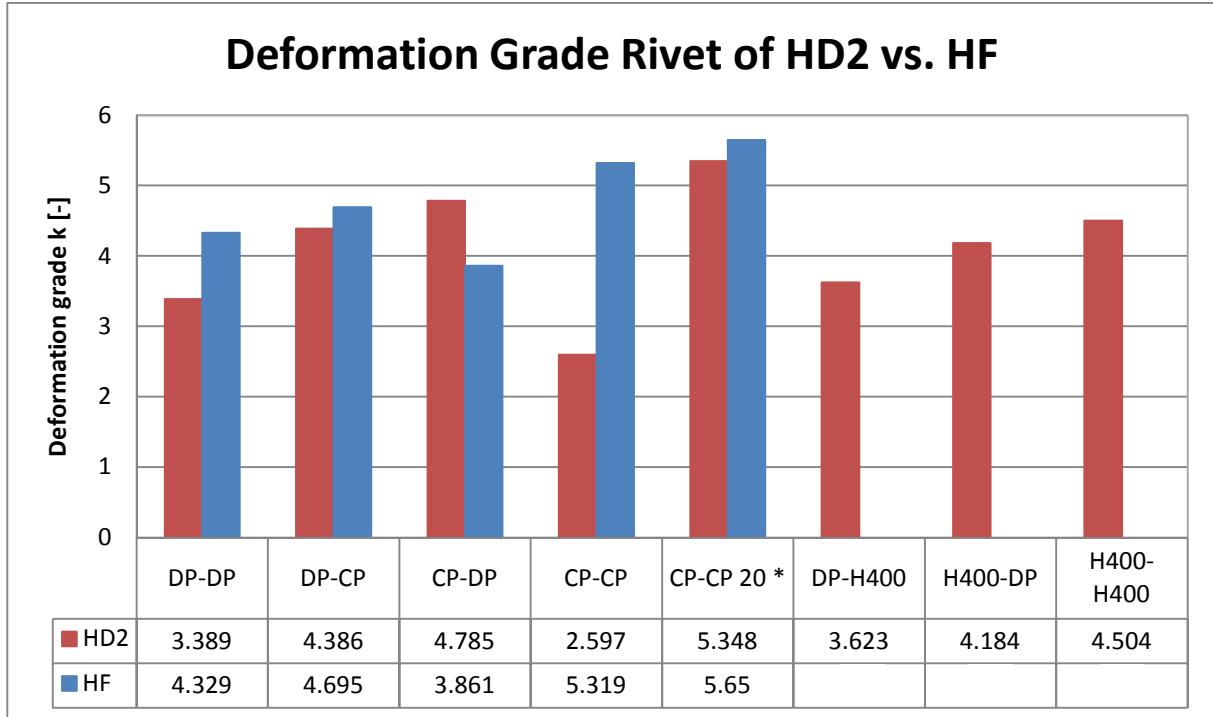


Fig. 90 Deformation grade for fatigue tests with  $\Delta f = -0.1$  as run-out condition

\*CP-CP 20: Deformation grade for CP-CP combination with  $\Delta f = -20$  Hz as run-out condition

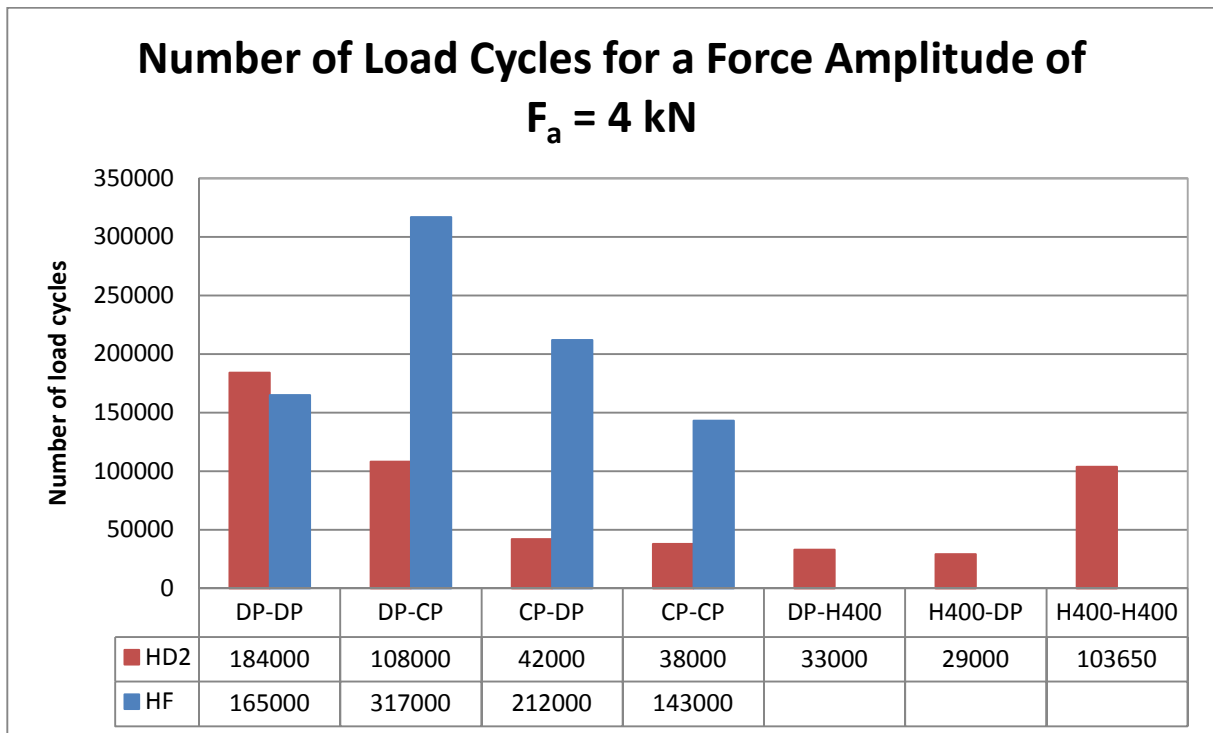
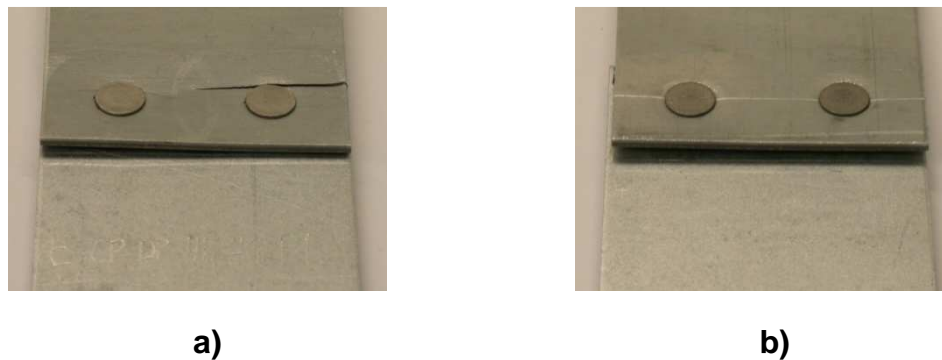


Fig. 91 Number of load cycles for a force amplitude of  $F_a = 4$  kN with run-out condition  $\Delta f = -0.1$  Hz

Except for CP-DP, the other tested sheet combinations for HF rivets have a better deformation's grade than for HD2 samples (appendix 12.5). This means that the HF Wöhler curves decrease more slowly next to the HD2 curves. Besides, HF rivets can last more load cycles than HD2 rivets for same force amplitude. This better behaviour of HF rivets comes probably from the filled shank hole. The conical feet of HF rivets give a better stability to the joint.

A possible explanation for the exception of CP-DP combination can be given with the failure mode. Indeed, for example the 4.5 kN CP-DP test, for HF the CP sheet has been a little bit deformed and torn. For HD2, the CP sheet had a bigger deformation and no visible cracks. The sheet deformation is a slow process in these fatigue tests, but cracks are much faster and change the rigidity of the sample very quickly.



**Fig. 92 CP-DP samples for fatigue test with 4.5 kN force amplitude: a) HF sample b) HD2 sample**

The reason why the CP sheet cracked only for the HF rivet could be that the required setting force is twice bigger than for the HD2 rivet. This has increased locally the hardness of the CP sheet and made it more brittle.

The fig. 91 gives an indication of the offset between the HF and the HD2 Wöhler curves. The force amplitude of 4 kN was taken, because it is the biggest force that was measured for all the samples.

The DP-DP combination shows that HD2 rivet has a better fatigue capacity than the HF rivet. But if the HD2 Wöhler curve is considered, it is obvious that the measure for 4 kN is bigger than the expected value.

The other combination measured with both HF and HD2 rivets indicate that HF rivets have a much better fatigue endurance.

### 8.2.5.1 HD2 Rivet Fatigue Tests

The main failure mode encountered for quasi-static tests, which is a crack that open the head, does not happen anymore for dynamic tests. The force amplitude for these tests is between 2 kN and 6 kN, which is obviously not enough for inducing cracks in the head.

The H400 combinations break mainly with cracks in the foot region. For DP-DP tests, cracks appear in the sheets. The reason for this different behavior is that H400 requires the H7 hardened rivets, which make the rivets more fragile. Therefore, the rivet gets destroyed before the upper sheet can crack. This also happened for the H400-H400 combination, which resisted better than for the quasi-static test.

The cracks in the upper sheets appear for the DP-DP and DP-CP combinations. They start always just below the rivet head and then progress on both sides. Sometimes, there is only one crack and in other cases two cracks appear simultaneously, one below each rivet head.



Fig. 93 Different HD2 fatigue samples: a) crack start b) crack grow c) two simultaneously cracks

### 8.2.5.2 HF Rivet Fatigue Tests

For HF rivets, all except H400 combinations have as failure mode a crack in the upper sheet. The second failure mode is that all except the DP-DP combination have a piece of foot torn off and blocked in the lower sheet.

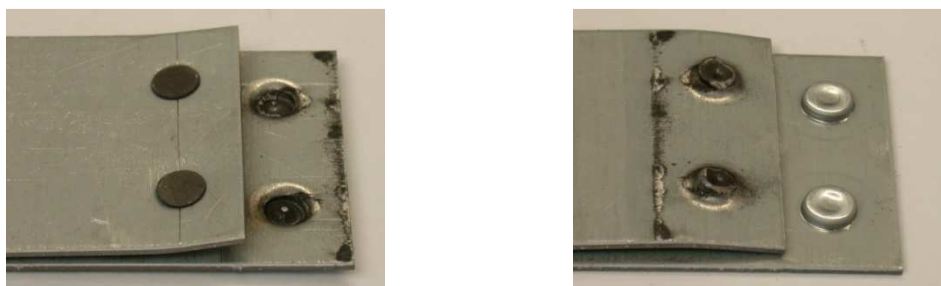


Fig. 94 CP-CP combination for a HF fatigue test

# 9. Conclusions and Recommendations

## 9.1 Conclusions

The G rivet prototype could not be tested, because of the insufficient quality of its shape processing and of its chemical composition. The rivet was too soft, but was not possible to harden because of a lack of carbon in its structure.

All the static tested combinations, for HF and HD2 rivets, resisted at least to a force of 8 kN and to a deformation energy of 7 Nm except the HD2 rivet with H400-H400 combination, for which the rivet is almost not able to create an interlock.

Besides, HF and HD2 rivets can bear at least 29,000 load cycles for all the dynamic fatigue tests. The HF rivet was not measured for the H400 combinations, but the HF rivet is better than the HD2 for the measured dynamic tests and is probably the same for the H400 combination.

The interlock as well as the setting direction had not a significant influence on the binding for the shear tests.

Globally for quasi-static loads, HD2 rivets are the more efficient, because they can absorb a lot of deformation energy by cracking their head and foot region. HF rivets are better for dynamic loads, because of their conical shanks and their capacity to fill the shank hole when riveted. On the other side, because of its thick shanks, the HF rivet has a less good dimensional stability than the HD2 rivet.

Even if HF and HD2 rivets can be used to bind ultra high-strength sheet steels, there is a big progression potential. Indeed, for the CP-CP and all the H400 combinations, both rivets need to be hardened in order to make the joining. A hardness of 630 HV is required for the rivets to work properly, which weaken them and increase the risk of cracks in them. Besides, HF rivets need a very high punching force (approx. 100 kN) that reaches the limits of what C-frames rigidity can support.

## 9.2 Recommendations

The G rivet prototype should be made with the good materials and shape processing in order to test them.

The dynamic tests with the HF rivet should be completed. Besides, at least some of the fatigue tested samples should be sectioned in the tensile length and analyzed for cracks presence. This would help to define more precise run-out conditions for the dynamic tests.

## 10. References

- [01] Singh, S.; Hahn, O.; Zhang, G.: *Lightweight design through optimized joining technology*, Materialprüfung in der Fügetechnik, München, (2003)
  
- [02] Hahn, O.; Philipuskötter, A.: *Entwicklung eines Halbholnietes für das Fügen von Mischbauweisen aus Aluminium und höherfesten Stählen*, Universität Paderborn, Band 72
  
- [03] Sun, X.; Stephens, E. V.; Khaleel, M. A.: *Fatigue behaviors of self-piercing rivets joining similar and dissimilar sheet metals*, Elsevier, (2006)
  
- [04] Hahn, O.; Flügge, W.: *Fügen von Edelstahlblechen mit verzinkten Feinblechen durch Stanznieten mit Halbhol- und Vollniet*, Europäische Forschungsgesellschaft für Blechverarbeitung e. V., Nr. 172
  
- [05] Hahn, O.; Philipuskötter, A.: *Neue Entwicklung auf dem Gebiet der mechanischen Fügetechnik*, 10. Paderborner Symposium Fügetechnik, (2003)
  
- [06] Schulz-Beenken, A.; Gössling, P.: *Einfluss der Vorverformung beim Stanznieten hochfester Stahlfeinbleche*, AIF-FH<sup>3</sup> Projekt Abschlussbericht, (2007)
  
- [07] Glowig, A.; Hahn, O.; Tölle, J.: *Anrisserkennung an Gefügten Proben bei schwingender Beanspruchung*, 12. Paderborner Symposium Fügetechnik, (2005)

# 11. Acknowledgment

This diploma work is the result of collaboration between the HES-SO Valais in Sion (Switzerland) and the Fachhochschule Südwestfalen in Soest (Germany). I would like to thank all the people that helped me in this work:

Prof. PhD Eng. Anne Schulz-Beenken for having given me this very interesting diploma work and being always very comprehensive and helpful

Eng. Peter Gössling who supervised and assisted me for the laboratory work and helped me for the scientific literature

The Laboratory for Materials crew at the Fachhochschule Südwestfalen in Soest who aided me for the experimentations

Ms Sabine Mahlstedt from the international student office who made my arrival in Germany easier

# 12. Appendices

## 12.1 HD2 Rivet Joining Formation

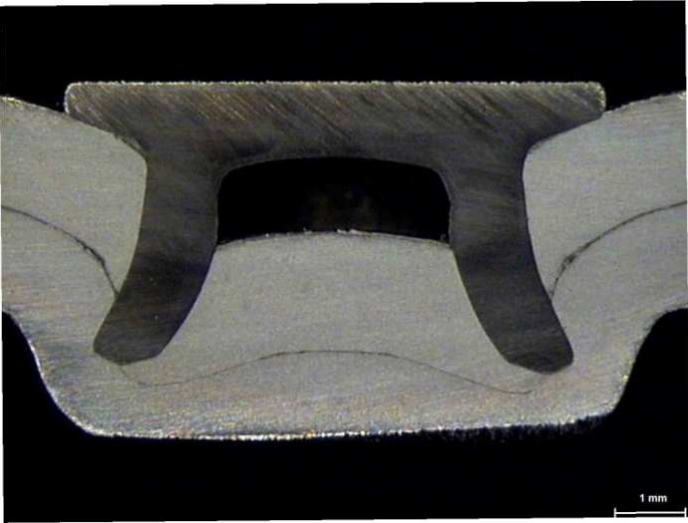
Joining Formation of Rivet HD2 with DP-DP Combination						
					Joined Sheets and Thickness	
					Punch side: DP-K 34/60 / 1.5mm Die side: DP-K 34/60 / 1.5mm	
					Joining Forces	
					Punch force: 53 kN Clamping force: 10 kN	
					SPR and Die	
SPR: HD2 / 5mm / 480 HV Die: G30						
Interlock [mm]		Residual Bottom Thickness [mm]		Swelled Length [mm]		Spread Diameter [mm]
Left	Right	Left	Right	Left	Right	Total
0.30	0.39	0.74	0.79	4.02	4.09	6.92

Fig. 95 Sample No.1 of rivet HD2 section with DP-DP combination

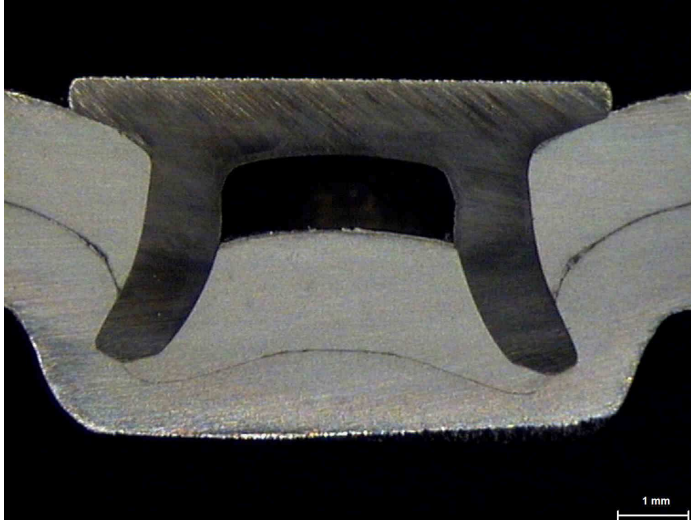
Joining Formation of Rivet HD2 with DP-DP Combination						
				Joined Sheets and Thickness		
				Punch side: DP-K 34/60 / 1.5mm Die side: DP-K 34/60 / 1.5mm		
				Joining Forces		
				Punch force: 53 kN Clamping force: 10 kN		
				SPR and Die		
SPR: HD2 / 5mm / 480 HV Die: G30						
Interlock [mm]		Residual Bottom Thickness [mm]		Swelled Length [mm]		Spread Diameter [mm]
Left	Right	Left	Right	Left	Right	Total
0.36	0.30	0.79	0.67	4.03	4.14	6.88

Fig. 96 Sample No.2 of rivet HD2 section with DP-DP combination

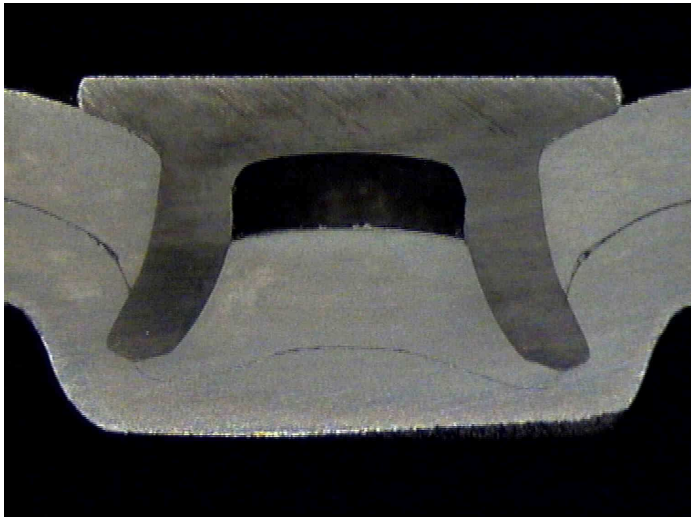
Joining Formation of Rivet HD2 with DP-DP Combination						
				Joined Sheets and Thickness		
				Punch side: DP-K 34/60 / 1.5mm Die side: DP-K 34/60 / 1.5mm		
				Joining Forces		
				Punch force: 53 kN Clamping force: 10 kN		
				SPR and Die		
SPR: HD2 / 5mm / 480 HV Die: G30						
Interlock [mm]		Residual Bottom Thickness [mm]		Swelled Length [mm]		Spread Diameter [mm]
Left	Right	Left	Right	Left	Right	Total
0.38	0.35	0.72	0.81	4.06	4.13	6.92

Fig. 97 Sample No.3 of rivet HD2 section with DP-DP combination

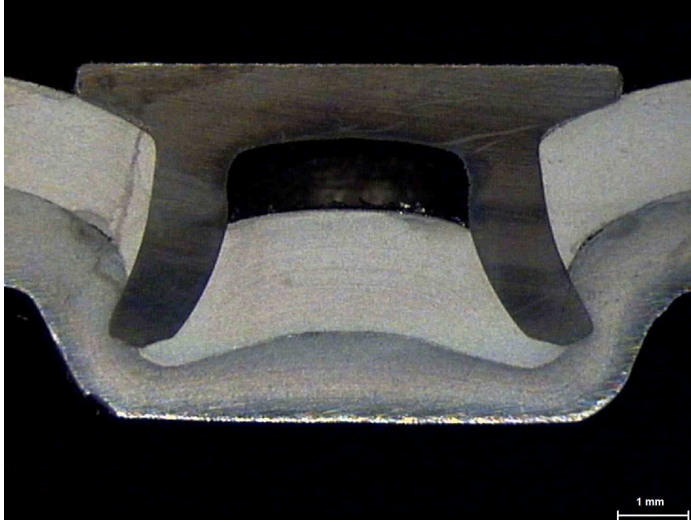
Joining Formation of Rivet HD2 with DP-CP Combination						
				Joined Sheets and Thickness		
				Punch side: DP-K 34/60 / 1.5mm Die side: CP-W 800 / 1.5mm		
				Joining Forces		
				Punch force: 53 kN Clamping force: 10 kN		
				SPR and Die		
SPR: HD2 / 5mm / 480 HV Die: G30						
Interlock [mm]		Residual Bottom Thickness [mm]		Swelled Length [mm]		Spread Diameter [mm]
Left	Right	Left	Right	Left	Right	Total
0.28	0.35	0.70	0.67	4.02	3.98	6.89

Fig. 98 Rivet HD2 section with DP-CP combination

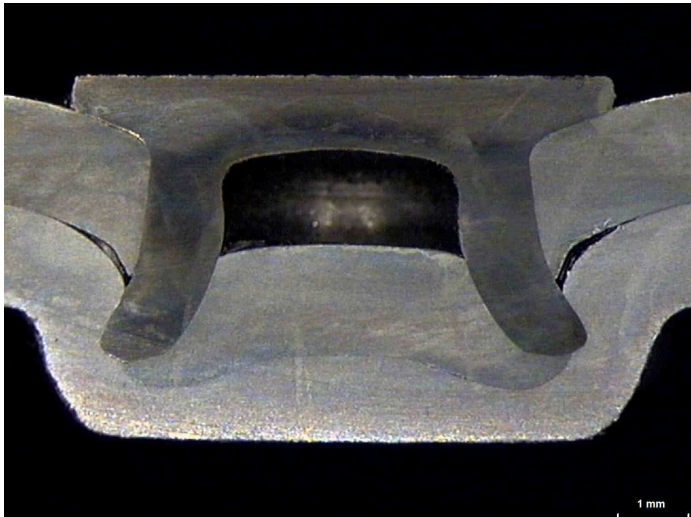
Joining Formation of Rivet HD2 with CP-DP Combination						
				Joined Sheets and Thickness		
				Punch side: CP-W 800 / 1.5mm Die side: DP-K 34/60 / 1.5mm		
				Joining Forces		
				Punch force: 53 kN Clamping force: 10 kN		
				SPR and Die		
SPR: HD2 / 5mm / 480 HV Die: G30						
Interlock [mm]		Residual Bottom Thickness [mm]		Swelled Length [mm]		Spread Diameter [mm]
Left	Right	Left	Right	Left	Right	Total
0.38	0.34	0.79	0.89	4.04	3.96	6.93

Fig. 99 Rivet HD2 section with CP-DP combination

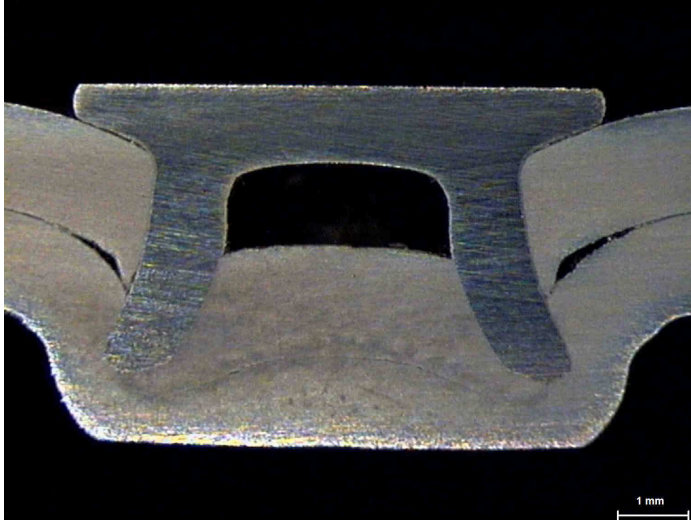
Joining Formation of Rivet HD2 with CP-CP Combination						
				Joined Sheets and Thickness		
				Punch side: CP-W 800 / 1.5mm Die side: CP-W 800 / 1.5mm		
				Joining Forces		
				Punch force: 58 kN Clamping force: 10 kN		
				SPR and Die		
SPR: HD2 / 5mm / 640 HV Die: G30						
Interlock [mm]		Residual Bottom Thickness [mm]		Swelled Length [mm]		Spread Diameter [mm]
Left	Right	Left	Right	Left	Right	Total
0.35	0.34	0.73	0.82	4.09	4.15	6.66

Fig. 100 Rivet HD2 section with CP-CP combination

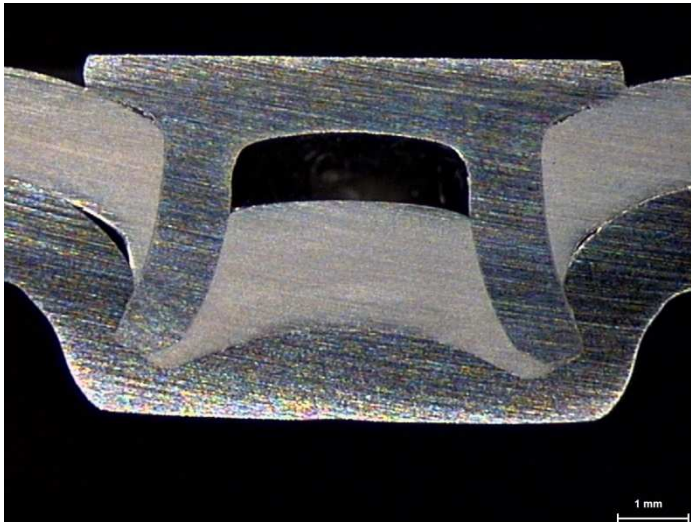
Joining Formation of Rivet HD2 with DP-H400 Combination						
				Joined Sheets and Thickness		
				Punch side: DP-K 34/60 / 1.5mm Die side: H400 / 1.5mm		
				Joining Forces		
				Punch force: 58 kN Clamping force: 10 kN		
				SPR and Die		
SPR: HD2 / 5mm / 640 HV Die: G30						
Interlock [mm]		Residual Bottom Thickness [mm]		Swelled Length [mm]		Spread Diameter [mm]
Left	Right	Left	Right	Left	Right	Total
0.27	0.27	0.72	0.77	4.06	4.06	6.82

Fig. 101 Rivet HD2 section with DP-H400 combination

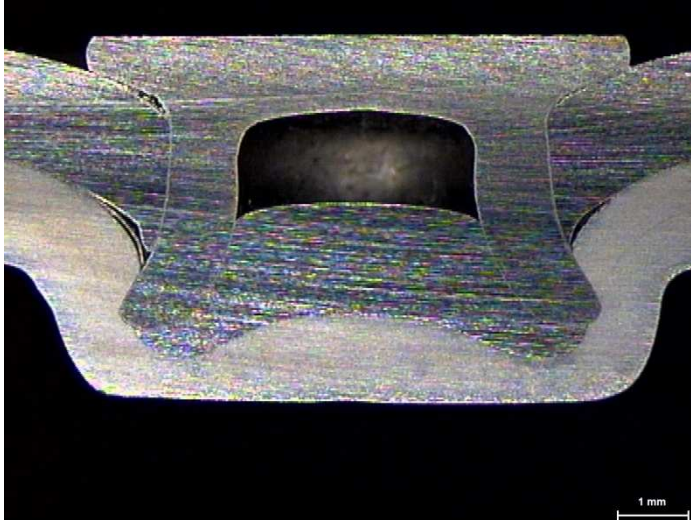
Joining Formation of Rivet HD2 with H400-DP Combination												
							Joined Sheets and Thickness					
							Punch side: H400 / 1.5mm Die side: DP-K 34/60 / 1.5mm					
							Joining Forces					
							Punch force: 58 kN Clamping force: 10 kN					
							SPR and Die					
SPR: HD2 / 5mm / 640 HV Die: G30												
Interlock [mm]		Residual Bottom Thickness [mm]		Swelled Length [mm]		Spread Diameter [mm]						
Left	Right	Left	Right	Left	Right	Total						
0.34	0.33	0.87	0.88	4.06	4.12	6.75						

Fig. 102 Rivet HD2 section with H400-DP combination

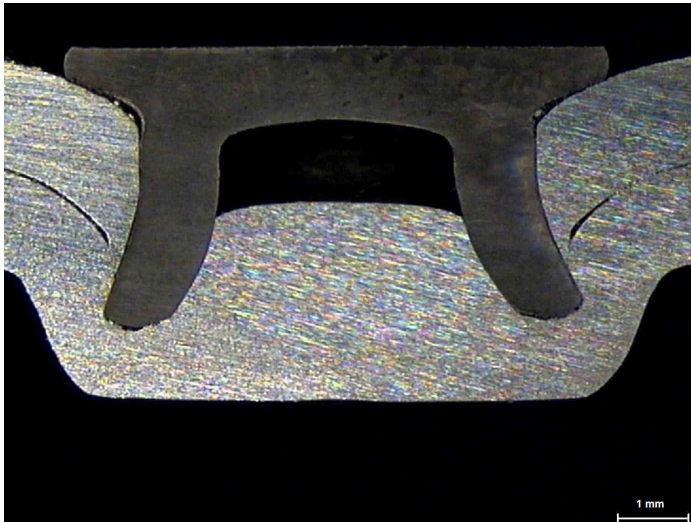
Joining Formation of Rivet HD2 with H400-H400 Combination												
							Joined Sheets and Thickness					
							Punch side: H400 / 1.5mm Die side: H400 / 1.5mm					
							Joining Forces					
							Punch force: 67 kN Clamping force: 10 kN					
							SPR and Die					
SPR: HD2 / 5mm / 640 HV Die: G30												
Interlock [mm]		Residual Bottom Thickness [mm]		Swelled Length [mm]		Spread Diameter [mm]						
Left	Right	Left	Right	Left	Right	Total						
0.18	0.22	0.83	0.84	3.99	3.87	6.82						

Fig. 103 Rivet HD2 section with H400-H400 combination

## 12.2 HF Rivet Joining Formation

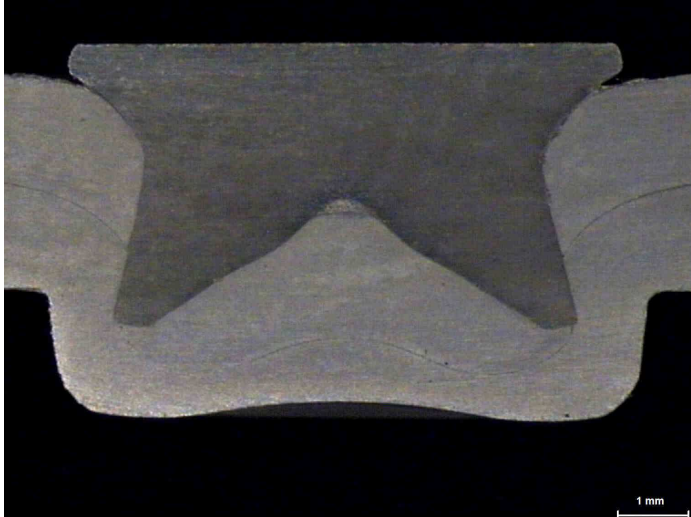
Joining Formation of Rivet HF with DP-DP Combination						
					Joined Sheets and Thickness	
					Punch side: DP-K 34/60 / 1.5mm Die side: DP-K 34/60 / 1.5mm	
					Joining Forces	
					Punch force: 91 kN Clamping force: 10 kN	
					SPR and Die	
SPR: HF / 5mm / 480 HV Die: F61801						
Interlock [mm]		Residual Bottom Thickness [mm]		Swelled Length [mm]		Spread Diameter [mm]
Left	Right	Left	Right	Left	Right	Total
0.21	0.22	0.84	0.93	4.01	4.03	6.63

Fig. 104 Sample No.1 of rivet HF section with DP-DP combination

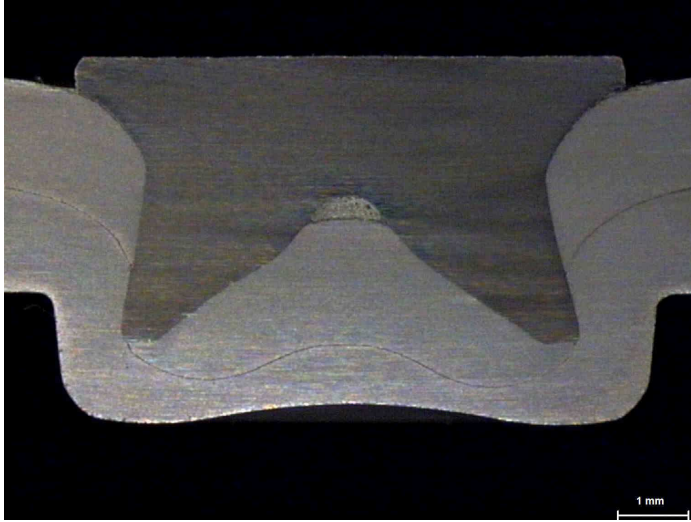
Joining Formation of Rivet HF with DP-DP Combination						
				Joined Sheets and Thickness		
				Punch side: DP-K 34/60 / 1.5mm Die side: DP-K 34/60 / 1.5mm		
				Joining Forces		
				Punch force: 91 kN Clamping force: 10 kN		
				SPR and Die		
SPR: HF / 5mm / 480 HV Die: F61801						
Interlock [mm]		Residual Bottom Thickness [mm]		Swelled Length [mm]		Spread Diameter [mm]
Left	Right	Left	Right	Left	Right	Total
0.16	0.19	0.89	1.02	4.07	4.07	6.52

Fig. 105 Sample No.2 of rivet HF section with DP-DP combination

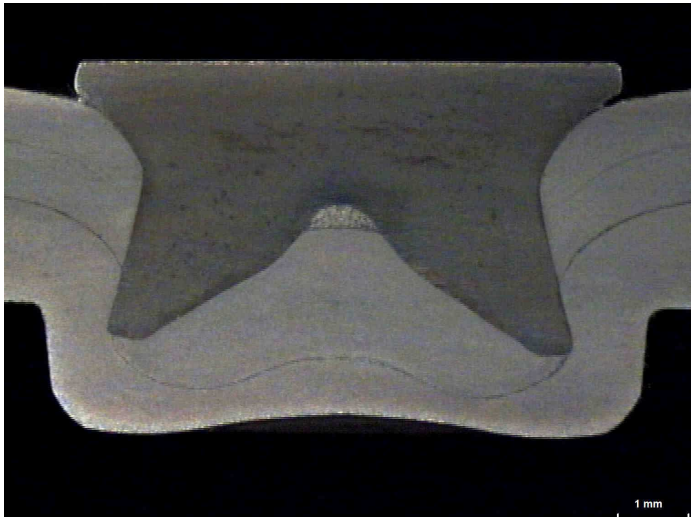
Joining Formation of Rivet HF with DP-DP Combination						
				Joined Sheets and Thickness		
				Punch side: DP-K 34/60 / 1.5mm Die side: DP-K 34/60 / 1.5mm		
				Joining Forces		
				Punch force: 91 kN Clamping force: 10 kN		
				SPR and Die		
SPR: HF / 5mm / 480 HV Die: F61801						
Interlock [mm]		Residual Bottom Thickness [mm]		Swelled Length [mm]		Spread Diameter [mm]
Left	Right	Left	Right	Left	Right	Total
0.21	0.20	0.85	1.01	3.93	4.13	6.63

Fig. 106 Sample No.3 of rivet HF section with DP-DP combination

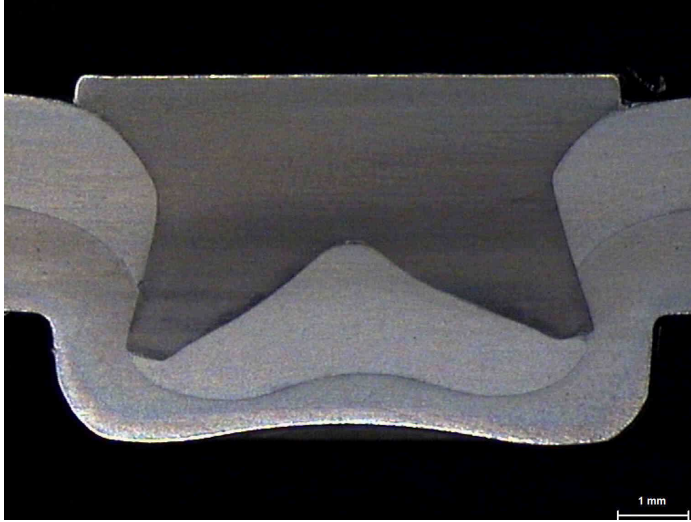
Joining Formation of Rivet HF with DP-CP Combination						
				Joined Sheets and Thickness		
				Punch side: DP-K 34/60 / 1.5mm Die side: CP-W 800 / 1.5mm		
				Joining Forces		
				Punch force: 96 kN Clamping force: 10 kN		
				SPR and Die		
SPR: HF / 5mm / 480 HV Die: F61801						
Interlock [mm]		Residual Bottom Thickness [mm]		Swelled Length [mm]		Spread Diameter [mm]
Left	Right	Left	Right	Left	Right	Total
0.21	0.24	1.00	0.83	3.98	3.75	6.64

Fig. 107 Rivet HF section with DP-CP combination

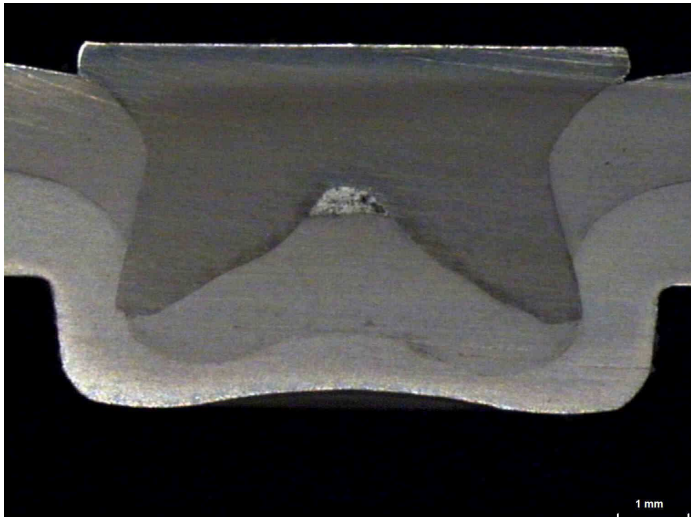
Joining Formation of Rivet HF with CP-DP Combination						
				Joined Sheets and Thickness		
				Punch side: CP-W 800 / 1.5mm Die side: DP-K 34/60 / 1.5mm		
				Joining Forces		
				Punch force: 100 kN Clamping force: 10 kN		
				SPR and Die		
SPR: HF / 5mm / 480 HV Die: F61801						
Interlock [mm]		Residual Bottom Thickness [mm]		Swelled Length [mm]		Spread Diameter [mm]
Left	Right	Left	Right	Left	Right	Total
0.19	0.16	0.84	1.02	3.84	3.93	6.64

Fig. 108 Rivet HF section with CP-DP combination

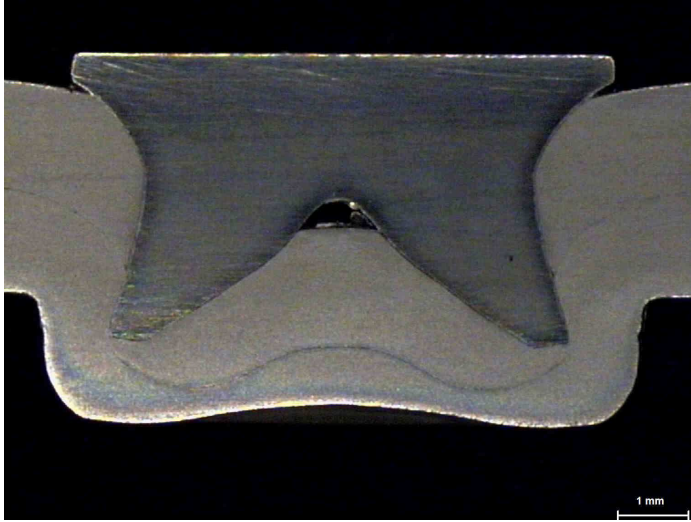
Joining Formation of Rivet HF with CP-CP Combination						
				Joined Sheets and Thickness		
				Punch side: CP-W 800 / 1.5mm Die side: CP-W 800 / 1.5mm		
				Joining Forces		
				Punch force: 100 kN Clamping force: 10 kN		
				SPR and Die		
SPR: HF / 5mm / 630 HV Die: F61801						
Interlock [mm]		Residual Bottom Thickness [mm]		Swelled Length [mm]		Spread Diameter [mm]
Left	Right	Left	Right	Left	Right	Total
0.25	0.23	0.88	0.99	4.04	4.16	6.54

Fig. 109 Rivet HF section with CP-CP combination

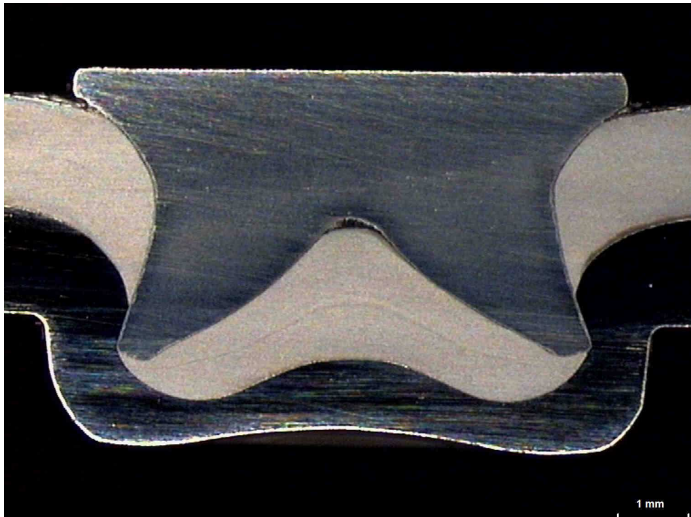
Joining Formation of Rivet HF with DP-H400 Combination						
				Joined Sheets and Thickness		
				Punch side: DP-K 34/60 / 1.5mm Die side: H400 / 1.5mm		
				Joining Forces		
				Punch force: 100 kN Clamping force: 10 kN		
				SPR and Die		
SPR: HF / 5mm / 630 HV Die: F61801						
Interlock [mm]		Residual Bottom Thickness [mm]		Swelled Length [mm]		Spread Diameter [mm]
Left	Right	Left	Right	Left	Right	Total
0.18	0.23	0.97	0.79	4.12	3.99	6.71

Fig. 110 Rivet HF section with DP-H400 combination

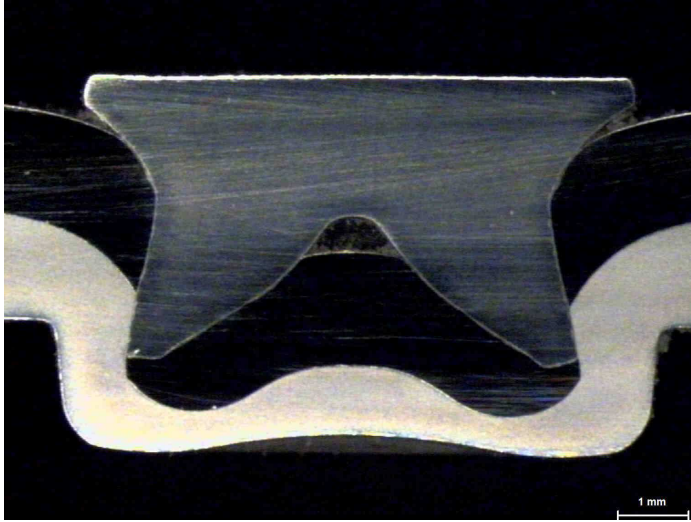
Joining Formation of Rivet HF with H400-DP Combination						
						Joined Sheets and Thickness
						Punch side: H400 / 1.5mm Die side: DP-K 34/60 / 1.5mm
						Joining Forces
						Punch force: 105 kN Clamping force: 10 kN
						SPR and Die
						SPR: HF / 5mm / 630 HV Die: F61801
Interlock [mm]		Residual Bottom Thickness [mm]		Swelled Length [mm]		Spread Diameter [mm]
Left	Right	Left	Right	Left	Right	Total
0.15	0.12	0.94	1.09	3.96	4.07	6.42

Fig. 111 Rivet HF section with H400-DP combination

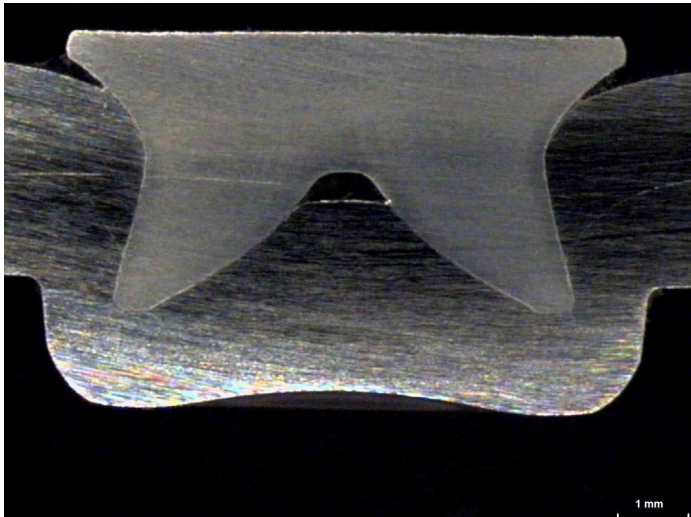
Joining Formation of Rivet HF with H400-H400 Combination						
						Joined Sheets and Thickness
						Punch side: H400 / 1.5mm Die side: H400 / 1.5mm
						Joining Forces
						Punch force: 105 kN Clamping force: 10 kN
						SPR and Die
						SPR: HF / 5mm / 630 HV Die: F61801
Interlock [mm]		Residual Bottom Thickness [mm]		Swelled Length [mm]		Spread Diameter [mm]
Left	Right	Left	Right	Left	Right	Total
0.13	0.12	0.98	1.04	3.98	3.92	6.54

Fig. 112 Rivet HF section with H400-H400 combination

## 12.3 G Rivet Joining Formation

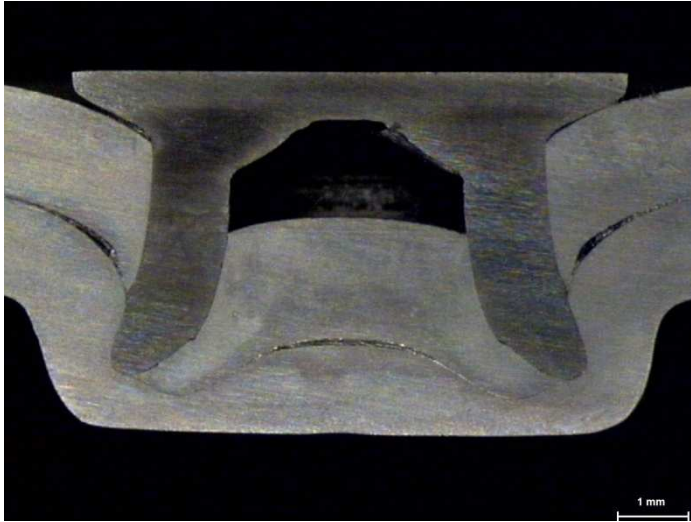
Joining Formation of Rivet G4 with DP-DP Combination						
				Joined Sheets and Thickness		
				Punch side: DP-K 34/60 / 1.5mm Die side: DP-K 34/60 / 1.5mm		
				Joining Forces		
				Punch force: 53 kN Clamping force: 10 kN		
				SPR and Die		
SPR: G4 / 5mm / 560 HV Die: G30						
Interlock [mm]		Residual Bottom Thickness [mm]		Swelled Length [mm]		Spread Diameter [mm]
Left	Right	Left	Right	Left	Right	Total
0.23	0.28	0.73	0.74	4.31	4.36	6.79

Fig. 113 Rivet G4 section with DP-DP combination

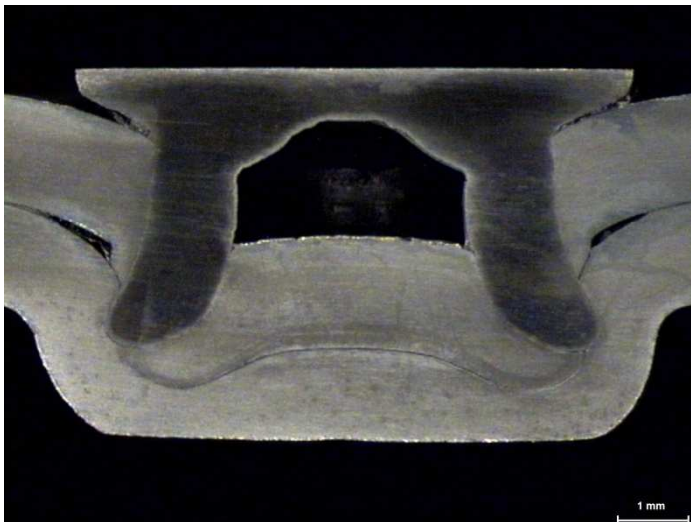
Joining Formation of Rivet G4 with CP-CP Combination						
				Joined Sheets and Thickness		
				Punch side: CP-W 800 / 1.5mm Die side: CP-W 800 / 1.5mm		
				Joining Forces		
				Punch force: 58 kN Clamping force: 10 kN		
				SPR and Die		
SPR: G4 / 5mm / 560 HV Die: G30						
Interlock [mm]		Residual Bottom Thickness [mm]		Swelled Length [mm]		Spread Diameter [mm]
Left	Right	Left	Right	Left	Right	Total
0.25	0.28	0.97	0.80	3.93	3.98	7.04

Fig. 114 Rivet G4 section with CP-CP combination

## 12.4 Quasi-Static Shear Test Comparison

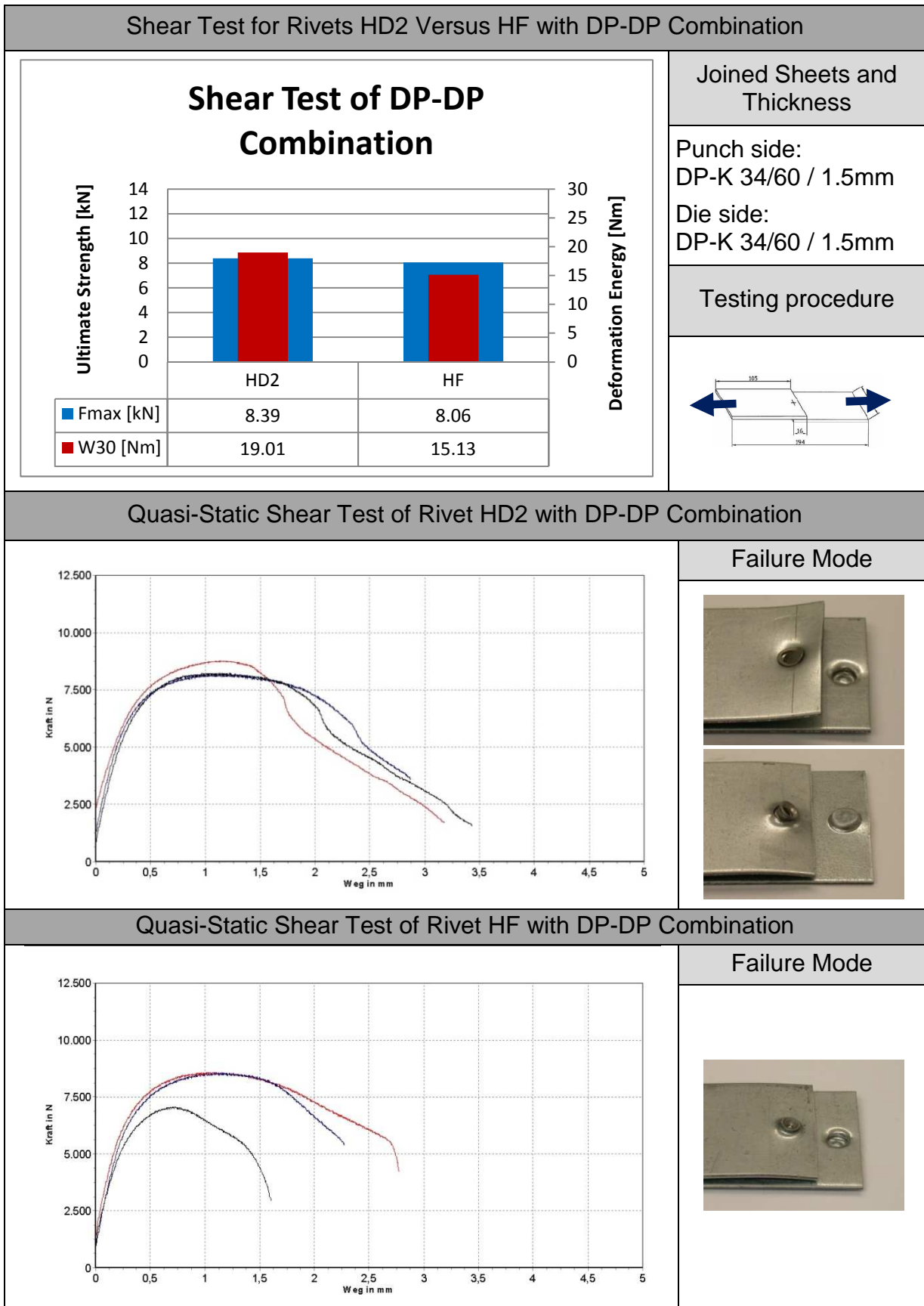
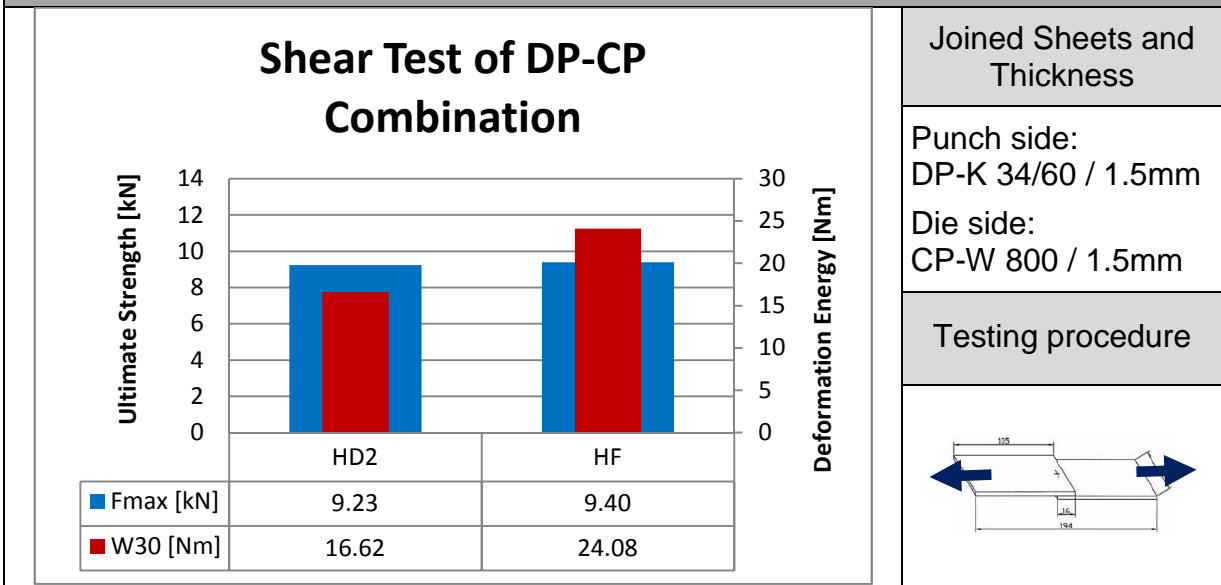
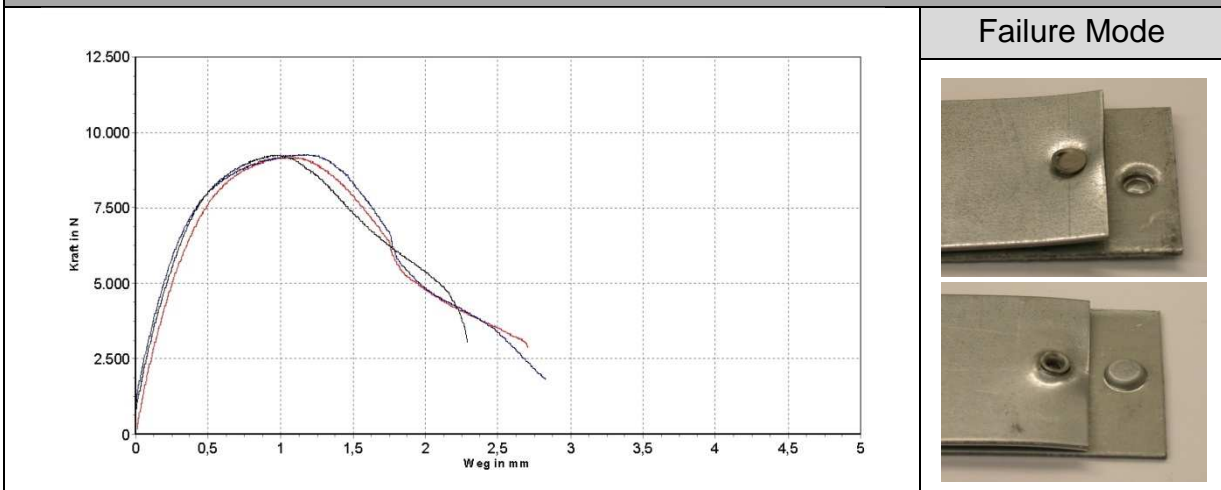


Fig. 115 Quasi-static shear test of DP-DP combination

Shear Test for Rivets HD2 Versus HF with DP-CP Combination



Quasi-Static Shear Test of Rivet HD2 with DP-CP Combination



Quasi-Static Shear Test of Rivet HF with DP-CP Combination

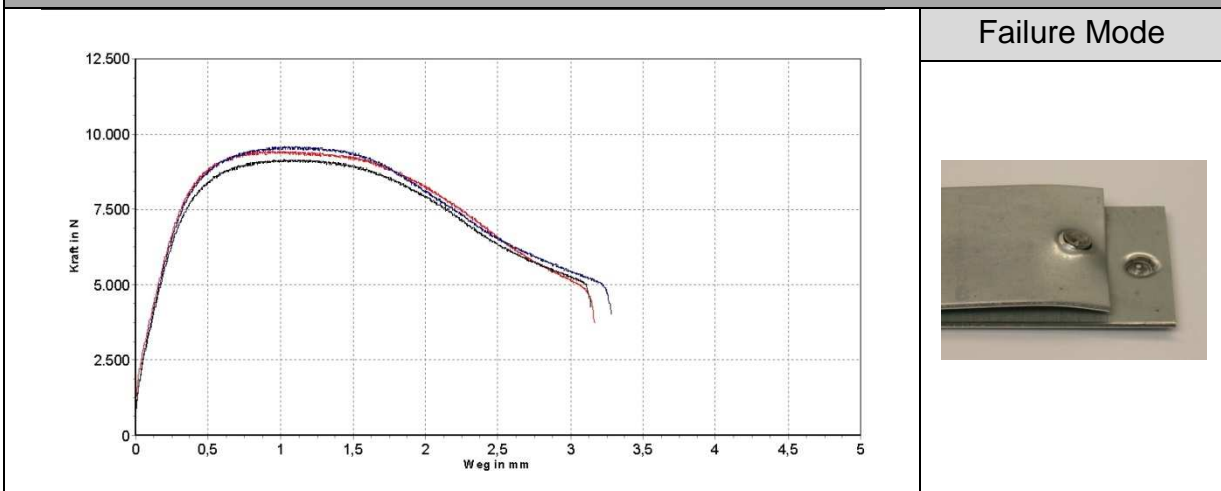
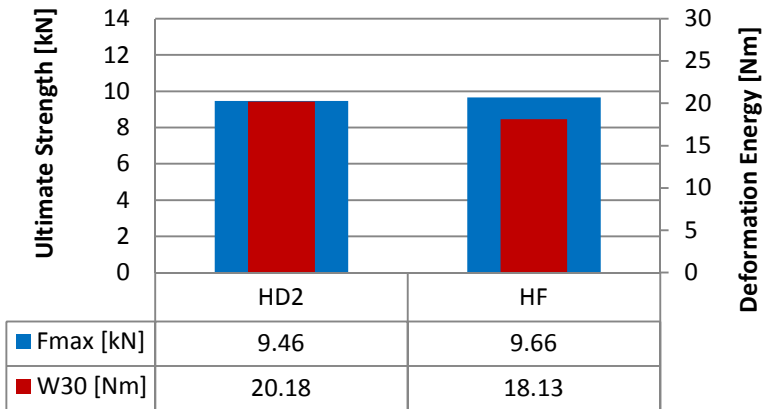


Fig. 116 Quasi-static shear test of DP-CP combination

Shear Test for Rivets HD2 Versus HF with CP-DP Combination

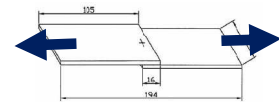
**Shear Test of CP-DP  
Combination**



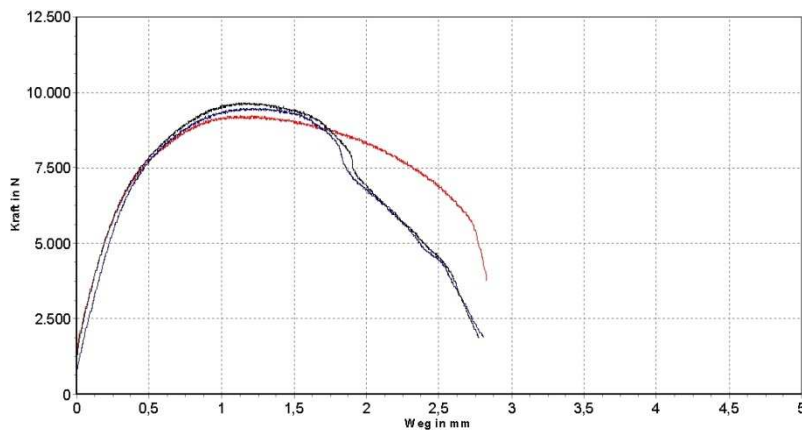
Joined Sheets and Thickness

Punch side:  
CP-W 800 / 1.5mm  
Die side:  
DP-K 34/60 / 1.5mm

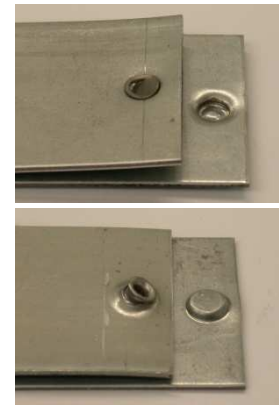
Testing procedure



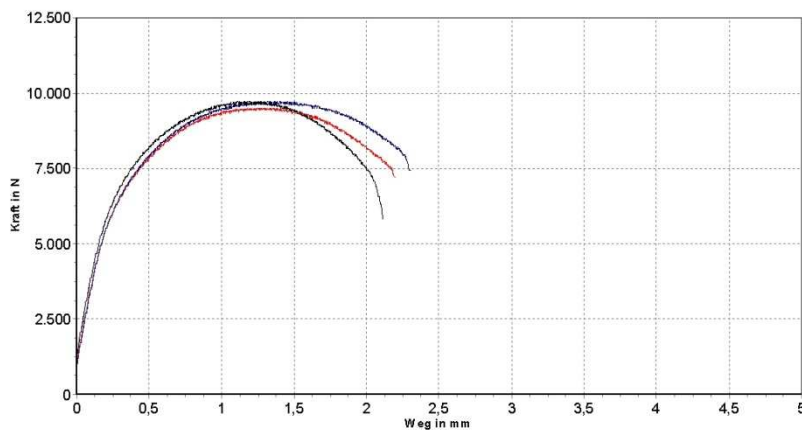
Quasi-Static Shear Test of Rivet HD2 with CP-DP Combination



Failure Mode



Quasi-Static Shear Test of Rivet HF with CP-DP Combination



Failure Mode

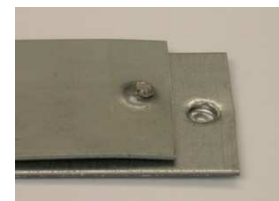
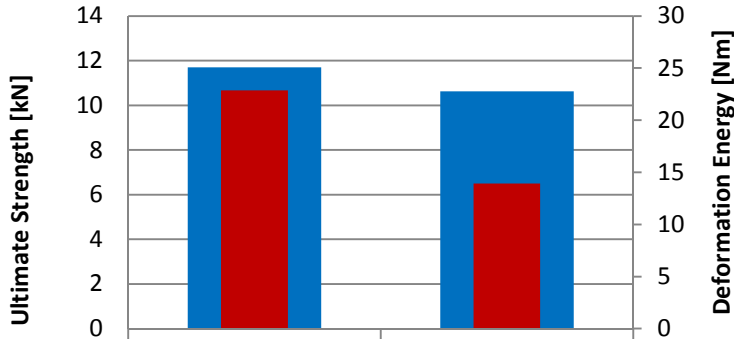


Fig. 117 Quasi-static shear test of CP-DP combination

Shear Test for Rivets HD2 Versus HF with CP-CP Combination

Shear Test of CP-CP Combination



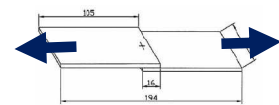
■ Fmax [kN]	11.71	10.62
■ W30 [Nm]	22.86	13.92

Joined Sheets and Thickness

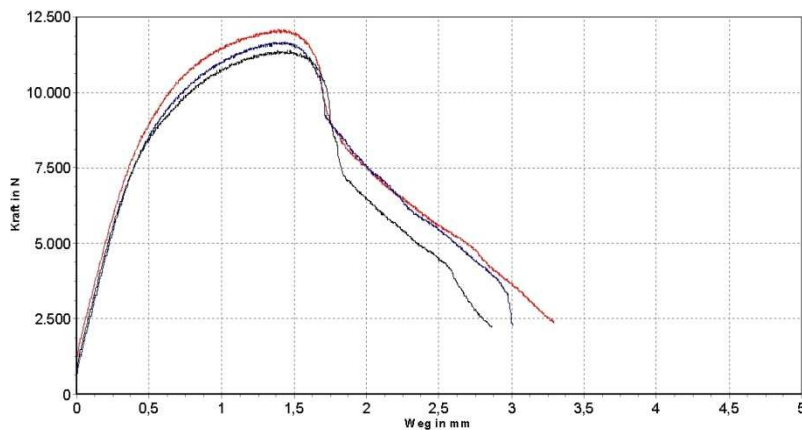
Punch side:  
CP-W 800 / 1.5mm

Die side:  
CP-W 800 / 1.5mm

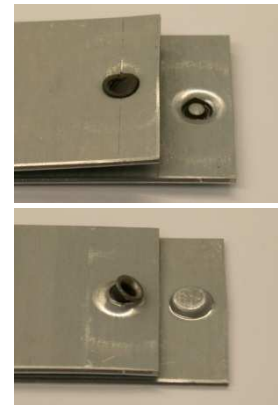
Testing procedure



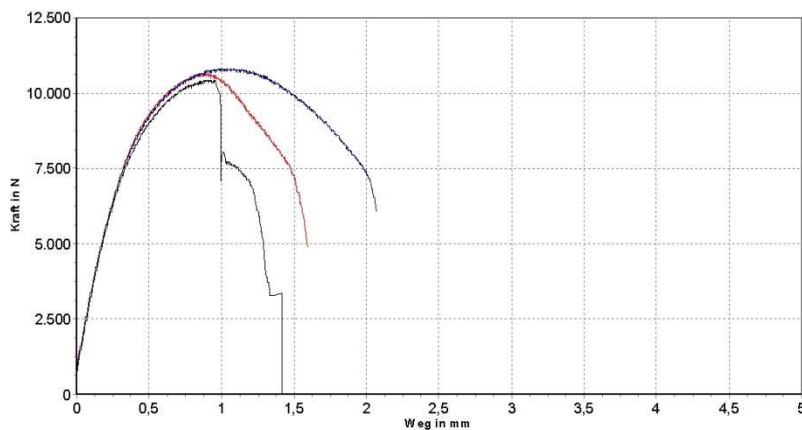
Quasi-Static Shear Test of Rivet HD2 with CP-CP Combination



Failure Mode



Quasi-Static Shear Test of Rivet HF with CP-CP Combination



Failure Mode

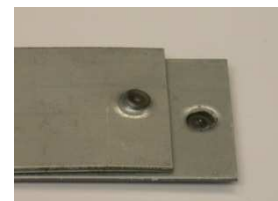


Fig. 118 Quasi-static shear test of CP-CP combination

Shear Test for Rivets HD2 Versus HF with DP-H400 Combination

### Shear Test of DP-H400 Combination

	HD2	HF
■ Fmax [kN]	10.05	8.96
■ W30 [Nm]	22.41	11.28

**Joined Sheets and Thickness**

Punch side:  
DP-K 34/60 / 1.5mm

Die side:  
H400 / 1.5mm

---

**Testing procedure**

Quasi-Static Shear Test of Rivet HD2 with DP-H400 Combination

**Failure Mode**

Quasi-Static Shear Test of Rivet HF with DP-H400 Combination

**Failure Mode**

Fig. 119 Quasi-static shear test of DP-H400 combination

Shear Test for Rivets HD2 Versus HF with H400-DP Combination

### Shear Test of H400-DP Combination

	HD2	HF
■ Fmax [kN]	9.87	8.55
■ W30 [Nm]	26.16	12.43

Joined Sheets and Thickness

Punch side:  
H400 / 1.5mm

Die side:  
DP-K 34/60 / 1.5mm

Testing procedure

Quasi-Static Shear Test of Rivet HD2 with H400-DP Combination

Failure Mode

Quasi-Static Shear Test of Rivet HF with H400-DP Combination

Failure Mode

Fig. 120 Quasi-static shear test of H400-DP combination

Shear Test for Rivets HD2 Versus HF with H400-H400 Combination

### Shear Test of H400-H400 Combination

	HD2	HF
■ Fmax [kN]	5.18	8.33
■ W30 [Nm]	1.27	7.03

**Joined Sheets and Thickness**

Punch side:  
H400 / 1.5mm

Die side:  
H400 / 1.5mm

---

**Testing procedure**

Quasi-Static Shear Test of Rivet HD2 with H400-H400 Combination

**Failure Mode**

Quasi-Static Shear Test of Rivet HF with H400-H400 Combination

**Failure Mode**

Fig. 121 Quasi-static shear test of H400-H400 combination

## 12.5 Fatigue Shear Test Rivet Comparison

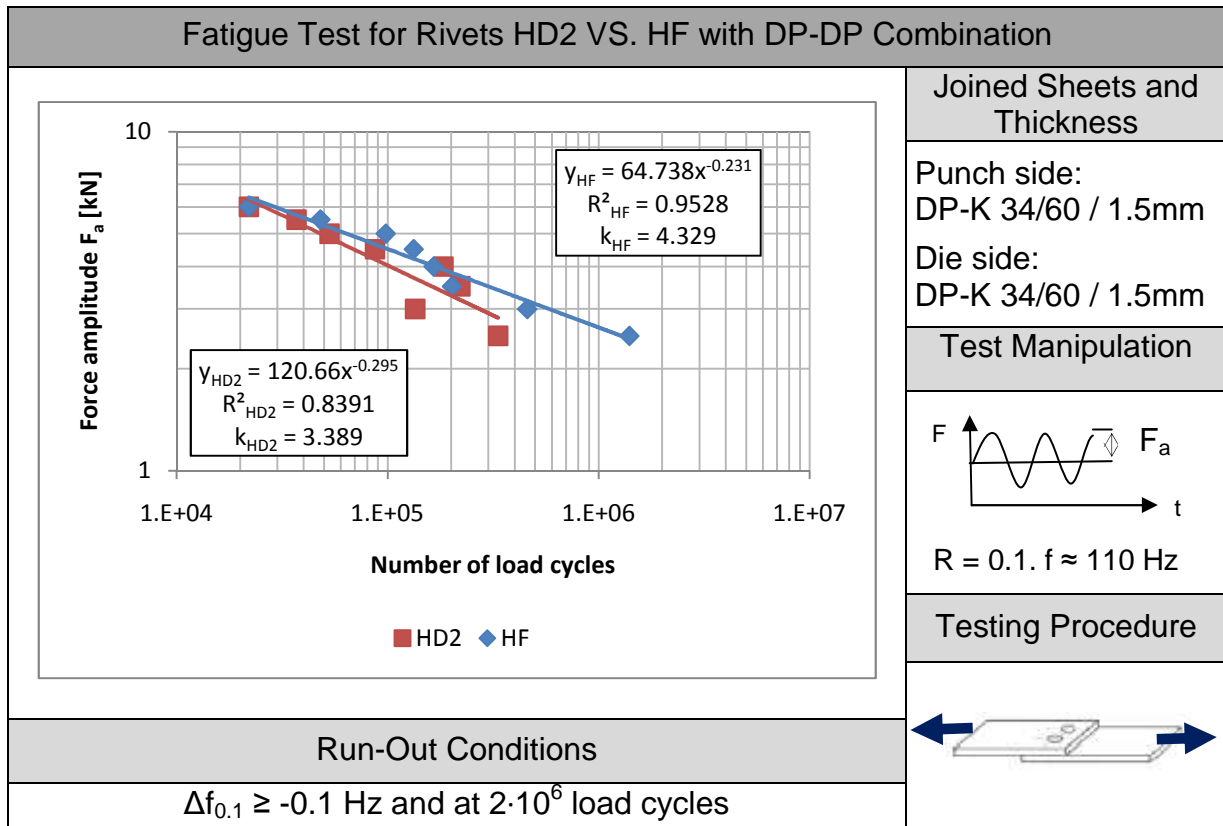


Fig. 122 Wöhler curves for rivets HD2 vs. HF with DP-DP combination

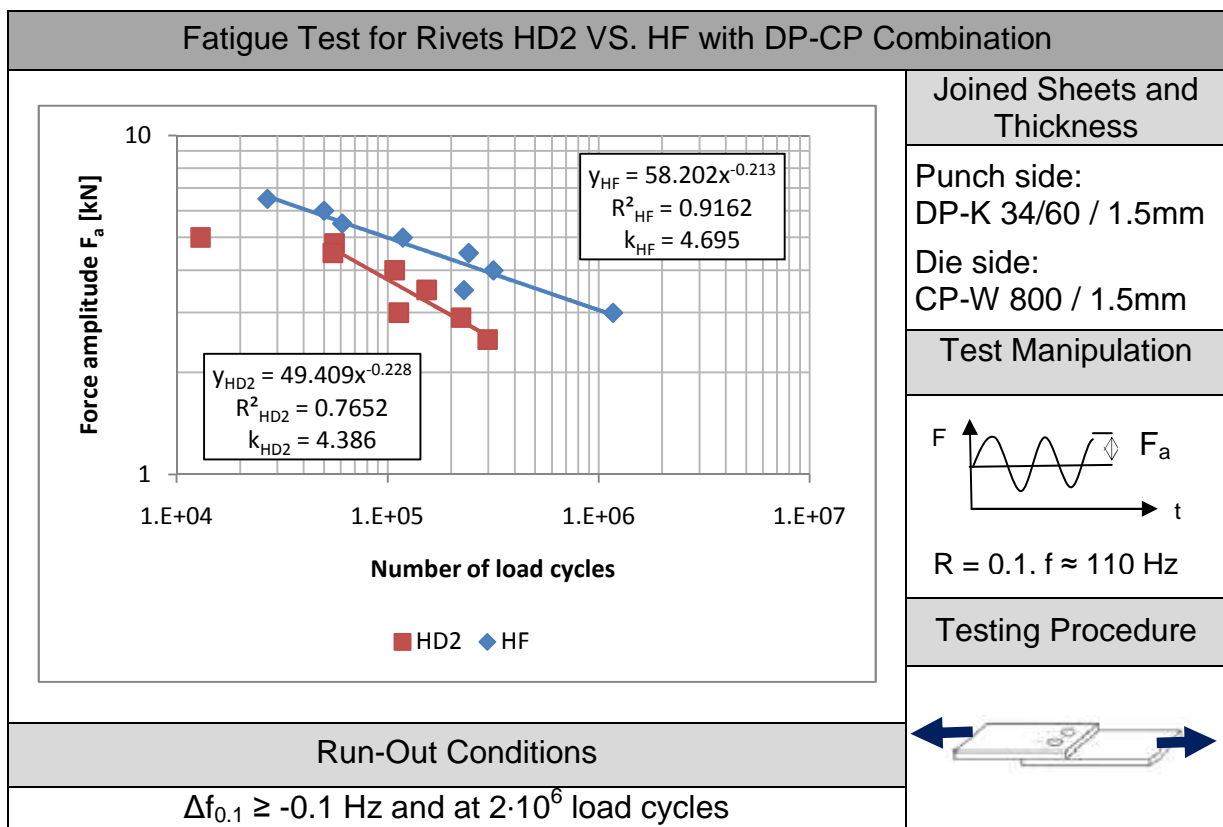


Fig. 123 Wöhler curves for rivets HD2 vs. HF with DP-CP combination

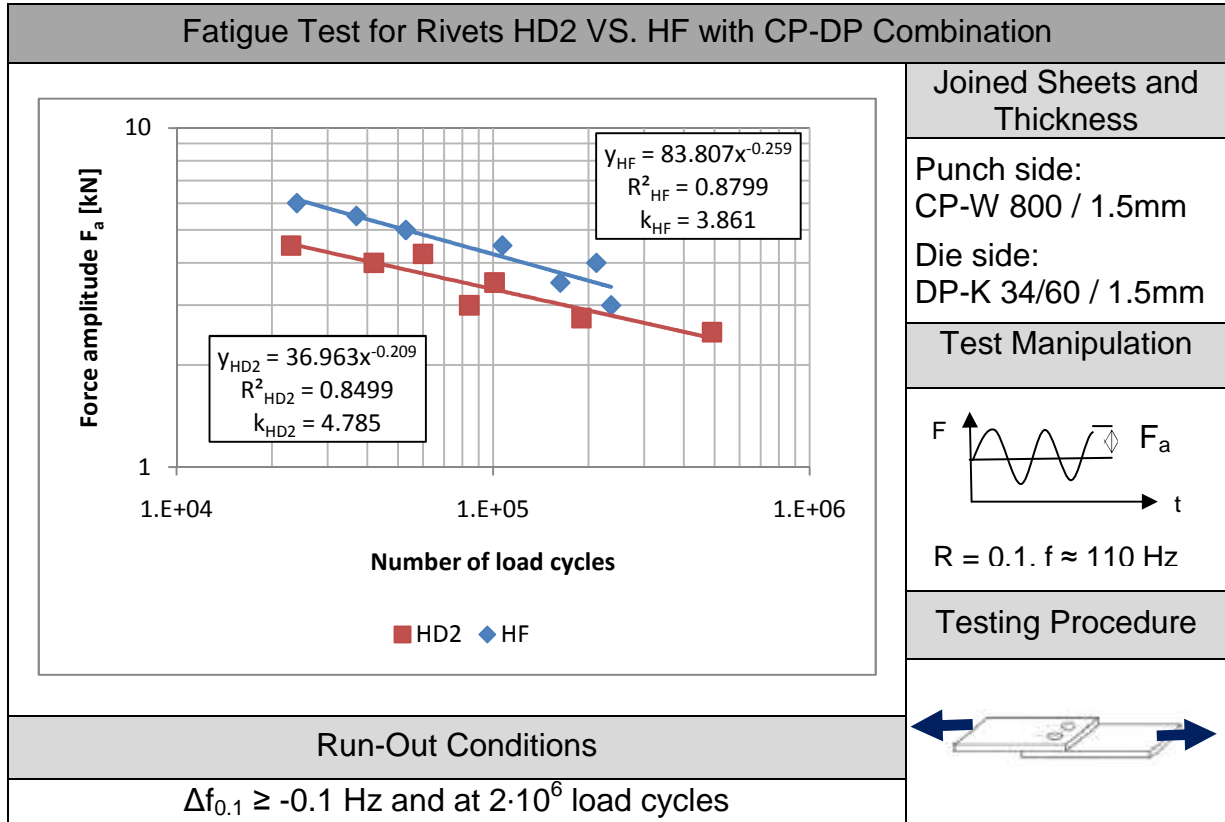


Fig. 124 Wöhler curves for rivets HD2 vs. HF with CP-DP combination

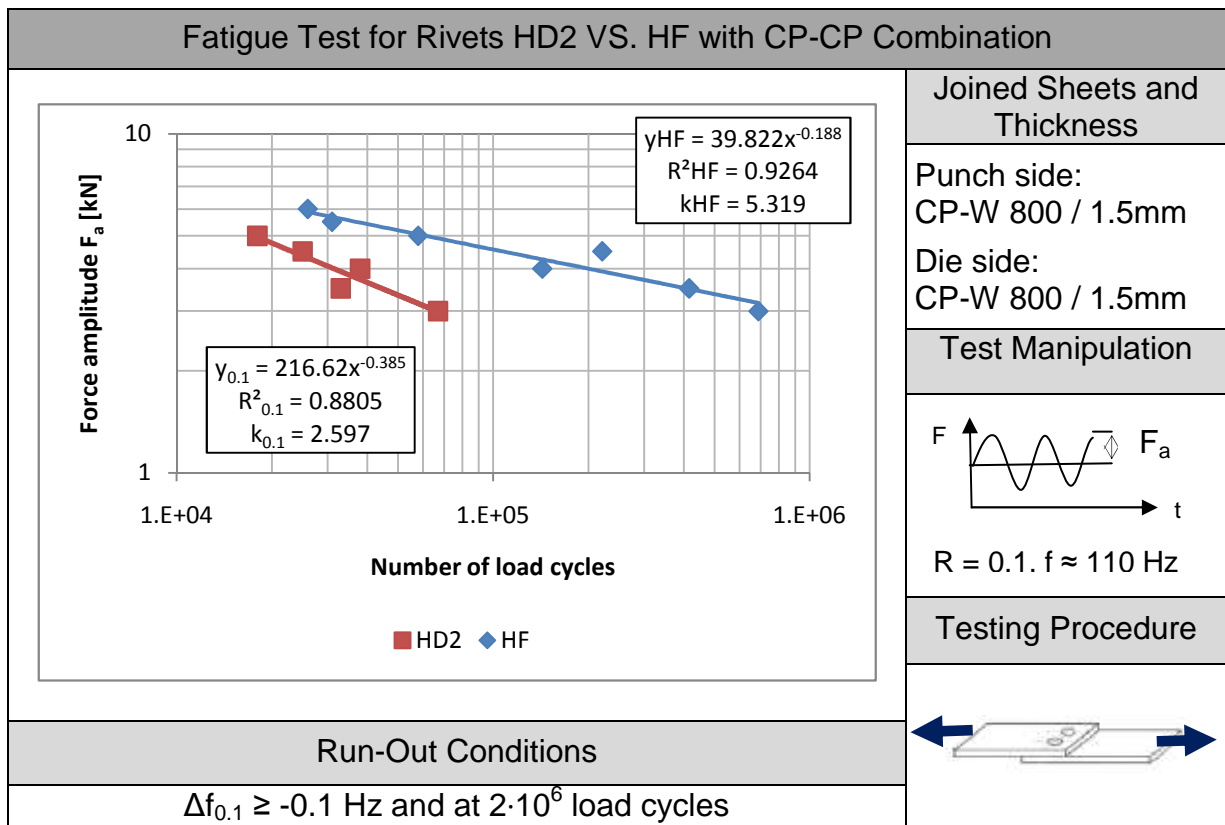


Fig. 125 Wöhler curves for rivets HD2 vs. HF with CP-CP combination

## 12.6 Fatigue Shear Test Frequency Comparison

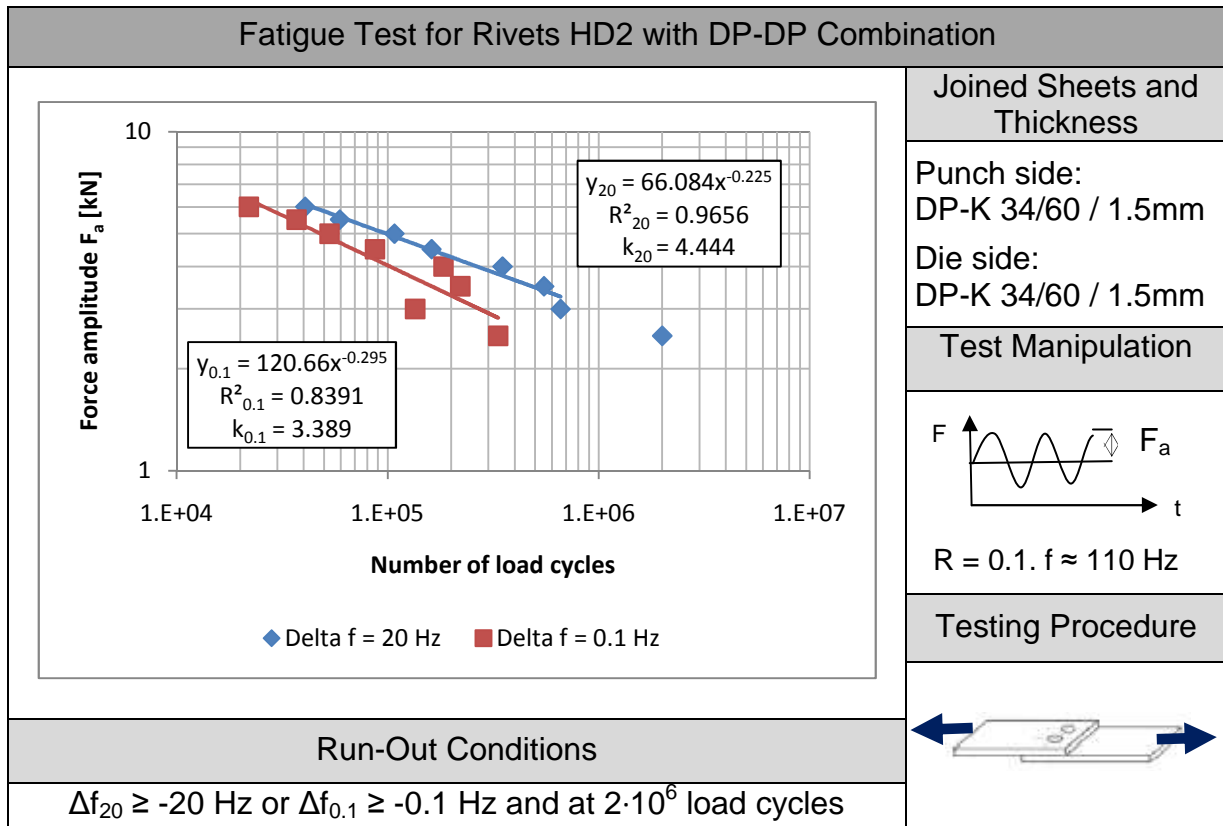


Fig. 126 Wöhler curves for DP-DP combination with HD2 rivet

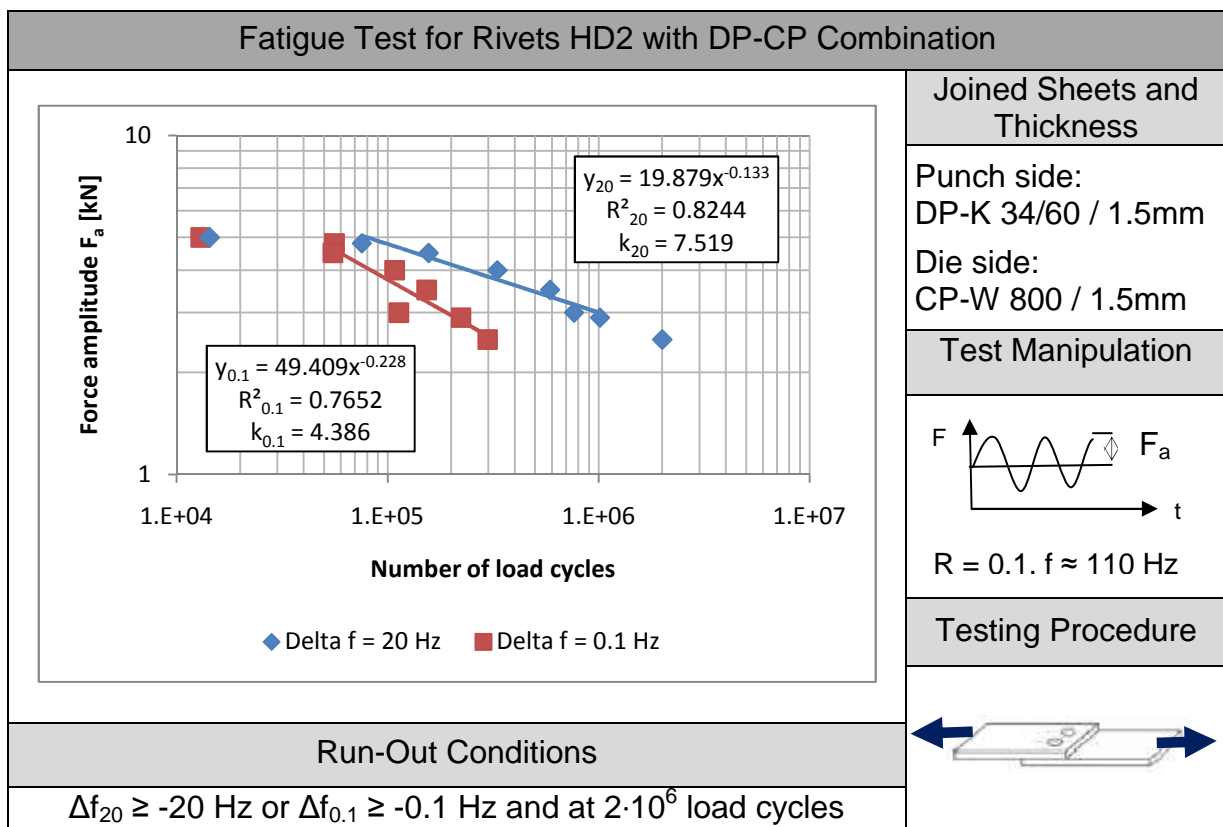


Fig. 127 Wöhler curves for DP-CP combination with HD2 rivet

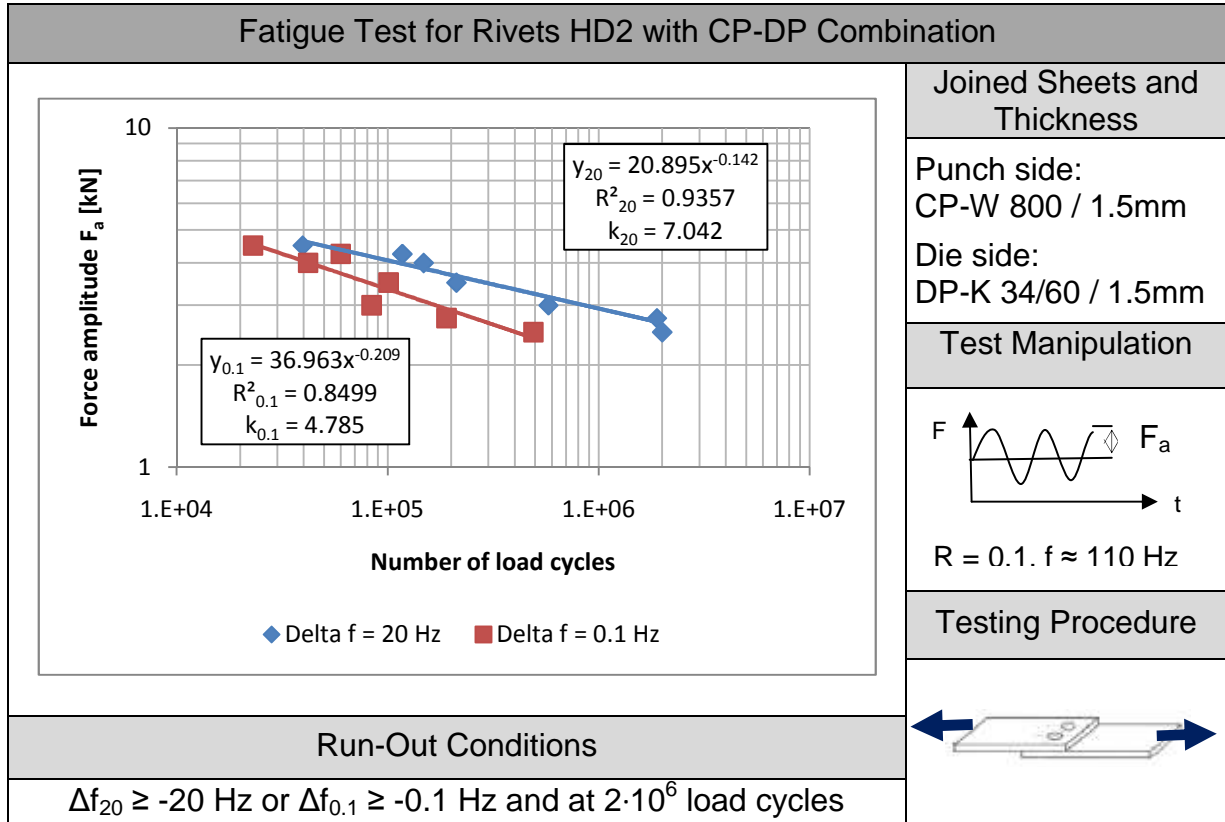


Fig. 128 Wöhler curves for CP-DP combination with HD2 rivet

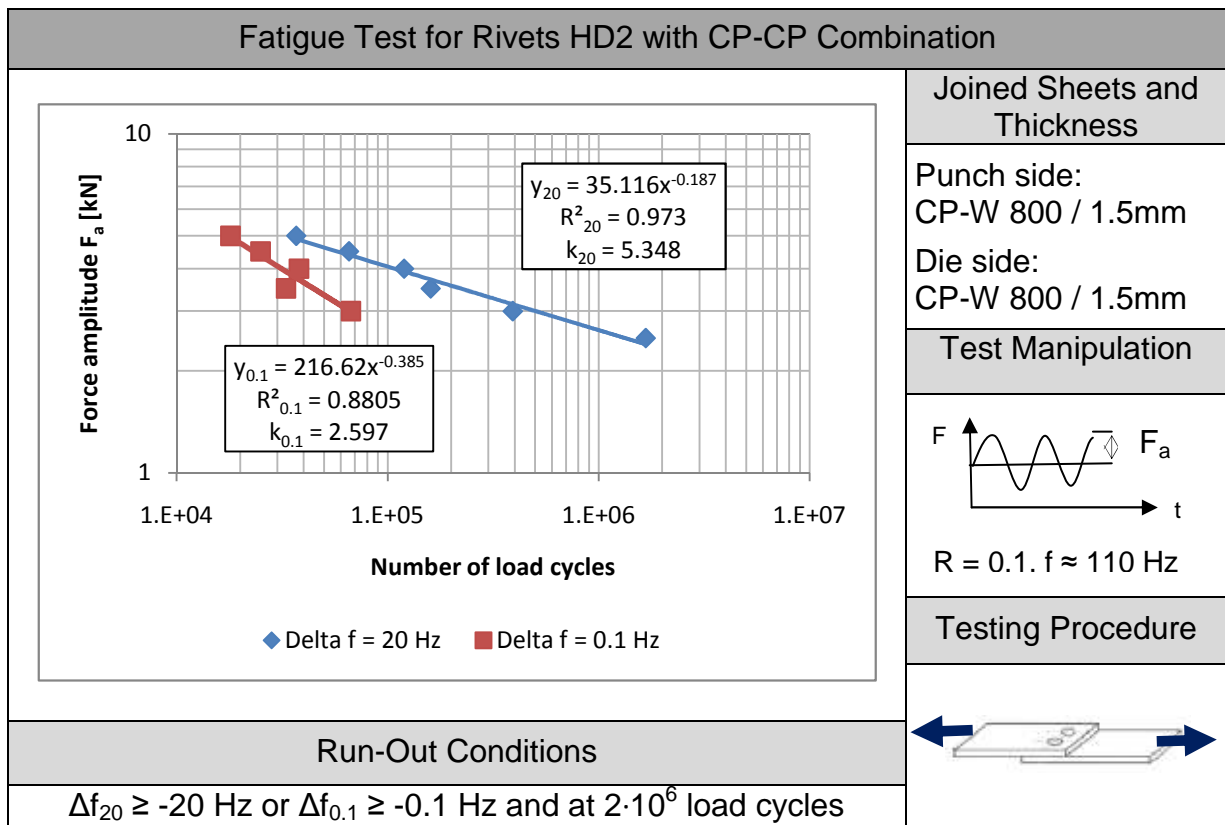


Fig. 129 Wöhler curves for CP-CP combination with HD2 rivet

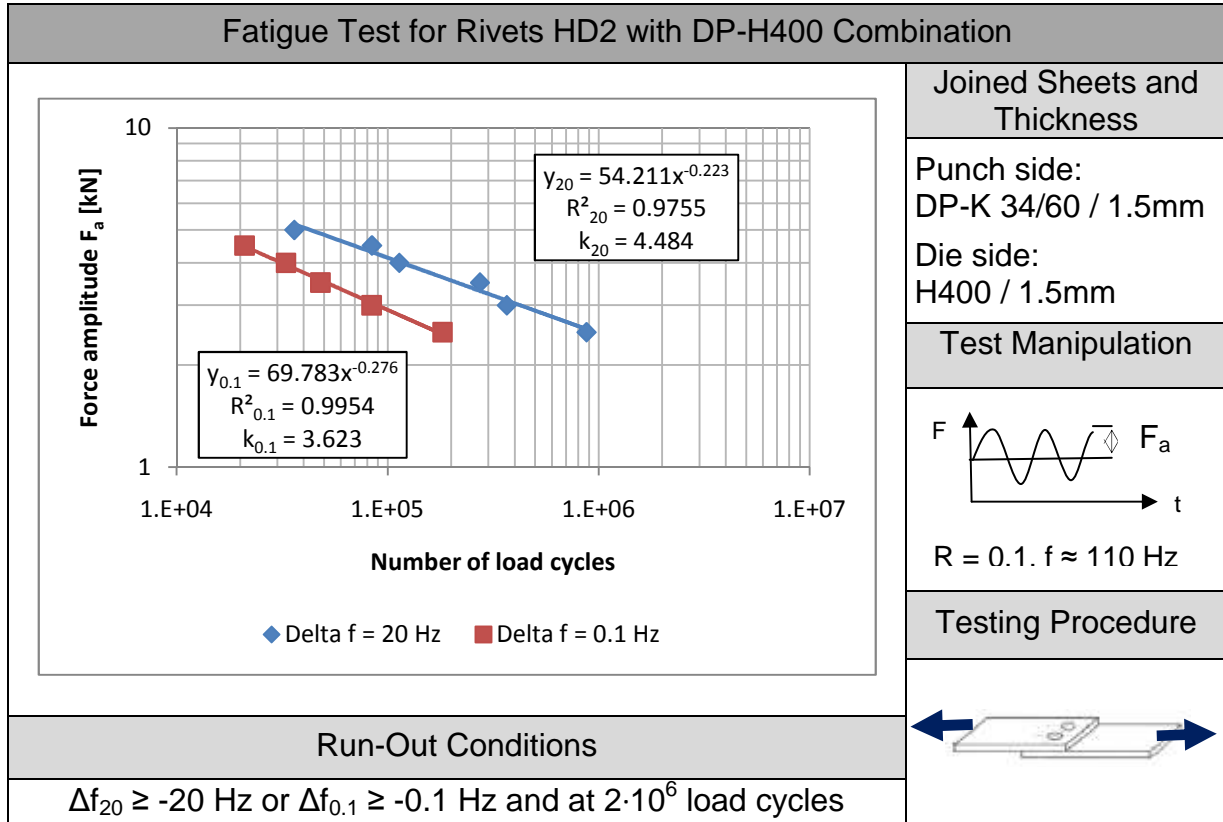


Fig. 130 Wöhler curves for DP-H400 combination with HD2 rivet

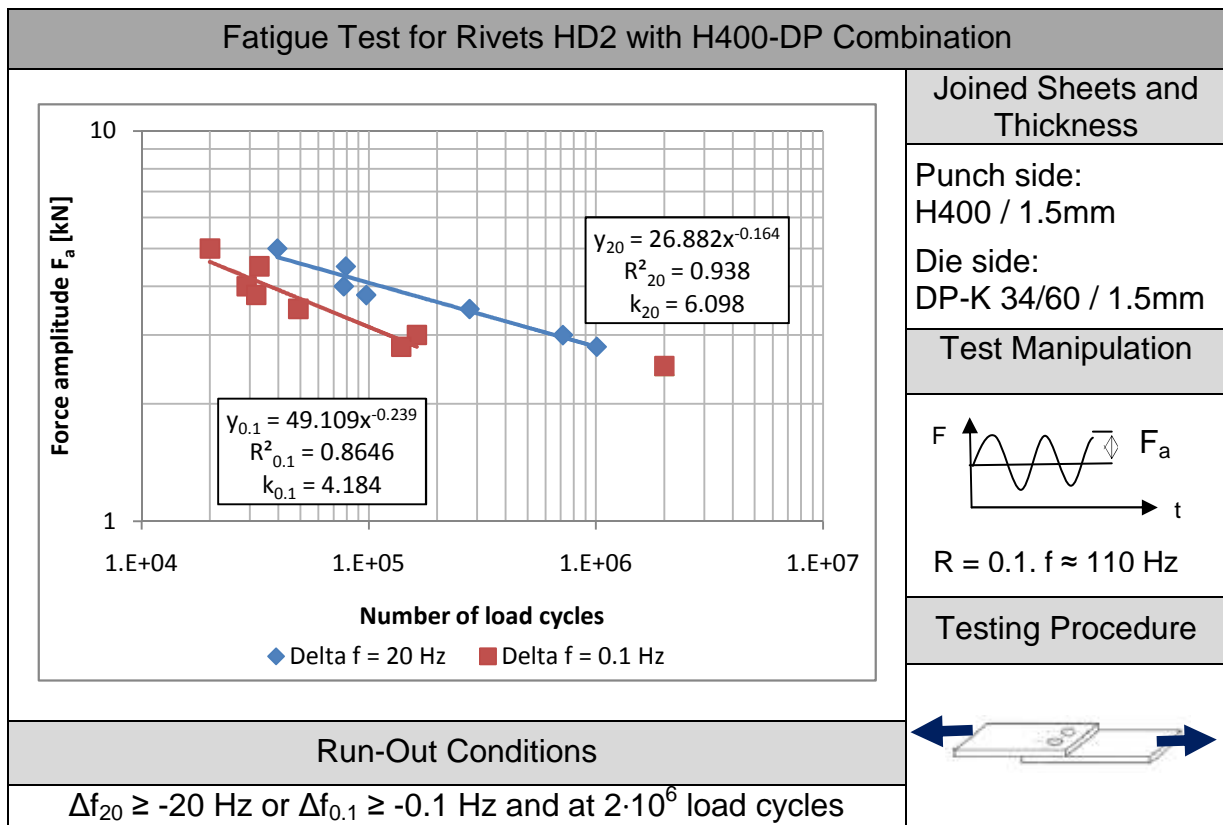


Fig. 131 Wöhler curves for H400-DP combination with HD2 rivet

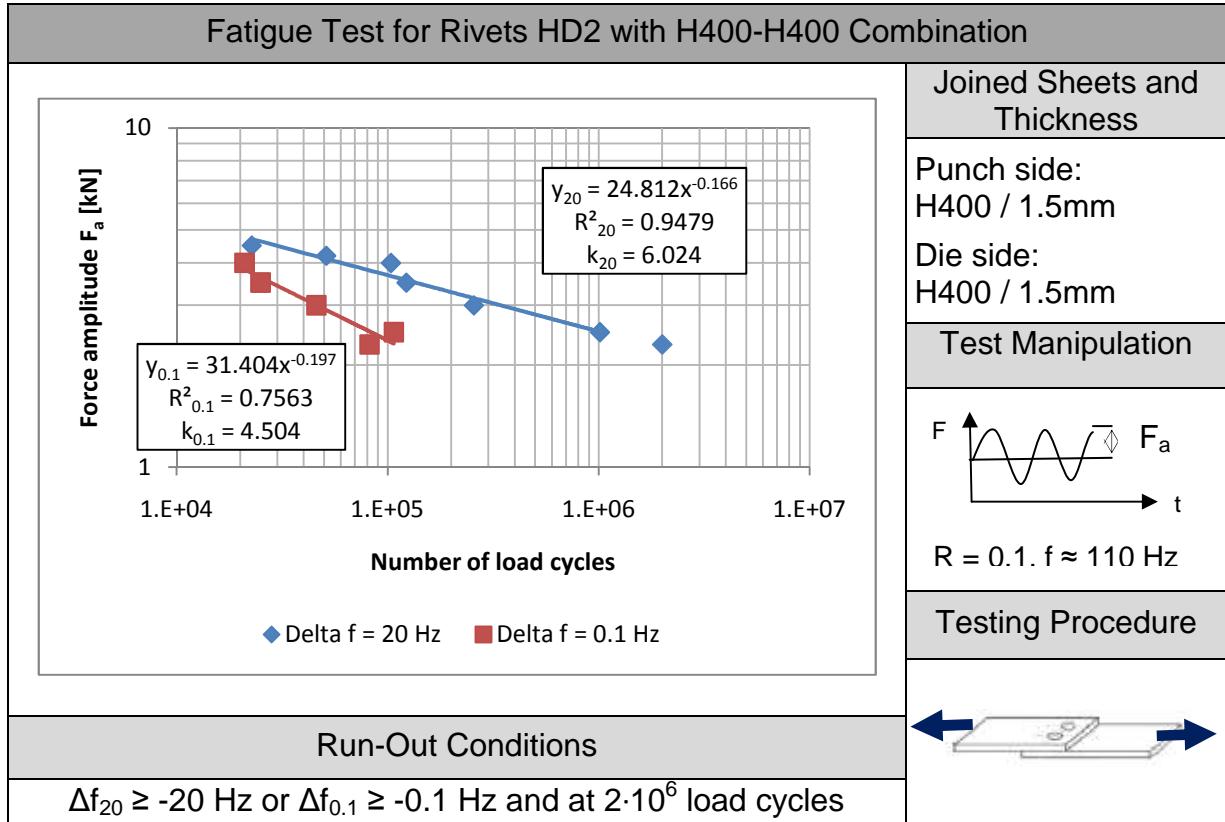


Fig. 132 Wöhler curves for H400-H400 combination with HD2 rivet

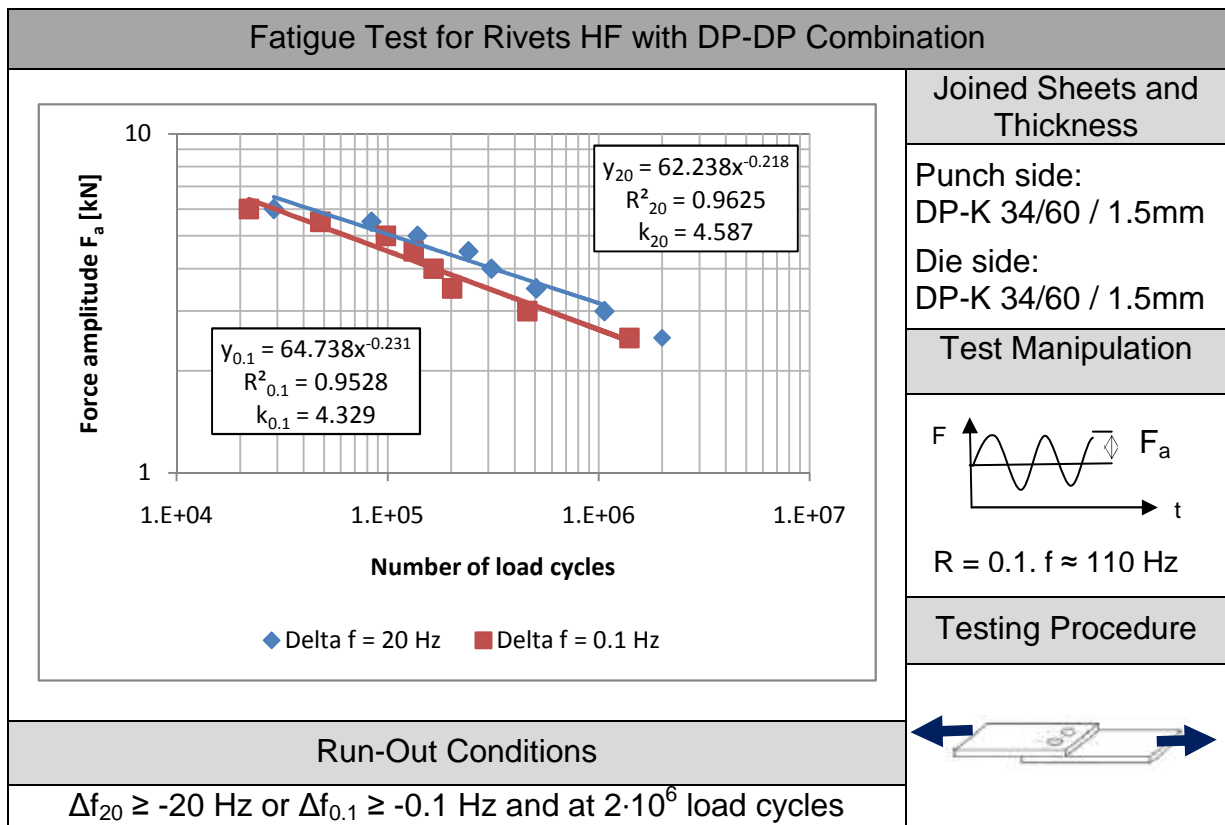


Fig. 133 Wöhler curves for DP-DP combination with HF rivet

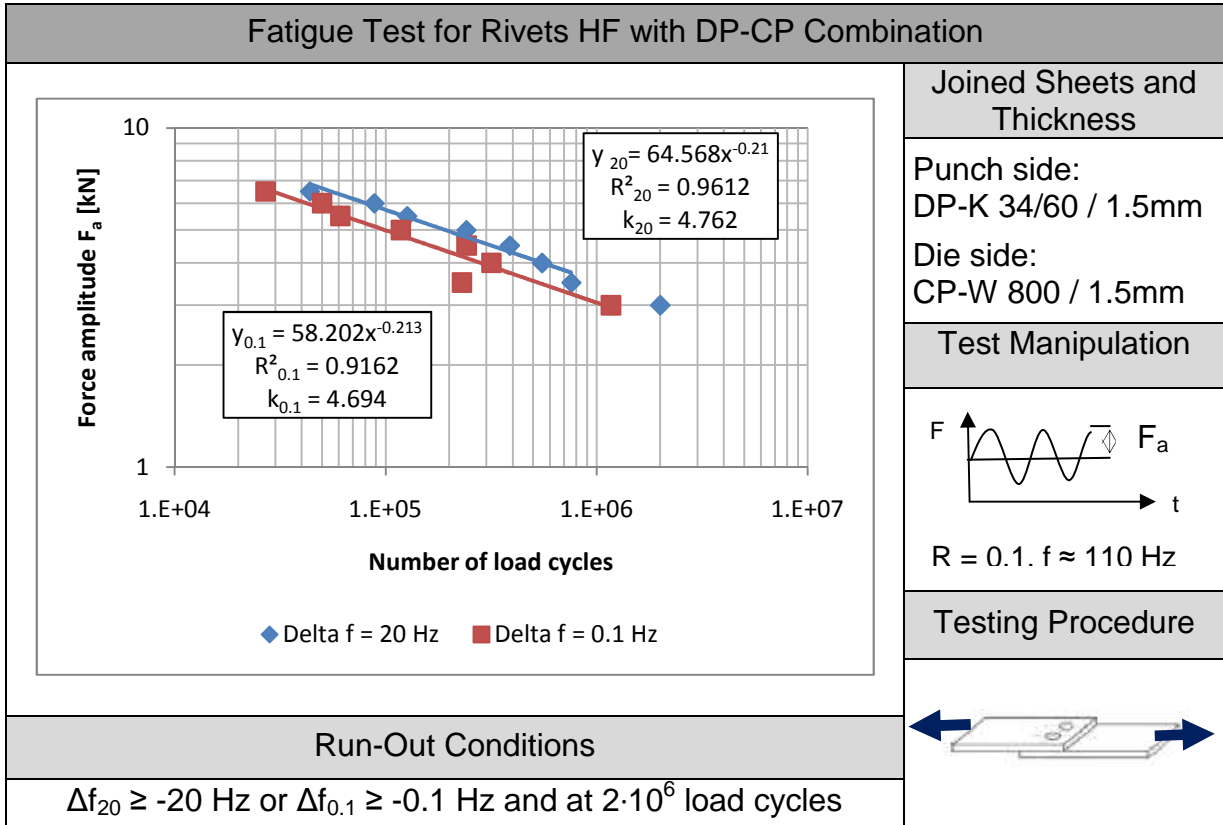


Fig. 134 Wöhler curves for DP-CP combination with HF rivet

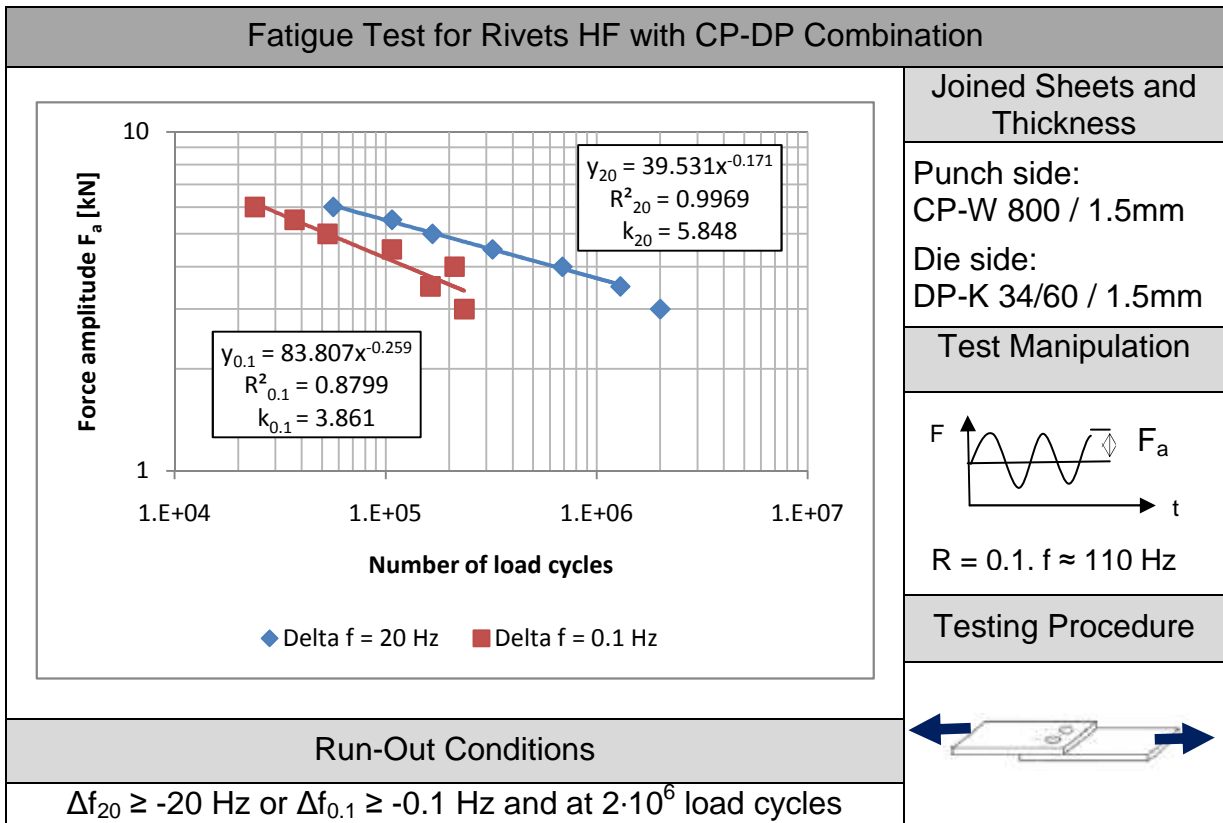


Fig. 135 Wöhler curves for CP-DP combination with HF rivet

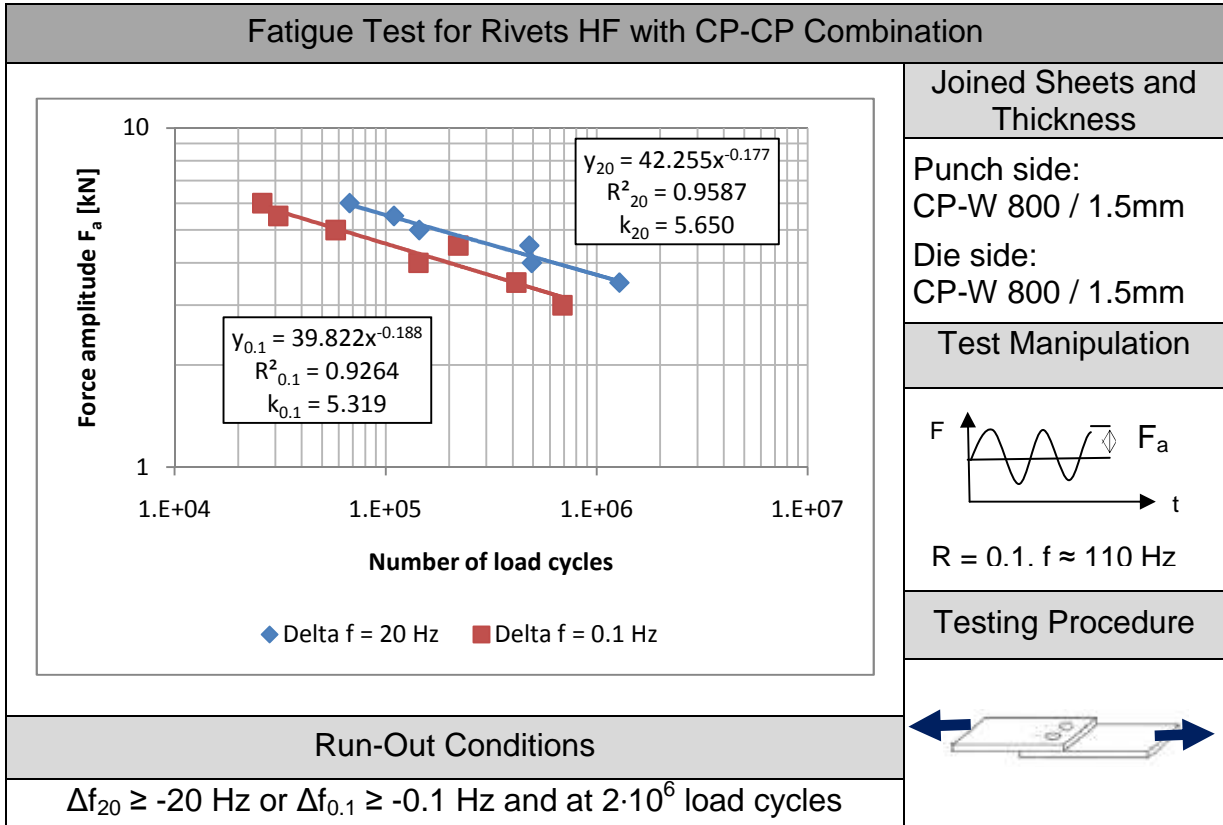


Fig. 136 Wöhler curves for CP-CP combination with HF rivet